I. SIMILARITY SOLUTIONS OF THE EQUATIONS OF THREE

PHASE FLOW THROUGH POROUS MEDIA

II. THE FINGERING PROBLEM IN A HELE-SHAW CELL

Thesis by

Louis Anthony Romero

In Partial Fullfillment of the Requirements

for the Degree of

Doctor of Philosophy

California Institute of Technology

Pasadena, California

1982

(submitted January 4, 1982)

ACKNOWLEDGEMENTS

I would like to thank my advisor Professor P.G. Saffman for his guidance during the course of my graduate studies here at Caltech. He has set an example of depth of understanding, and honesty in scientific research that will hopefully influence my future work.

My stay at Caltech was made possible due to the financial support of the Doctoral Studies Program at Sandia Labs. I would like to thank my boss Mel Scott for encouraging me to apply for the program, for helping me get accepted, and for his help throughout the course of my stay at Caltech. The numerical computations were made possible thanks to a grant from the Control Data Corporation.

Special thanks go out to my brother Ed for his help in filling in the equations by hand. I would also like to thank Betty Wood for her help in drawing the graphs, and Sheila Shull for her help in setting up the word processing system.

I would like to thank my wife Shelley for making my stay in school much more enjoyable than it would have been without her.

ABSTRACT

I

In part I of this thesis similarity solutions to the equations of three phase flow through porous media are examined. The three phases are water, steam, and a noncondensing phase, most likely oil. The main purpose of analyzing such flows is to gain understanding of the steam flooding of oil fields.

Provided steam is being injected at a higher pressure than the initial field pressure, it is shown that there will always be at least two saturation shocks. As one increases the pressure of the injected steam several regimes are encountered; first the flow develops a region where all the steam is completely condensed, then the position of two of the shocks are interchanged, and finally one of the shocks grows weaker and is eventually replaced by an expansion fan.

In sections 12 and 13 the stability of steadily moving condensation fronts in porous media is analyzed. For one special problem it is found that the sign of the jump in pressure gradient at the interface determines whether the interfaces are stable or unstable. This result is applied with some caution to the similarity solutions found in the earlier sections.

II

Recently McLean analyzed the shapes of fingers in a Hele-Shaw cell, including the effects of surface tension. His

work resolved the question of the uniqueness of the shapes
first brought up by Saffman and Taylor in their analysis that
did not include surface tension. It is however felt that
there are still unresolved problems.

In determining the pressure jump across an interface
there are two principal radii of curvature. McLean only took
into account the effect of the larger of these, assuming that
the other was constant along the outline of the finger.
Unless the smaller radius is very nearly constant, it should
in fact give a larger contribution to the jump in pressure.
In this thesis the effect of this smaller radius of curvature
is modelled by assuming that it is a function of the normal
velocity of the mean two dimensional surface of the finger.

It is found that if one only takes into account the
smaller radius of curvature, the problem is not uniquely
determined, as in the case with no surface tension at all.
When both radii of curvature are taken into account, the
effect of the smaller radius of curvature is to modify the
finger shapes in a way that is qualitatively in agreement with
experimental data. Also, McLean's results are checked by an
independent numerical scheme, and the results are found to be
in excellent agreement. Using both methods of solution a
second solution branch other than that described by McLean was
also found.

TABLE OF CONTENTS

II. THE FINGERING PROBLEM IN A HELE-SHAW CELL

Part I

SIMILARITY SOLUTIONS OF THE EQUATIONS OF THREE

PHASE FLOW THROUGH POROUS MEDIA

1) INTRODUCTION

The equations of motion of a fluid in a porous medium are almost always based on Darcy's law or one of its extensions. In its simplest form, Darcy's law states that for a homogeneous fluid the seepage velocity $\underline{U}$ (which is the net rate of transport of fluid) is proportional to the pressure gradient and a term due to gravity (ref 1).

1) $$\underline{U} = -\frac{k}{\mu}\left(\nabla P - \rho \hat{g}\right)$$

Here k is the permeability, which is a property of the porous medium, μ and ρ are the viscosity and density of the fluid, and $\hat{g}$ is the gravity vector. In this work the effect of gravity will be ignored.

If more than one fluid is present in the medium, one or more saturation functions must be introduced. In the case of a two fluid system the saturation function $S(x,t)$ tells what fraction of the volume of pore space is occupied by each of the two fluids. If the two fluids are labeled I and II, then S=1 indicates only fluid I is present, and S=0 indicates only fluid II is present. In these multicomponent systems Darcy's law is generalized to (ref 1)

2) $$\underline{U}_I = -k\,\alpha_I(s)\frac{\nabla P}{\mu_I}$$

$$\underline{U}_{II} = -k\,\alpha_{II}(s)\frac{\nabla P}{\mu_{II}}$$

Here $\underline{U}_I$ and $\underline{U}_{II}$ are the net rate of transport of each

component. This is an empirical formula. The functions α_I
and α_{II} are known as the relative permeabilities, and they are
obtained experimentally. One can however expect that they are
both monotone functions of S. As S varies from 0 to 1
α_I rises from 0 to 1, and α_{II} decreases from 1 to 0. This is
due to the fact that when S=0 the seepage velocity of fluid I
is zero, since none of it is present, so $\alpha_I(0)=0$. Also,
$\alpha_{II}(0)=1$ since at this extreme the result should agree with
equation 1) for a single component system. The corresponding
result at S=1 is valid for the same reason. In figure 1 a
typical pair of profiles for α_I and α_{II} is plotted.

The case of the flow of two immiscible fluids in a porous
medium was first analyzed by Buckley and Leverett (ref 2). In
this case the continuity equations for each phase yield

3a) $\quad \dfrac{\partial}{\partial t}\left(\epsilon \rho_I s\right) - \nabla\cdot\left(\rho_I \dfrac{k}{\mu_I}\alpha_I(s)\nabla P\right) = 0$

b) $\quad \dfrac{\partial}{\partial t}\left(\epsilon \rho_{II}(1-s)\right) - \nabla\cdot\left(\rho_{II}\dfrac{k}{\mu_{II}}\alpha_{II}(s)\nabla P\right) = 0$

Here ϵ, known as the porosity, tells how much of the
medium is available to be filled by fluid. For the one
dimensional problem a first order P.D.E. can be derived. By
combining 3ab) one gets

$$K P_x\left(\frac{\alpha_I(s)}{\mu_I} + \frac{\alpha_{II}(s)}{\mu_{II}}\right) = f(t)$$

where f(t) is an arbitrary function of time. Plugging this

back into 3a) one gets

$$\epsilon \frac{\partial s}{\partial t} - \frac{\partial}{\partial x}\left(\frac{f(t)\alpha_I(s)}{\alpha_I(s) + \frac{\mu_I}{\mu_{II}}\alpha_{II}(s)}\right) = 0$$

This equation is an equation for a kinematic wave (ref 3). Buckley and Leverett used this equation to show that for certain initial conditions saturation shocks develop in the flow.

In the above formulation it is assumed that the pressures of the two fluids are identical. This is not precisely true. Due to surface tension effects it is found that the pressures differ by a function of S. This function pc(S), known as the capillary pressure, is experimentally determined. If this function is included in equations 3ab) one has a term involving S_{xx}, and this term acts to replace the shocks by regions of sharp gradients in S and P_x.

In many problems of flow through porous media the capillary pressure is a dominant term in the equations, and cannot be ignored. It is important in problems such as the slow infiltration of groundwater, where no external pressure gradient is forced on the system. For problems such as the steam-flooding of oil fields, or the analysis of geothermal power systems, the capillary pressure may be ignored. This is because the pressure gradients due to capillarity are small compared to those forced on the system. It is this second class of problems that motivates the present work.

In recent papers (refs. 4,5) Romero and Nilson found similarity solutions to the problem of a fluid capable of undergoing phase change flowing through a porous medium. In this case the saturation, pressure, and temperature are the dependent variables. Neither phase is independently conserved, so there is only one continuity equation. However, one has in addition an energy equation, and the Clausius-Clapeyron equation.

As in the case of the Buckley-Leverett solutions, saturation shocks are obtained. A unique feature of the solutions is that depending on the boundary and initial conditions, there can be a variety of purely single phase regions imbedded in the flows. Unlike the Buckley-Leverett flows these regions may occur even when the boundary and initial conditions specify two-phase flow.

In the present work the similarity solutions of Romero and Nilson are extended to include a third phase that does not undergo phase change. The hope is that these solutions will be useful in the analysis of steam-flooding of oil fields.

The purpose of using steam-flooding as opposed to water-flooding in secondary and tertiary oil recovery is to raise the temperature of the oil, thereby lowering its viscosity, and enhancing its mobility. To model this effect, the temperature dependence on viscosity is included in the equations.

In order to reduce the equations to ordinary differential

equations by the use of a similarity variable, several factors important in an oil field must be ignored. In particular, no account can be taken of the effects of gravity, three dimensionality, or the finiteness of the oil field. Despite these limitations, it is felt that these solutions will still be useful. For the problem under consideration it is so difficult to do experiments, or to solve the full set of P.D.E.s, that very little is known about the basic structure of the flow. It is believed that the solutions in the following sections will serve as a guide to experimentalists, and builders of more general purpose P.D.E. codes, and possibly to oil reservoir engineers.

Figure 1
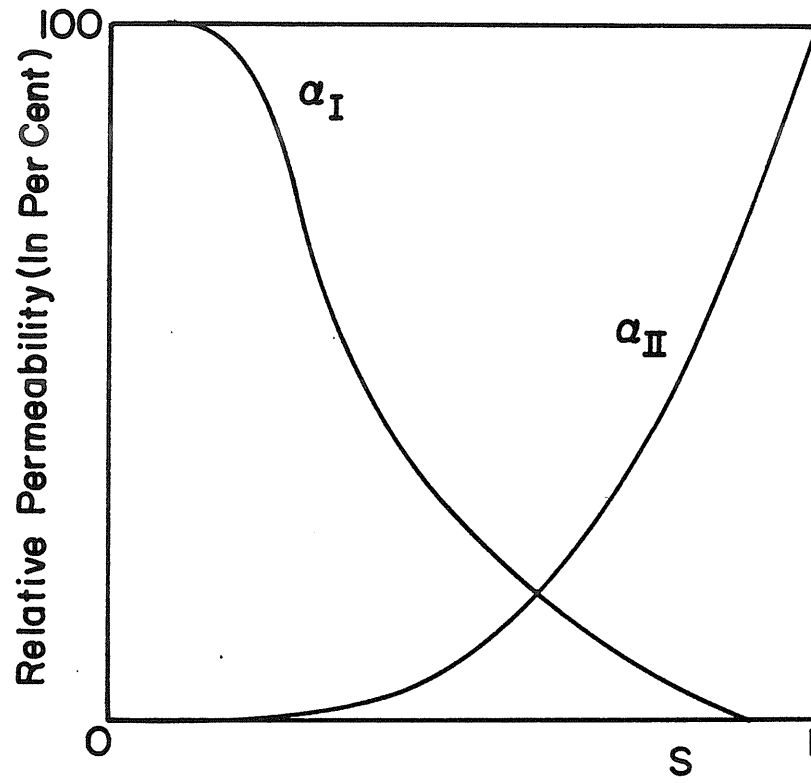
Relative Permeabilities For Typical
Gas Liquid Mixture

2) EQUATIONS OF THREE PHASE FLOW

In this section equations for flows containing oil, liquid water, and water vapor are derived. To describe such flows a second saturation function Z(x,t) is introduced. Z(x,t) is the volume fraction of pore space occupied by oil, (1-Z) is the volume fraction occupied by water in either its liquid or vapor form. Of the pore space occupied by water, S(x,t) denotes the fraction occupied by liquid, and (1-S) denotes the fraction occupied by vapor. By their definitions it is evident that 0<S<1, and 0<Z<1.

Oil, water, and energy must all be conserved. Below are the one dimensional conservation equations for these quantities in a porous medium.

4a) Oil

$$\frac{\partial}{\partial t}\left(\rho_o \, \epsilon \, Z\right) + \frac{\partial}{\partial x}\left(\rho_o \, u_o\right) = 0$$

b) Water

$$\frac{\partial}{\partial t}\left(\epsilon(1-Z)S\rho_\ell + \epsilon(1-Z)(1-S)\rho_v\right) + \frac{\partial}{\partial x}\left(\rho_\ell u_\ell + \rho_v u_v\right) = 0$$

c) Energy

$$\frac{\partial}{\partial t}\left(\epsilon Z\rho_o e_o + \epsilon(1-Z)S\rho_\ell e_\ell + \epsilon(1-Z)(1-S)\rho_v e_v + (1-\epsilon)\rho_s e_s\right)$$

$$+ \frac{\partial}{\partial x}\left(\rho_v h_v u_v + \rho_\ell h_\ell u_\ell + \rho_o h_o u_o\right) = 0$$

As is the case from now on, l, v, o, and s subscripts refer to liquid water, water vapor, oil, and the solid matrix (the porous medium itself). Also, from now on only one

dimensional flows are considered.

In equation 4) h_i (i=1,v,o,s) stand for the enthalpies per unit mass. These are assumed to be linear in T with slope c_i (i=1,v,o,s). The internal energies per unit mass are given by $e_i = h_i - P/\rho_i$.

No thermal conductivity or capillary pressure is included in the equations.

The water vapor is assumed to be ideal $\rho_v = \dfrac{P}{RT}$. A more realistic dependence could easily be used, but this is not felt to be essential. The water is assumed to be incompressible, and the oil density satisfies $(d\rho_o/dp)/\rho_o = \gamma$.

The oil viscosity is assumed to vary with temperature like $\dfrac{d\mu_o}{dT}\dfrac{1}{\mu_o} = \beta$. It is important to note that the inequalities $\mu_v < \mu_\ell < \mu_o$ will always be assumed to hold.

The velocities in equation 4) are given by the generalized form of Darcy's law (eq 2). To simplify the algebra, the relative permeabilities are taken to vary linearly with Z and S.

5)
$$U_\ell = -\alpha_\ell \frac{k}{\mu_\ell} \frac{\partial P}{\partial x} \qquad \alpha_\ell = (1-z)S$$

$$U_v = -\alpha_v \frac{k}{\mu_v} \frac{\partial P}{\partial x} \qquad \alpha_v = (1-z)(1-S)$$

$$U_o = -\alpha_o \frac{k}{\mu_o} \frac{\partial P}{\partial x} \qquad \alpha_o = z$$

In the case of two-phase condensing flows (where the algebra is less complicated), numerical tests were made that

showed that the flows with relative permeabilities varying linearly with S looked qualitatively the same as the flows where the permeabilities were chosen to better match experimental data. The flows were qualitatively the same in the sense that for both types of profiles the same sort of shocks and imbedded single phase regions occurred, and the dependence on the parameters of the flow were similar.

In regions with both phases of water present the pressure and temperature are constrained to lie on the Clausius-Clapeyron curve.

6a) T=Tsat(P) $\dfrac{dTsat}{dP} = \dfrac{V_{\ell v} Tsat}{h_{\ell v}}$ $h_{\ell v} = h_\ell - h_v < 0$ $V_{\ell v} = \dfrac{1}{\rho_\ell} - \dfrac{1}{\rho_v} < 0$

In regions with only one phase of water present the pressure and temperature are independent, but it is required that

6b) S=∅ and T>Tsat(P)

or

6c) S=1 and T<Tsat(P).

The above P.D.E.s cannot be classified as one of the standard types. In three-phase regions the equations are 4th order with S, Z, P, and P_κ being the independent variables (T is related directly to P by 6a)). In such regions there are 3 sets of characteristics. Two of these are as in a hyperbolic system, the third has dt/dx=∅, and is degenerate as in a parabolic system. More details on the characteristics may be found in appendix B.

In regions with S=1, or S=0, the temperature totally decouples from the other equations (it is a constant), one of the dependent variables drops out (S), and one of the hyperbolic type characteristics is no longer present.

In the following sections the problem to be analyzed is that of a semiinfinite region initially at uniform conditions, that at times t>0 is subjected to a new set of constant conditions at the plane wall x=0.

7)
$$S(o,t) = S_o \quad P(o,t) = P_o \quad \mathcal{z}(o,t) = \mathcal{z}_o \quad T(o,t) = T_o \quad t \geqslant o$$

$$S(x,o) = S_\infty \quad P(x,o) = P_\infty \quad \mathcal{z}(x,o) = \mathcal{z}_\infty \quad T(x,o) = T_\infty \quad x \geqslant o$$

In the above if 0<S<1, then T and P cannot be specified independently, but must lie on the Clausius-Clapeyron curve. Also, unless otherwise stated, it will be assumed that $P(0,t) > P(x,0)$.

3) <u>EQUATIONS</u> <u>IN</u> <u>THE</u> <u>SIMILARITY</u> <u>VARIABLE</u>

The equations and boundary conditions given by 4), 5), 6), and 7) are all invariant under the transformations $x \to \alpha x$, $t \to \alpha^2 t$. It follows that all quantities can be written as functions of a similarity variable $\theta = x/\sqrt{t}$. It should be noted that the particular assumptions on the forms of the enthalpies, densities, viscosities, and relative permeabilities are not necessary for obtaining a similarity solution.

When written in terms of the similarity variable, the system of P.D.E.'s reduces to the following set of O.D.E.'s

a) $\quad \dfrac{\theta}{2}\left(\epsilon \rho_o z\right)' + \left(\rho_o z \, P'\dfrac{k}{\mu_o}\right)' = 0$

8 b) $\quad \dfrac{\theta}{2}\left(\epsilon(1-z)s\rho_\ell + \epsilon(1-z)(1-s)\rho_v\right)'$

$\quad\quad + \left((1-z)s\rho_\ell P'\dfrac{k}{\mu_\ell} + (1-z)(1-s)\rho_v P'\dfrac{k}{\mu_v}\right)' = 0$

c) $\quad \dfrac{\theta}{2}\left(\epsilon(1-z)s\rho_\ell e_\ell + \epsilon(1-z)(1-s)\rho_v e_v + \epsilon z \rho_o e_o + (1-\epsilon)\rho_s e_s\right)$

$\quad\quad + \left(\rho_\ell(1-z)s h_\ell P'\dfrac{k}{\mu_\ell} + \rho_v(1-z)(1-s)h_v P'\dfrac{k}{\mu_v} + \rho_o z h_o \dfrac{k}{\mu_o}\right)' = 0$

Here the primes refer to derivatives with respect to θ. The boundary conditions 7) transform to

$\quad\quad S(0) = S_o \quad\quad P(0) = P_o \quad\quad z(0) = z_o \quad\quad T(0) = T_o$

9) $\quad S(\infty) = S_\infty \quad P(\infty) = P_\infty \quad z(\infty) = z_\infty \quad T(\infty) = T_\infty$

$\quad\quad T = T_{sat}(P) \quad$ unless $\quad s = 0$ or 1

The compressibility of the oil and the water vapor make it allowable to assign P at infinity rather than merely assigning P'. This is for basically the same reason as with

the case of a single homogeneous fluid flowing through a
porous medium. In such a case, assume that the density is
given by $\rho = Ae^{\gamma P}$, and that the boundary conditions admit the
use of a similarity variable. Using Darcy's law and the
equation of continuity one obtains

$$\frac{\theta}{2}\left(\epsilon \rho\right)' + \left(\frac{k \rho P'}{\mu}\right)' = 0$$

If the fluid is incompressible, the equation reduces to P''=0,
and it is obvious that one cannot specify P at infinity.
However, if the fluid is compressible, P'→0 as θ→∞. It is
thus legitimate to assign the value of P at infinity.

It should be emphasized that $P_0 > P_\infty$. It will soon be
shown that as a consequence of this P'<0 for all θ.

In regions with all 3 phases present it is convenient to
write the equations in matrix form.

$$A \begin{pmatrix} P'' \\ S' \\ z' \end{pmatrix} = \underset{\sim}{b}$$

10)

$$A = \begin{pmatrix} F_0 & 0 & z/\mu_0 \\ -\rho_\ell h_{\ell v} s F_\ell & \rho_\ell h_{\ell v}(1-z)F_\ell & s(1-z)\rho_\ell h_{\ell v}/\mu_\ell \\ -\rho_v h_{\ell v}(1-s)F_v & -\rho_v h_{\ell v}(1-z)F_v & (1-s)(1-z)\rho_v h_{\ell v}/\mu_v \end{pmatrix}$$

$$\underset{\sim}{b} = \begin{pmatrix} -\gamma P' z F_0 + z F_0 T'\beta \\ -T' F_H \\ T' F_H - \rho_v'(1-s)(1-z)F_v \end{pmatrix}$$

Here the following notations are introduced.

$$F_V = \frac{\theta}{2}\epsilon + \frac{kP'}{\mu_V} \qquad F_\ell = \frac{\theta}{2}\epsilon + \frac{kP'}{\mu_\ell} \qquad F_o = \frac{\theta}{2}\epsilon + \frac{kP'}{\mu_o}$$

$$F_H = \rho_\ell C_\ell S(1-z)F_\ell + \rho_V C_V(1-z)(1-s)F_V + \rho_o C_o z F_o + \frac{\theta}{2}\epsilon\rho_s C_s$$

The quantities F_V, F_ℓ, F_o, and F_H will be used frequently from now on. Their physical significance will be described in the next section. At the present it is important to note that due to the inequalities $\mu_V < \mu_\ell < \mu_o$ and $P' < 0$, $F_V < F_\ell < F_o$.

From equation 10) it can be seen that P' always has the same sign unless some sort of degeneracy exists in the equations. This is because if it ever passed through zero, the vector $\underset{\sim}{b}$ would vanish. This is because P and T are related by the Clausius-Clapeyron, so if P'=0, then T' and ρ'_V both also vanish. As a consequence of this P'', S', and Z' would vanish. Assuming the solutions are unique, this would imply that all the variables S, Z, and P were constant throughout the whole flow. The numerics were never found to contradict the fact that P' is always the same sign. Except for the solutions in section 10, it will always be so that $P_\infty < P_o$, so P' is less than zero.

The determinant of A turns out to be a significant quantity. After factoring out $\rho_\ell \rho_V h_{\ell V}^2 (1-z)$ it is given by

11)

$$\det A = (1-s)(1-z)\frac{F_\ell F_o}{\mu_V} + (1-z)s\frac{F_V F_o}{\mu_\ell} + z\frac{F_\ell F_V}{\mu_o}$$

In regions with only one phase of water present the energy equation reduces to

12a) $$T' = 0$$

In such a region the oil continuity equation is the same as in the three phase case, but the water continuity equation simplifies to

12b) $$-z'F_\ell + \frac{(1-z)P''}{\mu_\ell} = 0 \qquad \text{for } S = 1$$

or

c) $$-z'F_v + \frac{(1-z)P''}{\mu_v} = -\rho_v'F_v(1-z) \qquad \text{for } S = 0$$

In the actual steam-flooding of an oil field the field would most likely initially be subcooled. That is $S_\infty = 1$ T_∞ <$Tsat(P_\infty)$. Despite this, the case with $S_\infty < 1$ will first be analyzed. After seeing the variety of solutions available for these initial conditions the more realistic case with $S_\infty = 1$ will be considered. There are several reasons for analyzing the case with $S_\infty < 1$ first. The simplest solutions satisfy this condition, and confidence in the other solutions is obtained when one sees how the various regimes of flow evolve into each other as one varies the boundary conditions. Also, when $S_\infty < 1$ there are several interesting regimes of flow which do not occur in the similarity solutions with $S_\infty = 1$; and it is possible that these regimes might occur when less restrictive boundary conditions are used that do not lead to similarity solutons.

With these remarks in mind, assume that equations 8) and boundary conditions 9) hold with $S_\infty < 1$. Also assume that no superheated (S=0) or subcooled regions (S=1) exist in the flow

(later it will be seen for what boundary conditions this is in fact true). As with the case of two-phase flow (ref 5) one can obtain information about the structure of the flow by comparing the order of the equations with the number of boundary conditions, and also by examining detA. There are two indications that 2 shocks must be present in the flow.

1) Equation 8) is a 4th order equation with 6 independent boundary conditions.

One knows S, Z, and P at $\theta=0$. By just adjusting P'(0) one cannot satisfy all 3 boundary conditions at $\theta=\infty$. If one puts two shocks in the flow the position of these shocks may be treated as extra shooting parameters. These may be adjusted along with P'(0) so that all 3 conditions at $\theta=\infty$ are satisfied.

2) Note that at $\theta=0$ F_v, F_ρ, and F_ω are all negative, but at $\theta=\infty$ they are all positive. From looking at equation 11) it is easy to see that at $\theta=0$ and∞, detA>0. There must be a point at which $F_\rho=0$. At this point equation 11) easily yields detA<0. If no shocks were present in the flow detA would have to pass through at least 2 zeroes as θ went from 0 to∞. The equations would thus pass through two singularities. The possibility of doing this in a continuous fashion was examined and found not to be feasible. To have such continuous solutions be feasible, it would be necessary that whenever the determinant of A vanished, the vector $\underset{\sim}{b}$ was automatically in the range of A. This does not in fact happen. The conclusion

is that shocks must be present in order to jump over the zeroes of detA. Consideration of the problem shows that the singularities must be jumped over one at a time (appendix A), so that two shocks must be present.

4) SHOCK CONDITIONS

By equating fluxes of oil, water, energy, and momentum on both sides of a shock moving with velocity U, one obtains the following jump conditions.

a) $\quad \epsilon U [\rho_o z] + [\rho_o z \frac{k P_x}{\mu_o}] = 0$

13) b) $\quad \epsilon U [\rho_\ell (1-z) s + \rho_v (1-z)(1-s)] + [\rho_\ell (1-z) s \frac{k P_x}{\mu_\ell} + \rho_v (1-z)(1-s) \frac{k P_x}{\mu_v}] = 0$

c) $\quad U [\epsilon \rho_\ell (1-z) s e_\ell + \epsilon \rho_v (1-z)(1-s) e_v + \epsilon \rho_o z e_o + (1-\epsilon) \rho_s e_s]$

$\quad + [\rho_\ell h_\ell k \frac{P_x}{\mu_\ell} (1-z) s + \rho_v h_v k \frac{P_x}{\mu_v} (1-z)(1-s) + \rho_o h_o k \frac{P_x}{\mu_o} z] = 0$

d) $\quad [P] = 0$

The continuity of pressure across a shock is consistent with the fact that the equations of flow through porous media describe low Reynolds flow. This condition is usually used at the interface of two fluids in a porous medium, and is also used at the Buckley-Leverett shock described in section 1.

In the similarity variable if the shock occurs at $\theta = \theta_s$, then the position of the shock is x $= \theta_s \sqrt{t}$. The velocity is thus $u_s = \frac{\theta_s}{2\sqrt{t}}$. Also, $P_x = \frac{1}{\sqrt{t}} \frac{dP}{d\theta}$. Using these relations one obtains the shock conditions in terms of the similarity variable.

14) a) $\quad [\rho_o z F_o] = 0$

b) $\quad [\rho_\ell (1-z) s F_\ell + \rho_v (1-z)(1-s) F_v] = 0$

and after a little manipulation,

c) $\quad [T] F_H + \hat{h}_{\ell v} [\rho_v (1-z)(1-s) F_v] = 0$

d) $\quad [P] = 0$

Here the hat on $\hat{h}_{\ell v}$ indicates that it is to be evaluated on the opposite side of the shock as the quantities in F_H. The formula is true no matter on which side of the shock $\hat{h}_{\ell v}$ is evaluated provided it is a different side than the quantities in F_H.

Note that $F_\ell = \frac{1}{\sqrt{t}} \left(\epsilon v + \frac{k P_x}{\mu_\ell} \right)$, so except for the factor $\frac{1}{\sqrt{t}}$ F_ℓ measures the flux of liquid relative to the point $x = \theta \sqrt{t}$. Similarly F_v, F_o, and F_H measure the fluxes of vapor, oil, and heat relative to $x = \theta \sqrt{t}$.

If $[T] \neq 0$ certain inequalities on F_H must be satisfied. These can be derived by including a thermal conductivity term in the energy equation and looking at the behavior as this term approaches zero. When thermal conductivity is included the energy equation 8c) has a term involving $T_{\theta\theta}$. When this term is included, the jump in T is replaced by a region with large gradients in T. Note that there are no large gradients in P since $[P] = 0$, so all large gradients in T must occur in a region where T and P are not related by the Clausius-Clapeyron equation. That is, in a region where $S = 0$ or 1. In such a region the energy equation including thermal conductivity is

15) $\quad K_T T'' + T' F_H = 0 \qquad 1 \gg K_T > 0$

It can easily be seen that if T is to have boundary layer type

behavior, it is necessary that

16 a) $F_H > 0$ if the boundary layer (jump in T) occurs on the

   L.H.S. of the region with S=0,or 1.

   b) $F_H < 0$ if the boundary layer occurs on the R.H.S. of the

   region with S=0, or 1.

   In reference 5) the relations 16ab) were derived by
requiring that the jump in entropy be positive in crossing a
shock.

   It should be noted that for the case of a shock where
both sides have $0 < S < 1$,   [T]=0 since [P]=0, and the pressure
and temperature are related by the Clausius-Clapeyron
equation.

5) FLOWS WITH TWO SHOCKS

The simplest flows to analyze are those that contain no imbedded regions with S identically 0 or 1. In this case P and T are always related by the Clausius-Clapeyron equation. It will be seen that provided P_∞/P_o and S_o are not too small, and S_∞ and Z_∞ are not too large, these simple flows are the ones that occur.

In this case the jump conditions 14) reduce to

17) $[zF_o]=[(1-Z)(1-S)F_v]=[(1-Z)SF_\ell]=[P]=[T]=0$

The following simple identity is used frequently.

$[AB]=[A]B+\hat{A}[B]$

Here the hat on $\hat{A}$ indicates that it is to be evaluated on a different side of the shock than the term B multiplying [A].

Using this identity the jump conditions may be written (the hatted quantities have the same meaning as above)

17')
$$[z]F_o \quad + \quad [s]\cdot 0 \quad + \quad [P']\,\hat{z}/\mu_o \quad = 0$$
$$-[z]\hat{S}F_\ell \quad + \quad [s](1-\hat{z})F_\ell \quad + \quad [P']\hat{S}(1-\hat{z})/\mu_\ell = 0$$
$$-[z](1-\hat{S})F_v \quad + \quad [s]F_v(1-\hat{z}) \quad + \quad \frac{(1-\hat{z})(1-\hat{S})[P']}{\mu_v} = 0$$

In order for this system to have nontrivial solutions the determinant must vanish, so

18) $\quad \dfrac{F_o F_\ell}{\mu_v}(1-\hat{z})(1-\hat{S})+F_o F_v(1-\hat{z})\dfrac{\hat{S}}{\mu_\ell} + F_\ell F_v\dfrac{\hat{z}}{\mu_o} = 0$

If in the above formula $\hat{S}$ and $\hat{Z}$ were replaced by S and Z,

the left hand side would be identical to detA in equation 11).
Equation 18) proves to be useful in determining the signs of
[Z], [S], [P'], and also in determining necessary and
sufficient conditions for detA to change sign in crossing
shocks (appendices A and B).

In order to integrate the equations from $\theta=0$ to $\theta=\infty$
without encountering any singularities (having detA=0), F_ϱ, F_V,
and F_σ must have certain signs at the two shocks. At the
first shock, $F_V<0$ and $F_\varrho<0$. An examination of equation 11)
shows that if this were not so, detA would have already
changed sign, and the equations would have passed through a
singularity. Also, at the first shock $F_\sigma>0$. It can be shown
(appendix A) that this (along with $F_V<0$, and $F_\varrho<0$) is a
necessary and sufficient condition for detA to change sign in
crossing the first shock. As mentioned in section 3, detA
must change sign at a shock in order to avoid later having to
pass through a singularity. The above can also be shown to be
necessary and sufficient conditions for the characteristics on
the left to be overtaking those on the right (appendix B).
This condition should be satisfied in order to have the shocks
be meaningful in terms of the original P.D.E.s.

At the second shock it is necessary that $F_V<0$, otherwise
by similar arguments as above one can show that detA would
have passed through zero. To have detA change sign at the
shock, and have the characteristics overlapping it is also
required that $F_\varrho>0$ (appendices A and B).

Given values S_1, Z_1, and P_1' on the L.H.S. of the shock satisfying $0 < S_1 < 1$, $0 < Z_1 < 1$ it is not clear that the jump conditions 17) yield unique solutions S_2, Z_2 and P_2' on the R.H.S. satisfying $0 < S_2 < 1$, $0 < Z_2 < 1$. By eliminating S_2 and P_2' from equations 17) one arrives at a quadratic equation for Z_2.

19)
$$A Z_2^2 + B Z_2 + C = 0$$

$$A = \mu_0 \left(\frac{1}{\mu_v} - \frac{1}{\mu_0} \right) \left(\frac{1}{\mu_0} - \frac{1}{\mu_\ell} \right) \left(\frac{\theta}{2} \epsilon \right)^2$$

$$B = \frac{\theta}{2} \epsilon F_0 \left(\frac{\mu_0}{\mu_\ell \mu_v} (1 + Z) - \frac{1}{\mu_v} + \frac{S(1-Z)}{\mu_v} - \frac{Z}{\mu_0} - \frac{S(1-Z)}{\mu_\ell} \right)$$

$$C = -\frac{Z \mu_0 F_0}{\mu_\ell \mu_v}$$

One can however show that the conditions on F_ℓ, F_v and F_0 that insure that detA changes are also necessary and sufficient conditions for 19) to have a unique solution $0 < Z_2 < 1$, that in combination with the other equations in 17) yield $0 < S_2 < 1$ (appendix C).

To summarize, if at the first shock $F_v < F_\ell < 0$, and $F_0 > 0$, and at the second shock $F_v < 0$, $F_0 > F_\ell > 0$, then:

1) There is one and only one solution to the system 17) satisfying $0 < S_2 < 1$, $0 < Z_2 < 1$.

2) Other than the trivial characteristic $dt/dx = 0$, the partial differential equations have 2 families of characteristics. At both shocks the characteristics on the left are overtaking those on the right.

3) At both shocks detA changes sign. After the second shock

the equations may be integrated out to infinity without encountering any singularities.

4) It can be shown (appendix A) that $[P'] > 0$ at both shocks. In sections 12 and 13 it will be seen that this gives at least some indication that the shocks are stable to 3 dimensional disturbances.

5) In appendix A it is also shown that $[Z] < 0$ at both shocks. At the first shock $[S] > 0$, at the second $[S] < 0$.

In the flow of oil and noncondensing water there is a shock, the Buckley- Leverett shock. In a two-phase condensing flow there is a shock with $[S] < 0$ at which $F_V < 0$, and $F_\ell > 0$. Due to the signs of $[S]$, F_ℓ, and F_V at the two shocks it is reasonable to call the first shock a Buckley-Leverett shock, and the second shock a condensation shock.

The equations and jump conditions were solved numerically for a variety of parameters. The values of S, Z, and P were given at $\theta = 0$, then $P'(0)$, θ_1, and θ_2 (the values of θ at the two shocks) were adjusted using Newton's method until $S(\infty)$, $Z(\infty)$, and $P(\infty)$ were equal to their prescribed values. An Adams-Bashforth predictor corrector code obtained from the Sandia Laboratories math library was used to integrate the equations. Rather than integrating out to infinity, the equations were integrated out to a large but finite value of θ (usually $\theta = 2$ was adequate). The Jacobian was evaluated by differentiating both the differential equations and the shock conditions with respect to the parameters $P'(0)$, θ_1, and θ_2;

and solving the resulting equations along with the equations for P, S, and Z. Figure 2 shows some sample solutions for various values of P_∞ with the other parameters held fixed. Except for the values of P_∞ and T_∞ the physical parameters were chosen to be typical of a real oil field (ref 6).

Similar to the case of two-phase condensing flow one finds that if one keeps all parameters fixed and lowers P_∞/P_0, the value of S on the L.H.S. of the second shock increases. If one lowers P_∞/P_0 far enough one finds that at the second shock S eventually equals 1. Lowering P_∞ further causes the solutions to have regions with S>1, which is not allowed physically. The only way out is to introduce a region which will be called a liquid slug where S=1, and T<Tsat(P). This will be done in the next section.

Before doing this it should be mentioned what effects varying the other boundary conditions other than P_∞ has on whether or not a slug develops. If one keeps all other parameters fixed one finds that

1) if one raises Z_∞ enough a slug will develop

2) if one raises S_∞ enough a slug will develop

3) lowering Z_0 helps a slug to develop, but for many values of the parameters it can be lowered to 0 without a slug developing

4) raising S_0 helps a slug to develop, but it can be raised to 1 without a slug developing.
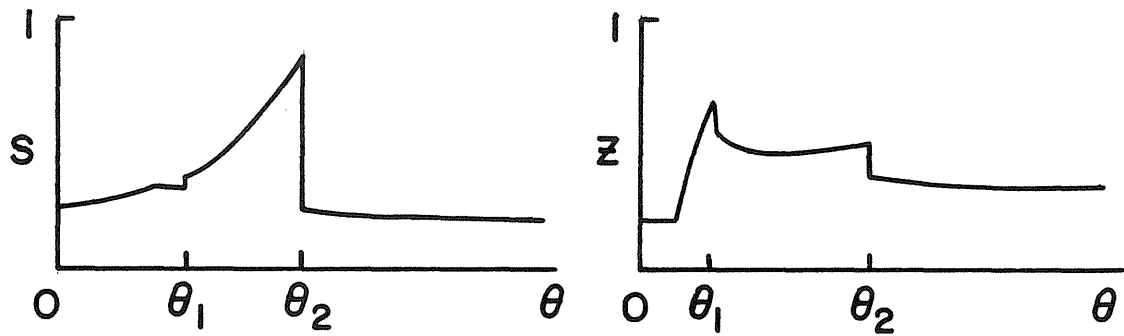
$$P_\infty/P_0 = .996$$
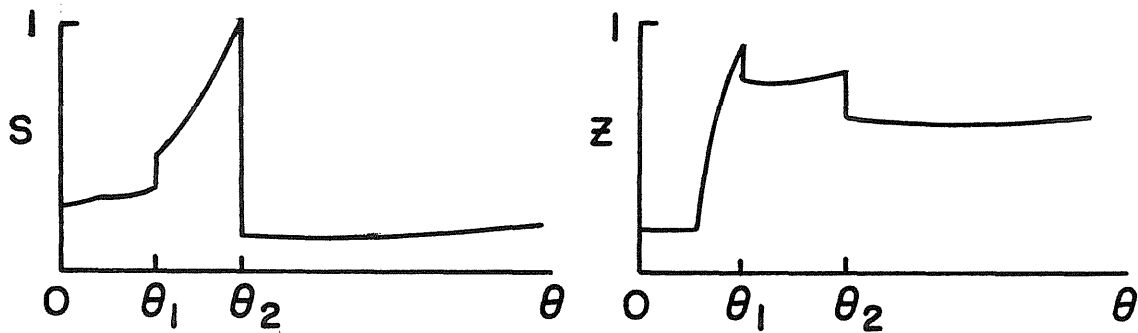
$$P_\infty/P_0 = .995$$

Figure 2

Typical profiles described in section 5. As one lowers p_∞/p_0 the saturation profile S eventually reaches 1 just before the second shock.

6) LIQUID SLUG

On entering into a region containing a liquid slug there must be a jump in both temperature and saturation. The reason for this is that inside the slug T'=∅ (equation 12a), but dTsat(P(θ))/dθ<∅ (since P'<∅). If there was no jump in temperature, the temperature inside the slug would immediately rise above the saturation temperature as θ increased. This is the opposite of what should occur in a liquid slug. The conclusion is that on jumping into the slug [T]<∅, hence from 14) it can be seen that [S], [Z], and [P'] are all nonzero.

A jump in temperature on the right hand side of the slug must be ruled out. The reason is that 16a) requires F_H >∅ on the L.H.S., but dF_H/dθ >∅, so that F_H >∅ on the right hand side of the slug. Since this is so 16b) rules out a jump in temperature. The fact that dF_H/dθ >∅ can be seen by plugging S=1 into 8a and b)

$$\frac{d}{d\theta}\left(\rho_o \, z \, F_o\right) = \frac{\epsilon}{2} \rho_o \, z$$

$$\frac{d}{d\theta}\left(\rho_\ell (1-z) F_\ell\right) = \rho_\ell \frac{\epsilon}{2}(1-z)$$

so that

$$\frac{d}{d\theta} F_H = \frac{\epsilon}{2}(1-z)\rho_\ell C_\ell + \frac{\epsilon}{2} z \rho_o C_o + (1-\epsilon)\rho_s C_s > 0$$

On moving out of the slug there must still be a jump in the saturations and the pressure gradient. Otherwise one would always have a region where S~1 just to the right of the

slug. Since this is not the case for flows without a slug, there would have to be discontinuous dependence on initial data. This argument is similar to the one used in reference 5.

Attention should be called to a certain detail in solving the jump conditions 14) to find the values T_2, Z_2, and P_2' on the right hand side of the jump into the slug. Using 14c) alone one can solve for T_2. By eliminating P_2' from 14a) and b) one gets a quadratic equation for Z_2.

$$20) \quad \rho_\ell \frac{\theta}{2} \epsilon \left(\mu_{o2} - \mu_\ell \right) \dot{z}_2 (\dot{z}_2 - 1) + \rho_\ell (1 - \dot{z}_2) \dot{z} F_o \mu_{o2} - \dot{z}_2 \mu_\ell \left(\rho_\ell s F_\ell + \rho_v (1-s) F_v \right) = 0$$

$$\mu_{o2} = \mu_o (T_2)$$

In general there may be more than one solution to this equation satisfying $0 < Z_2 < 1$. The fact that two solutions may exist will in fact be useful in the next section. However, when the slug first forms, there is one and only one valid solution to 20). This is because in this case, due to continuous dependence on initial data, one has $S \sim 1$ immediatley to the left of the shock into the slug. When this condition is satisfied, it can be shown (appendix D) that 20) has one solution with $0 < Z_2 < 1$, and one with $Z_2 > 1$. As the slug widens the second root may come to satisfy $0 < Z_2 < 1$, but by continuous dependence on data one continues using the same branch. Ambiguity would arise only if the two roots were to coincide. Numerically this was not found to occur.

Now that the basic structure of the flow is known, the equations may be integrated numerically. One uses $P'(0)$, θ,

,and θ_2 as the shooting parameters. Here θ_1 is the position of the first shock, and θ_2 is the position of the shock into the slug. Note that once P', θ_1 , and θ_2 are given, the position of the shock out of the slug is not arbitrary. This shock must occur at the point where T=Tsat(P).

Figure 3) shows some profiles for this regime of flow. As one raises P_∞ the slug grows narrower, and the jumps of S and T as they enter the slug grow smaller. The flow merges continuously into the flows without a slug. As one lowers P_∞ the first shock (Buckley-Leverett) gets closer to the shock into the slug. Eventually it catches up with it. At this point two possibilities exist.

1) The two shocks are replaced by a single shock.

2) The Buckley-leverett shock occurs inside the slug instead of before the slug.

If the first possibility occurs, one of the shooting parameters will no longer be available. A boundary condition would have to be dropped. If this were the case one would expect to see a type change of the equations or a characteristic qualitatively changing the way it transmits data. There is no evidence of either of these, so the conclusion is that the second possibility is the correct one.

Figure 3
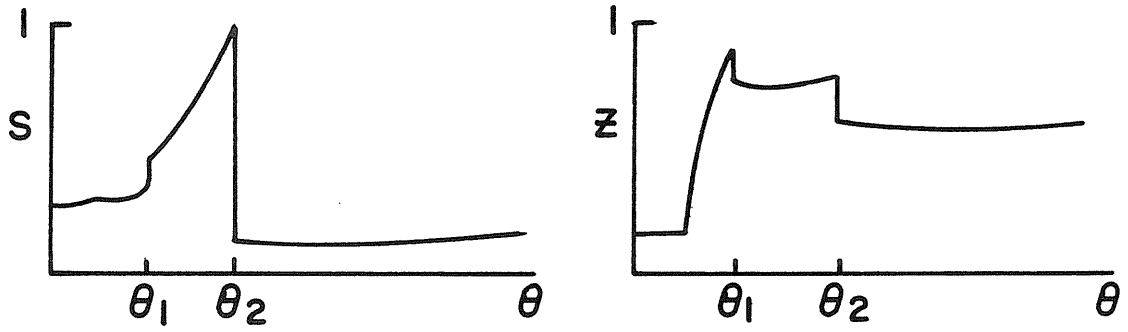
$P_\infty/P_0 = .995$
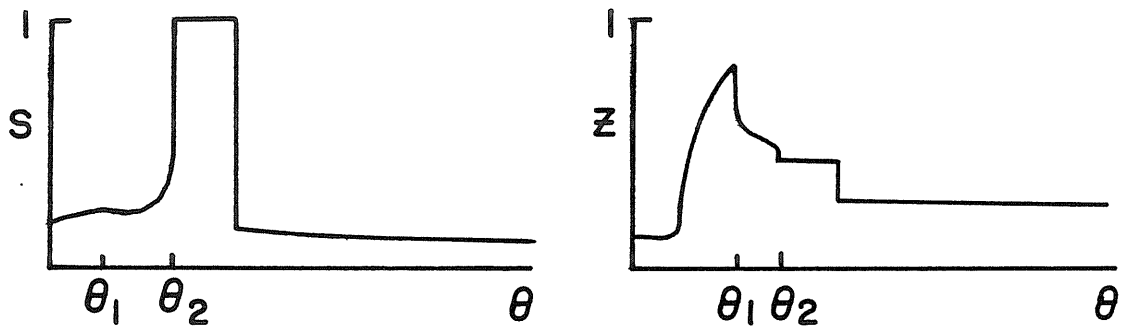
$P_\infty/P_0 = .994$
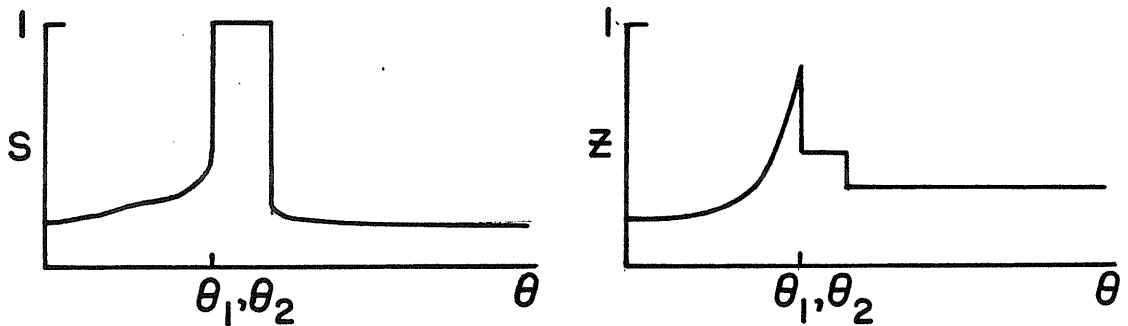
$P_\infty/P_0 = .993$

Typical profiles described in section 6. At first the width of the slug is infinitesimally small. As one lowers p_∞/p_0, the slug widens, and θ_1 approaches θ_2. Eventually θ_1 catches up with θ_2.

7) BUCKLEY LEVERETT SHOCK INSIDE SLUG

As just described, when one lowers P_∞ eventually the Buckley-Leverett shock passes the shock into the slug. At the precise value of P_∞ such that the two shocks coincide, one uses either of two methods to solve the equations. To have continuous dependence on data one must obtain the same results whether,

A) One first has a shock with $[T]=o$, followed by a shock with $[T]<\emptyset$ into the slug. On jumping into the slug one uses the same root of equation 2$\emptyset$) as before the Buckley-Leverett shock catches up. This is the method one would use immediately before the shock catches up with the slug.

B) One first does a shock into the slug with $[T]\neq\emptyset$, followed by a shock with $[T]=\emptyset$. This is the method one would use immediately after the Buckley-Leverett shock passes into the slug.

It is simple to show that for case B one jumps first to one root $z_2^{\prime}$ of 2$\emptyset$) then to a different root z_2^{2} of 2$\emptyset$). After passing through both shocks one must end up with the same value of Z_2 as one does in A. In order for this to happen z_2^{2} must be the same as Z_2 in A, so $z_2^{\prime}$ is on a different branch than Z_2 in A.

To have this transition between the two regions occur, it is necessary that two roots of 2$\emptyset$) be available with $\emptyset<Z_2<1$. It can be shown that at the point where the two shocks merge, two such roots always are available (appendix B).

Figure 4) gives examples of some of these flows. As one

raises P_∞ the butte of high saturation grows thinner until it disappears. It grows continuously into the flows described earlier. However, at the point where the butte vanishes there is an infinitesimal strip where the saturation jumps up and then right back down. One would be surprised to see an infinitesimally small zone of high saturation in a real flow. However, it should be noted that when the strip gets very thin one finds numerically that [P']<0 on entering the slug. In sections 12 and 13 this will be shown to be an indication of instability. As one continues to lower P_∞ the butte of high saturation widens, and [P'] eventually becomes positive indicating that the flow has stabilized.

If the compressibility of the oil is set to zero (the compressible case will be discussed later), one finds that as one lowers P_∞ further the shock inside the slug grows weaker and at the shock detA starts approaching 0. Eventually there is a value of P_∞ such that at the shock [Z]=[P']=detA=0. If one continues to solve the equations as before, one finds that the solutions are defective in several ways.

First, the solutions pass through a singularity. They can do this without blowing up due to the homogeneous nature of the equations inside the slug.

21)
$$A^* \begin{pmatrix} P'' \\ z' \end{pmatrix} = 0 \qquad A^* = \begin{pmatrix} F_o & z/\mu_o \\ -F_\ell & (1-z)/\mu_\ell \end{pmatrix}$$

$$\det A^* = \frac{1-z}{\mu_\ell} F_o + \frac{z F_\ell}{\mu_o}$$

However, if even a small compressibility for the oil was included, the equations could not be integrated through detA=∅ since 21) would in this case have a nonzero right-hand side. Because of this the validity of the solutions must be doubted.

Second, if one looks at the characteristics of these solutions (in a manner almost identical to that in Appendix B) one finds that they do not overlap as they should at the jump inside the slug. The conclusion is that one cannot continue to integrate the solutions and have a shock inside the slug.

At this point either a boundary condition must be dropped, or a new shooting parameter must be found. For the same reason as in the last section it is not plausible to drop a boundary condition. In the next section it will be explained that the new shooting parameter is essentially the width of an expansion fan.

Figure 4
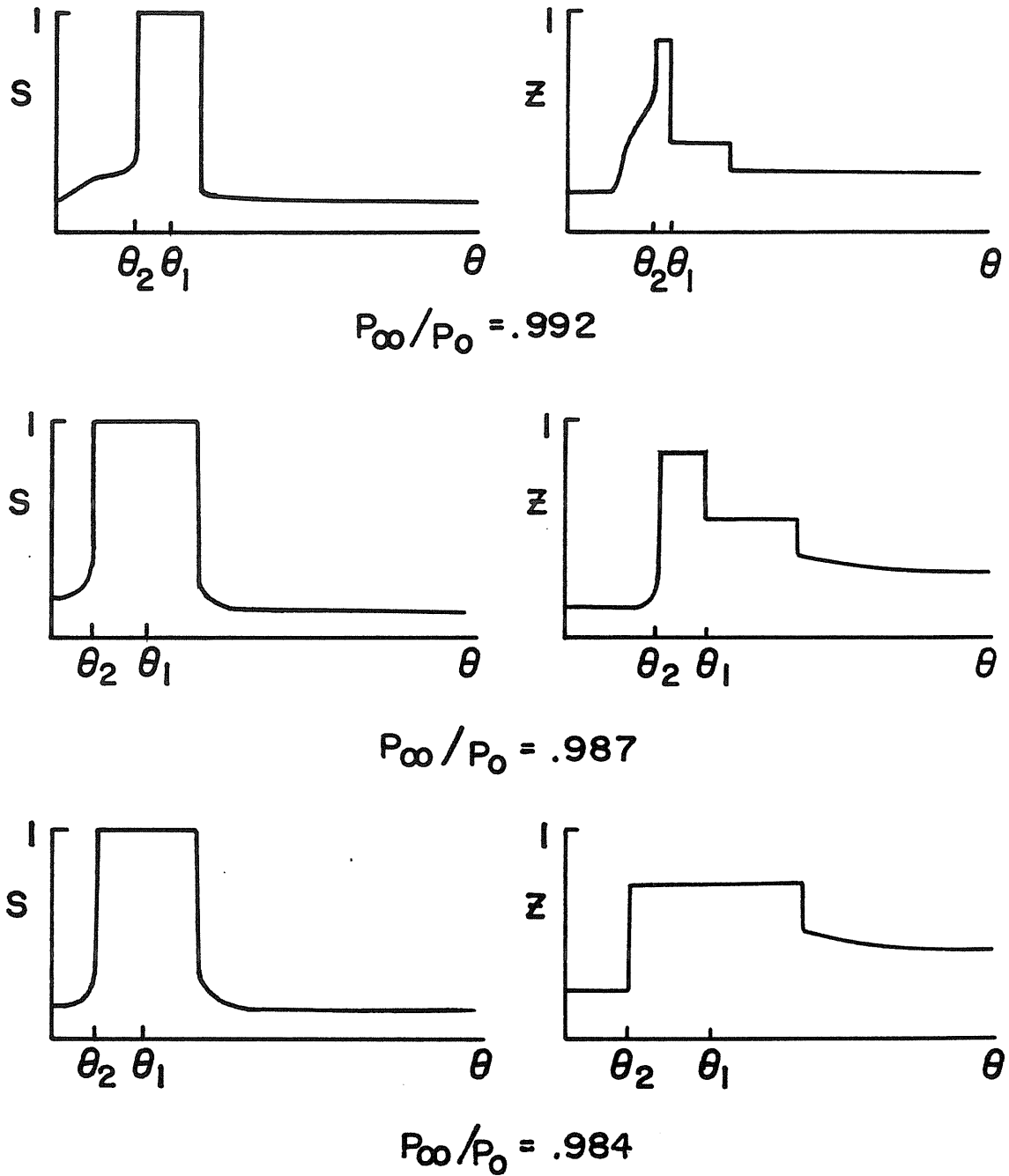
Typical profiles described in section 7. At first there is a very thin region where the oil saturation jumps up, and then right back down. As one lowers p_∞/p_0 this region widens, and the second jump grows smaller until it eventually disappears.

8) EXPANSION FAN INSIDE SLUG

There are two possible solutions to equation 21. One solution has $P''=Z'=\emptyset$. The other has nonzero values for Z' and P'', but has $\det A(\theta)=\emptyset$. When the slug first forms there is no doubt that $Z'=P''=\emptyset$ is the correct choice since $\det A \neq \emptyset$. However, as was seen in the last section, as one lowers P_∞ one reaches a point where $\det A=\emptyset$ at a point in the flow, and the shock inside the slug has disappeared. At this point one can introduce a singular subinterval where $\det A=\emptyset$. The length of this subinterval may be used to replace the location of the shock as a shooting parameter.

As in Appendix B it can be shown that at points θ where $\det A(\theta)=\emptyset$, $x=\theta\sqrt{t}$ is a characteristic. In the (x,t) plane this singular subinterval is bounded by two diverging characteristics. It is a type of expansion fan.

In figure 5 are some examples of flows with this expansion fan. After the expansion fan has been introduced one may lower P_∞ arbitrarily without introducing any new regimes of flow. By adjusting the other boundary conditions no new regimes of flow are encountered except for various types of superheated regions at the left-hand side of the flow. These regions are almost identical to those in reference 5.

If the oil is compressible the above expansion fan cannot occur. In this case equation 21) would have a nonzero R.H.S.. The solution with $\det A=\emptyset$ on a finite interval is no longer

feasible. Fortunately, in this case the problem of the shock disappearing and the equations becoming singular is found not to occur. For a small oil compressibility detA is small but nonzero over a finite interval. As the compressibility goes to zero these results are consistent with the results containing an expansion fan. It should be remarked that in these regimes where detA is a small over a finite interval it can be quite difficult to integrate the equations. In particular if one is using a continuation method to input initial guesses to Newton's method, one can use very much larger continuation steps if one ignores compressibility and introduces an expansion fan.
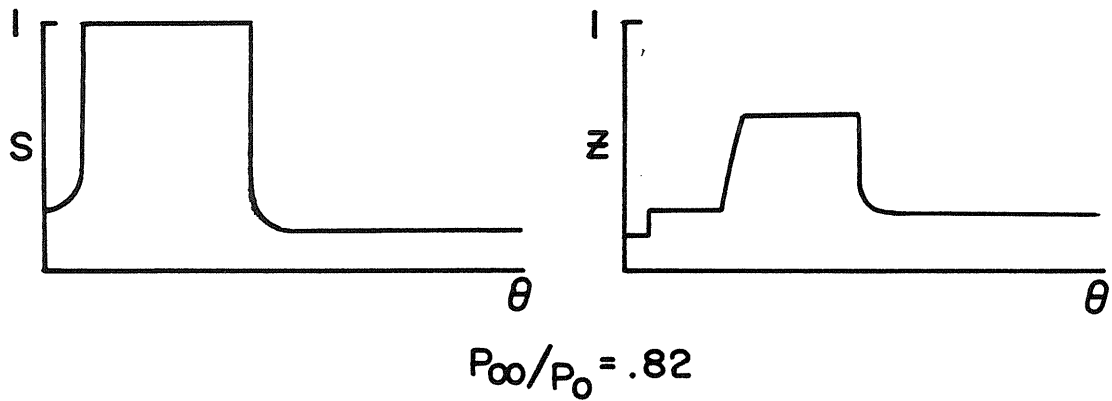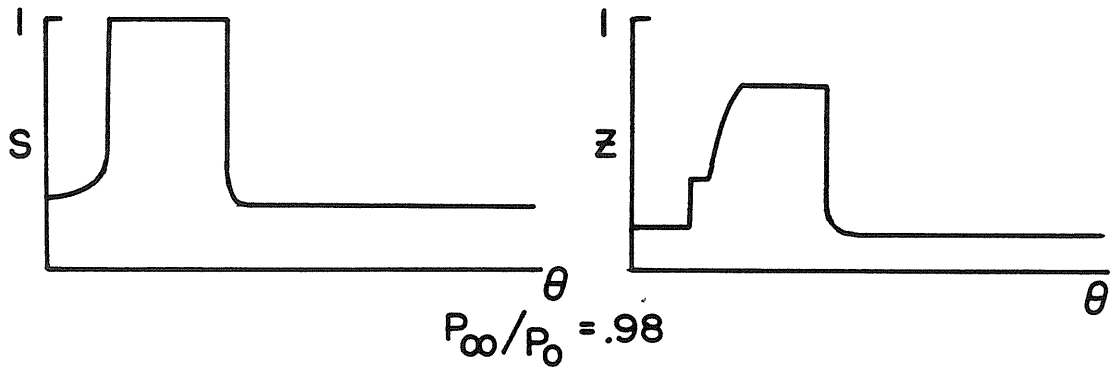
Figure 5

Typical profiles described in section 8. Expansion fan occurs inside liquid slug. As one lowers p_∞/p_0 further no new difficulties are encountered.

9) INITIALLY SUBCOOLED FIELD

As has already been mentioned, in a real oil field the initial conditions would satisfy T<Tsat and S=1. In terms of the solutions already obtained this means that after jumping into the slug the fluid remains subcooled all the way out to infinity. If the oil was incompressible this would mean that P''=0 in the slug, so P' would not approach zero automatically as $\theta \to \infty$. Thus, specifying P at ∞ would really be specifying two conditions, $P'(\infty)=0$, and $P(\infty)=P_\infty$. The similarity solutions could not be solved in this case.

If compressibility is included in the equations $P' \to 0$ as $\theta \to \infty$, and the above problem does not arise. It was with this problem in mind that compressibility was originally included in the equations.

When somewhat realistic data for an oil field are used, the flows look quite simple. The regime that occurs is the one with a Buckley-Leverett shock inside the slug. It appears that the pressure ratio P_∞/P_0 must be very close to unity (not realistic of a real oil field) in order for the Buckley-Leverett shock to occur before the saturation shock. In figure 6 are a variety of these flows for different values of S_0.

Figure 6
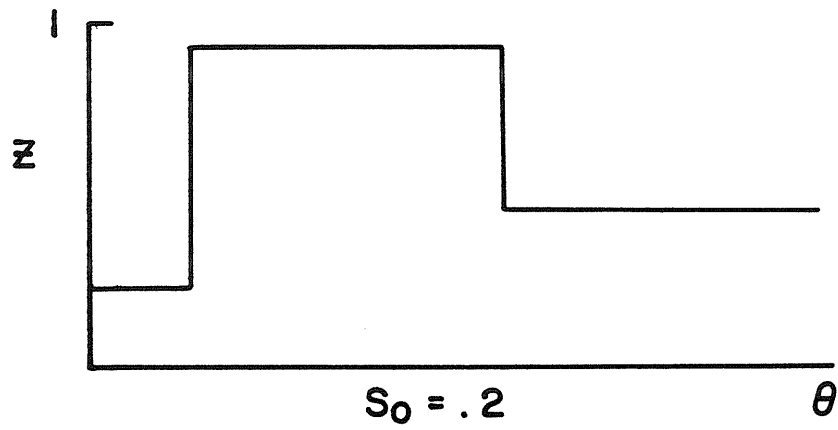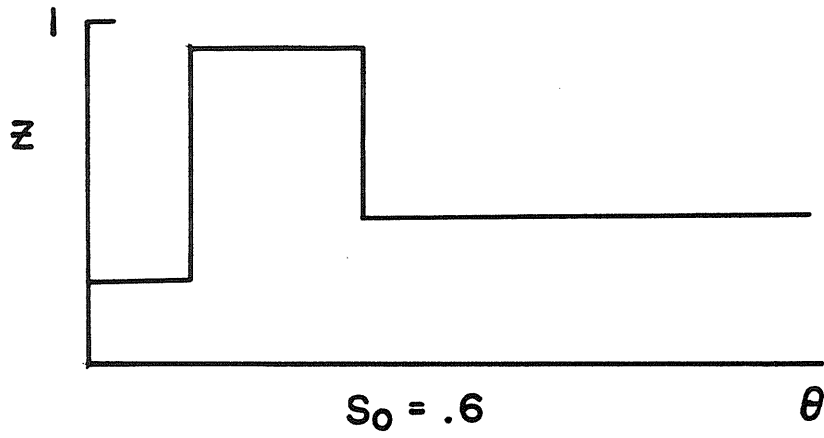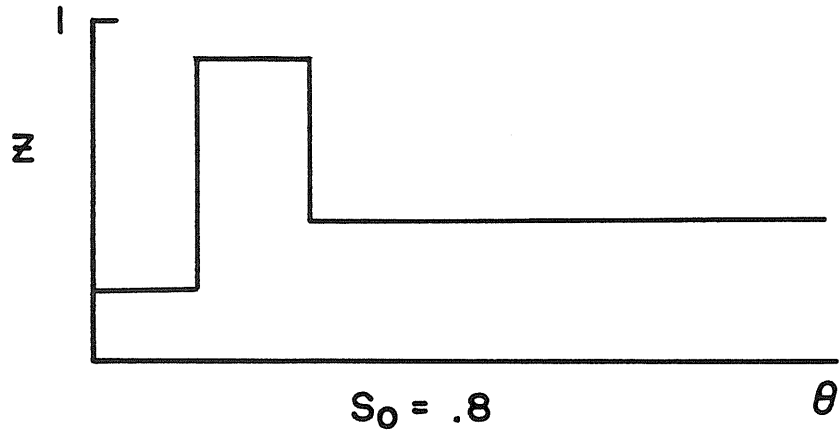
Oil saturation profiles for an initially subcooled field.
Note that lowering S_0 widens the region of high z saturation.

10) FLOWS WITHOUT SHOCKS

It should be mentioned what happens when the injection pressure P_0 is less than the initial pressure P_∞. In this case $P'(\theta) > 0$, so F_ρ, F_v, and F_o are always positive. If one looks at detA it is easy to see that in this case there is no reason to pass through any singularities as θ increases from 0 to ∞. This is evidence that no shocks are needed in the flow.

When one examines the two sets of characteristics of the P.D.E.'s one finds that the characteristics emerging from the line $t=0$ intersect the line $x=0$ if $P_0 < P_\infty$. For the previously analyzed case of $P_0 > P_\infty$ these characteristics pointed inwards and did not intersect $x=0$. Because of this, two conditions at $x=0$ must be dropped.

The above facts indicate that if $P_0 < P_\infty$, two shooting parameters are lost, but two boundary conditions are dropped, so everything still adds up properly.

It makes a certain amount of physical sense that when $P_0 < P_\infty$ the saturations Z_0 and S_0 cannot be specified. If at $x=0$ one forces material into the medium at high pressure, it is reasonable to expect that one is free to control what one puts in. However, if one lets material out of the medium by exposing it to a low pressure $P_0 < P_\infty$ at $x=0$, it is reasonable to expect that one has little control of what comes out.

Solutions for these unshocked flows were computed. In the compressed flows ($P_0 > P_\infty$), as P_0 is increased a liquid slug develops in the interior. In these flows, as P_0 is

decreased, a superheated steam region develops near $\theta = 0$.

These expansion flows will not be analyzed in any further detail here. It should be mentioned that these flows might be of interest for several applications. If oil is not included, these flows would be of interest in the analysis of geothermal energy systems. Also, with the oil included, they might be useful in analyzing the "puff" stage of a "huff and puff" steam-flooding process. In this process one injects steam at high pressure to lower the viscosity of the oil, then one pumps the oil back at the same point that one injected the steam.

11) SUMMARY OF FLOWS

Before considering the question of the stability of these

flows, it is worth summarizing all the various regimes of

flow.

For the case where $P_\infty < P_o$, as one lowers the pressure

ratio P_∞/P_o from 1 to 0 (keeping all other parameters fixed),

the following regimes of flow are encountered in order.

1) Three phases are always present. There are two shocks in

the flow. First a Buckley-Leverett type shock where [S]>0.

[Z]<0, and [P']>0, then a condensation shock where [S]<0,

[Z]<0, and [P']>0.

2) There is a subcooled slug in the flow where T<Tsat(P), and

S=1. There are 3 shocks, first a Buckley-Leverett shock as in

1), then a shock into the slug with [S]>0, [T]<0, [P']>0, then a

jump out of the slug with [S]<0, [T]=0, [P']>0.

3) The flow is the same as in 2) except the Buckley-Leverett

shock occurs inside the slug. At the left end of the slug

there is a thin stip of high oil saturation. The jump into the

slug has [P']<0, indicating that it is unstable.

4) The flow is the same as in 3) but the strip of high oil

saturation has widened, and the jump into the slug satisfies

[P']>0, indicating stability.

5) The flow is as in 4), but the shock inside the slug is

replaced by an expansion fan where Z is an increasing function

of θ .

By lowering S_o , flows can be obtained that are similar to

the above flows, but that near $\theta = \emptyset$ have various types of superheated steam regions. By varying the other parameters, no other regimes were found to occur provided $P_\infty < P_o$.

For the case with $P_o < P_\infty$ no shocks occur in the flow. As one raises P_∞ / P_o a superheated steam region forms near $\theta = \emptyset$.

12) STABILITY – PRELIMINARY CONSIDERATIONS

It would be nice if a stability analysis could be done directly on the similarity solutions, but this would be difficult. The problem is that the flows are time developing. We will be content with analyzing a steady problem that has many of the significant features that are relevant. In particular, it seems plausible to focus attention on the stability of steadily moving shocks.

Saffman and Taylor (ref 7) were the first to analyze the stability of plane interfaces in a porous medium. They analyzed the case where one fluid with viscosity μ_I and density ρ_I, was pushing another fluid, with viscosity μ_{II} and density ρ_{II}, upwards with velocity U. With gravity included, the neutral stability criterion is found to be

22)
$$\epsilon k u \left(\mu_{II} - \mu_I \right) + \left(\rho_{II} - \rho_I \right) g = 0$$

The first term indicates that when a fluid with a small viscosity pushes one with a larger viscosity, the interface is destabilized. The second term is basically just a contribution from the Rayleigh-Taylor stability criterion. It should be mentioned that if one uses Darcy's law, the neutral stability criterion may be simplified to [P']=0.

The Saffman-Taylor analysis is not sufficient to analyze the flows that have been considered here. The main feature that must be added to their analysis is the possibility of having condensation occur at the interface. This effect was

considered before by Miller (ref 8), but his analysis seems to be defective. He does not constrain his temperature perturbation to lie on the Clausius-Clapeyron curve, and as a result his result differs from the result in the next section.

The Saffman-Taylor analysis applies to the case where one homogeneous fluid is pushing another homogeneous fluid. In terms of the saturation function this means that S=0 on one side, and 1 on the other side. Before considering the effect of condensation on the stability of the shocks, at least some mention should be made of the effect of having S lie between 0 and 1 on one or both sides of the shock. It is completely straightforward to analyze the stability of a steadily moving interface with constant saturation on both sides. In this case the neutral stability criterion is precisely the same as in 22). This is essentially obvious, but it shows that the saturation function does not have a signficant effect on the neutral stability analysis.

One can similarly analyze the case where there are 3 phases present, but still no phase change. This analysis is also quite simple. Again the neutral stability criterion turns out to be [P']=0. This result does not seem to be quite as obvious as the case where there are only two phases present.

When no phase change is allowed to occur it is as easy to evaluate the stability of a steadily moving interface where S lies between 0 and 1 on each side of the shock, as it is to

analyze the case where S=0 or 1 on each side. When phase change takes place this is no longer the case. The complication arises due to the fact that a simple steady flow does not exist when S is nonzero on either side. In this case the fact that P and T are related by the Clausius-Clapeyron equation makes it impossible to have S, T, and P be constant on either side of the shock. The fact that these simple conditions are not allowed would greatly complicate the analysis. To avoid this problem, when analyzing the effect of phase change it will be assumed that S=0 or 1 on each side of the shock.

13) STABILITY WITH PHASE CHANGE

Consider an interface moving to the right with liquid water on the left, and water vapor on the right. Assume that no gravity is present, and let there be a jump in temperature at the interface. On both sides of the interface Darcy's law and the continuity equation combine to give

23a)
$$\nabla^2 P = 0$$

on the left the energy equation is

b)
$$\frac{\partial}{\partial t}\left(\rho_\ell \epsilon\, e_\ell + (1-\epsilon)\rho_s\, e_s\right) - \nabla\cdot\left(\rho_\ell h_\ell \frac{k}{\mu_\ell}\nabla P\right) = 0$$

and on the right the energy equation is

c)
$$\frac{\partial}{\partial t}\left(\rho_v \epsilon\, e_v + (1-\epsilon)\rho_s\, e_s\right) - \nabla\cdot\left(\rho_v h_v \frac{k}{\mu_v}\nabla P\right) = 0$$

For a steadily moving one dimensional interface the above equations yield P''=T'=0 on both sides. Let the interface be moving with velocity U, then the continuity of mass and energy flux put 2 constraints on the values of P' and T on the two sides of the interface.

24a)
$$\rho_\ell\left(\epsilon U + \frac{k P_\ell'}{\mu_\ell}\right) = \rho_v\left(\epsilon U + \frac{k P_v'}{\mu_v}\right)$$

b)
$$[T]\left(\rho_v c_v\left(\epsilon U + \frac{k P_v'}{\mu_v}\right) + (1-\epsilon)\rho_s c_s U\right) - \rho_\ell \overline{h}_{\ell v}\left(\epsilon U + \frac{k P_\ell'}{\mu_\ell}\right) = 0$$

or equivalently

b')
$$[T]\left(\rho_\ell c_\ell\left(\epsilon U + \frac{k P_\ell'}{\mu_\ell}\right) + (1-\epsilon)\rho_s c_s U\right) - \rho_\ell h_{\ell v}\left(\epsilon U + \frac{k P_\ell'}{\mu_\ell}\right) = 0$$

Here P_ℓ', and P_v' stand for the pressure gradients on the liquid and the vapor sides. The equations 24b and b') are identical, but written in different ways. In the first one, $\overline{h}_{\ell v}$ is evaluated on the liquid side, in the second $h_{\ell v}$ is evaluated on the vapor side

Given U, T_ℓ, and T_v equations 24ab) may be solved to determine P_ℓ', and P_v'.

25a)
$$\frac{k P_\ell'}{\mu_\ell} = \frac{[T]\left(\epsilon U c_v + \frac{\rho_s}{\rho_\ell} c_s (1-\epsilon) U\right) - \overline{h}_{\ell v} \epsilon U}{-[T] c_v + \overline{h}_{\ell v}}$$

b)
$$\frac{k P_v'}{\mu_v} = \frac{[T]\left(\epsilon U c_v + \frac{\rho_s}{\rho_v} c_s (1-\epsilon) U\right) - \overline{h}_{\ell v} \epsilon U}{-[T] c_v + \overline{h}_{\ell v}}$$

It will be convenient to introduce the following notation which is analogous to that introduced earlier.

$$F_\ell = \epsilon U + \frac{k P_\ell'}{\mu_\ell}$$

$$F_v = \epsilon U + \frac{k P_v'}{\mu_v}$$

$$F_H = \rho_\ell c_\ell F_\ell + (1-\epsilon) \rho_s c_s U$$

For future reference the signs of these quantities should be noted. Since the vapor must be hotter than the liquid, $[T] > 0$. It can be seen from 24b' that F_H and F_ℓ must be of opposite signs, but if $F_\ell > 0$, then obviously $F_H > 0$. Thus, it is

seen that $F_{\ell} < 0$, and $F_H > 0$. From 24a) it is thus seen that $F_v < 0$.

To analyze the stability of these solutions, assume that the steady solutions are perturbed by quantities that vary like

$$\hat{f}(x) \, e^{\omega t} \, e^{i(\alpha_y y + \alpha_z z)} \qquad\qquad \alpha_y^2 + \alpha_z^2 = \alpha^2$$

When equations 23abc) are linearized about the mean flow, and written in a frame moving with the velocity of the interface, they reduce to

26a)
$$\hat{P}'' = \alpha^2 \, \hat{P} \qquad \text{on both sides of the interface}$$

b)
$$-\omega \hat{T}_v \left(\epsilon \rho_v c_v + (1-\epsilon) \rho_s c_s \right) + \hat{T}_v' F_H = 0 \qquad \text{on the R.H.S.}$$

c)
$$-\omega \hat{T}_\ell \left(\epsilon \rho_\ell c_\ell + (1-\epsilon) \rho_s c_s \right) + \hat{T}_\ell' F_H = 0 \qquad \text{on the L.H.S.}$$

In order to have the solutions decay at $\pm\infty$ it is necessary that they be of the following form.

$$\hat{P} = \hat{P}_\ell \, e^{\alpha x} \qquad \hat{T} = \hat{T}_\ell \, e^{\sigma x} \qquad \text{on the L.H.S.}$$

$$\hat{P} = \hat{P}_v \, e^{-\alpha x} \qquad \hat{T} = 0 \qquad \text{on the R.H.S.} \qquad \sigma = \omega \, \frac{\left(\epsilon \rho_v c_v + (1-\epsilon) \rho_s c_s \right)}{F_H}$$

In finding the form of the solution for $\hat{T}$ it is assumed that ω is positive, even though the time dependence may not necessarily yield a positive ω. This can be rigorously justified by taking the Laplace transform in time, and then finding the growth rate by finding the poles in the transform

plane.

If one allows the interface itself to be perturbed by

$$\eta(y,z,t) = \eta\, e^{\omega t}\, e^{i(\alpha_y y + \alpha_z z)}$$

the perturbed boudary conditions may be written

27a)
$$\rho_\ell\left(\epsilon\omega\eta + \frac{k\,\hat{P}_\ell'}{\mu_\ell}\right) = \rho_v\left(\epsilon\omega\eta + \frac{k\,\hat{P}_v'}{\mu_v}\right) \quad (\text{continuity of mass})$$

b)
$$\hat{P}_\ell + \eta\, P_\ell' = \hat{P}_v + \eta\, P_v' \quad (\text{continuity of pressure})$$

c)
$$[\hat{T}]\,F_\mu + [T]\left(\rho_v c_v\left(\epsilon\omega\eta + \frac{k\,\hat{P}_v'}{\mu_v}\right) + (1-\epsilon)\rho_s c_s \omega \eta\right)$$
$$-\rho_\ell \bar{h}_{\ell v}\left(\epsilon\omega\eta + \frac{k\,\hat{P}_\ell'}{\mu_\ell}\right) = 0 \quad (\text{continuity of energy flux})$$

A condition requiring that the pressure and temperature
lie on the Clausius-Clapeyron curve must also be given. One
must be careful in deriving this condition. For simplicity
thermal conductivity has been ignored, but if it were left in,
there would be several consequences. The temperature profile
would be continuous, the boundary between the liquid and vapor
region would lie on the Clausius-Clapeyron curve, and the
perturbed energy equation would be of the following form.

$$k\hat{T}'' + a\hat{T}' - b\hat{T} = 0 \quad a>0 \quad b>0 \quad 0<k\ll1$$

The solutions would be of the form.

$$\gamma + e^{\lambda_+ x} + \gamma - e^{\lambda_- x} = \hat{T}$$

$$\lambda_\pm = \frac{-a + \sqrt{a^2 + 4bk}}{2k} \qquad \begin{array}{l}\lambda_+ = O(1)\\[4pt]\lambda_- = O\left(\frac{1}{k}\right)\end{array} \quad \text{for } k\ll1$$

To have $\hat{T}$ vanish at $x=\pm\infty$ it is necessary that $\gamma_+=0$ on the R.H.S., and $\gamma_-=0$ on the L.H.S. As $k\to 0$ it is simple to show that the temperature profile on the R.H.S. is of boundary layer type, while that on the L.H.S. has no sharp gradients. Thus when thermal conductivity is completely ignored $\hat{T}$ and $\hat{P}$ must lie on the Clausius-Clapeyron equation on the L.H.S., but not on the R.H.S.. The same type of argument also holds for the unperturbed flow. That is $T_\ell=\text{Tsat}(P_\ell)$ at the interface, but $T_v \neq \text{Tsat}(P_v)$.

The 4th condition on the perturbation is thus

27d) $\quad \dfrac{dT}{dP}\left(\hat{P}_\ell + \eta\, P_\ell'\right) = \hat{T}_\ell \quad$ (on the L.H.S. the perturbed pressure and temperature must lie on the Clausius-Clapeyron curve)

There are 4 unknowns, η, $\hat{P}_\ell$, $\hat{P}_v$, $\hat{T}_\ell$, and 4 equations. To have nontrivial solutions, ω must be chosen properly. This eigenvalue problem can easily be solved, but it is more convenient to just do a neutral stability analysis. If one sets $\omega=0$ in equation 27), one finds that the criterion for a nontrivial solution to exist is.

28) $\quad -F_H\, \dfrac{dT}{dP}\left(\dfrac{\rho_v}{\mu_v}P_v' + \dfrac{\rho_\ell}{\mu_\ell}P_\ell'\right) + \dfrac{\alpha \rho_\ell \rho_v}{\mu_\ell \mu_v}\left(P_v' - P_\ell'\right)\left([T]c_v - \bar{h}_{\ell v}\right) = 0$

This is of course the neutral stability criterion. For short wavelengths ($\alpha\to\infty$) this criterion is identical to the case for no condensation $[P']=0$. It is for short wavelengths that the analysis is meaningful when applied to the nonuniform

profiles of the earlier sections. The term

$$F_H \frac{dT}{dP} \left(\frac{\rho_v}{\mu_v} P'_v + \frac{\rho_\ell}{\mu_\ell} P'_\ell \right)$$

can be shown to be a stabilizing effect for longer

wavelengths.

Formally, the above stability analysis can be done for

the case where vapor is on the left and liquid is on the

right. This analysis yields the same criterion for stability.

The unperturbed profiles in this case are however not proper

physically. The reason is that on the R.H.S. $\frac{\partial T}{\partial x} = 0$, but $\frac{\partial P}{\partial x} < 0$,

so the liquid would eventually go superheated. This

obviously detracts from the result in this case, but it is not

unreasonable to expect that the result $[P']=0$ is a suitable

neutral stability criterion for similar flows that do not have

this difficulty.

The results of the various stability analyses indicate

that the neutral stability criterion $[P']=0$ may likely be

applied in some generality to the problems under

consideration. The result holds for steadily moving

saturation shocks with three noncondensing fluids on each side

of the shock, and it holds for small wavelength disturbances

of a steadily moving condensation shock with liquid on one

side and vapor on the other.

APPENDIX A

It will be shown that the conditions on F_ρ, F_v, and F_o stated in section 5 are necessary and sufficient conditions for detA to change sign. The signs of [S], [Z], and [P'] will also be determined.

As mentioned in section 5 detA>0 at the first shock, and F_ρ<0, F_v<0, otherwise the equations would have passed through a singularity. From the jump conditions 17) we see that F_ρ, F_v, and F_o cannot change sign in crossing a shock provided 0<S<1, 0<Z<1, on both sides. So, if F_o<0 on the L.H.S. of the shock, then F_v<F_ρ<F_o<0 on the R.H.S. From the form of detA we would thus have detA>0 on the R.H.S. This establishes the necessity of having F_v<0, F_ρ<0, and F_o>0 at the first shock.

Now assume that at the first shock F_v<F_ρ<0, F_o>0. The equations for the jumps may be written:

29a)
$$[Z]F_o + \frac{Z_2}{\mu_v}[P'] = 0$$

b)
$$[(1-Z)(1-S)]F_v + (1-Z_2)(1-S_2)\frac{[P']}{\mu_v} = 0$$

c)
$$[(1-Z)S]F_\rho + (1-Z_2)S_2\frac{[P']}{\mu_\rho} = 0 \qquad Z_2, S_2 \text{ are evaluated on the R.H.S.}$$

These show that [Z] has the opposite sign as [(1-Z)S], and [(1-Z)(1-S)]. Let detA be the determinant on the L.H.S., and det$\hat{A}$ be the determinant on the R.H.S. Equation 18) implies that

$$\det A = \frac{F_0 F_\varrho}{\mu_v} (1-z)(1-s) + \frac{F_0 F_v}{\mu_\varrho} (1-z)s + \frac{F_\varrho F_v}{\mu_0} z$$

$$= -\frac{F_0 F_\varrho}{\mu_v} \left[(1-z)(1-s)\right] - \frac{F_0 F_v}{\mu_\varrho} \left[(1-z)(1-s)\right] - \frac{F_\varrho F_v}{\mu_0} \left[z\right]$$

Now since $F_\varrho F_v > 0$, $F_\varrho F_0 < 0$, and $F_v F_0 < 0$, it is easy to see that since $\det A > 0$, $[Z] < 0$. Similar manipulations show that

$$\det \hat{A} = [z] \frac{F_{\varrho 2} F_{v2}}{\mu_0} + [(1-z)s] \frac{F_{v2} F_{02}}{\mu_\varrho} + [(1-z)(1-s)] \frac{F_{02} F_{\varrho 2}}{\mu_v}$$

Where $F_{\varrho 2}, F_{v2}, F_{02}$ are just F_ϱ, F_v, and F_0 evaluated on the R.H.S. The signs of F_ϱ, F_v, and F_0 do not change in crossing the shock, so similar arguments as above show that

$$\text{sgn}(\det \hat{A}) = \text{sgn} [z] < 0$$

So $\det A$ does in fact change sign in crossing the shock provided $F_v < 0$, $F_\varrho < 0$, and $F_0 > 0$.

One also gets that $[P'] > 0$ from $[Z] < 0$, $F_0 > 0$, and 2⁹a). If one considers 17'bc) as equations for $[S]$, and $[P']$, with $[Z]$ given one gets

$$[s] = \frac{(1-S_2) S_2 \frac{\Theta}{2} \left(\frac{1}{\mu_v} - \frac{1}{\mu_0}\right) [z]}{(1-z_2)\left((1-S_2)\frac{F_\varrho}{\mu_v} + S_2 \frac{F_v}{\mu_\varrho}\right)}$$

so $[S] > 0$.

At the second shock it is necessary that $F_\varrho > 0$ in order to get over the last zero of $\det A$. Assuming that this is so and that $F_v < 0$, $F_\varrho > 0$ it can be shown by arguments similar to those above that $\det A$ changes sign, and that $[Z] < 0$, $[P'] > 0$, and

$[S] < 0.$

In section 3) it was mentioned that it was not possible to jump over both zeros of detA in one jump. This is obviously true because of the fact that F_ρ, F_v, and F_o do not change sign in crossing a shock. At the shock it would be necessary that $F_\rho < 0$ (otherwise detA would have already changed sign), but it would be necessary to have $F_\rho > 0$ on the R.H.S. of the shock to avoid any further zeroes.

APPENDIX B

Here it will be shown that if at a shock, F_ℓ , F_v , and F_o satisfy the conditions stated in section 5, then the characteristics on the left are overtaking those on the right. First it should be noted that if these conditions are satisfied, then $[P_x]>0$ (as shown in appendix A).

Let $V=dx/dt$ be a characteristic. After factoring out the solutions with $dx/dt=\infty$, the following is the characteristic equation.

30)
$$\left(\epsilon V+\frac{kP_x}{\mu_\ell}\right)\left(\epsilon V+\frac{kP_x}{\mu_v}\right)\frac{z}{\mu_o} + \left(\epsilon V+\frac{kP_x}{\mu_\ell}\right)\left(\epsilon V+\frac{kP_x}{\mu_o}\right)\frac{(1-z)(1-s)}{\mu_v}$$

$$+ \left(\epsilon V+\frac{kP_x}{\mu_o}\right)\left(\epsilon V+\frac{kP_x}{\mu_v}\right)\frac{(1-z)s}{\mu_\ell} = 0$$

This is similar to equation 4) for detA. From the shock conditions one can derive an equation similar to equation 18.

31)
$$\left(\epsilon U+\frac{k\hat{P}_x}{\mu_\ell}\right)\left(\epsilon U+\frac{k\hat{P}_x}{\mu_v}\right)\frac{z}{\mu_o} + \left(\epsilon U+\frac{k\hat{P}_x}{\mu_\ell}\right)\left(\epsilon U+\frac{k\hat{P}_x}{\mu_o}\right)\frac{(1-z)(1-s)}{\mu_v}$$

$$+ \left(\epsilon U+\frac{k\hat{P}_x}{\mu_o}\right)\left(\epsilon U+\frac{k\hat{P}_x}{\mu_v}\right)\frac{(1-z)s}{\mu_\ell} = 0$$

Again the hat on $\hat{P}_x$ indicates that it is to be evaluated on a different side of the shock than Z and S. If equation 30) is considered as a polynomial in V/P_x , and equation 31) is considered as a polynomial in $U/\hat{P}_x$, then the two polynomials are identical. Thus it follows that one of the characteristics satisfies

$$\frac{V_1}{P_x} = \frac{U}{\hat{P}_x}$$

similarly, on the other side of the shock

$$\frac{\hat{V_1}}{P_x} = \frac{U}{P_x}$$

thus, $\hat{V_1} = V_1 \, \hat{P_x}^2 / P_x^2$

If hatted quantities are chosen to represent quantities on the R.H.S. of the shock, it is clear that $\hat{V_1} < V_1$ iff $[\rho_x] > 0$. This proves the result for one of the characteristics.

To prove it for the other characteristic, note that from 30) one can easily derive a formula for the product of the two roots $V_1 V_2$. Evaluating this expression on both the left and the right (hatted quantities), and taking the ratio, one gets

$$\frac{V_1 V_2}{P_x^2}\left(\frac{z}{\mu_0} + \frac{(1-z)(1-s)}{\mu_v} + \frac{(1-z)s}{\mu_\rho}\right) = \frac{\hat{V_1}\hat{V_2}}{\hat{P_x}^2}\left(\frac{\hat{z}}{\mu_0} + \frac{(1-\hat{z})(1-\hat{s})}{\mu_v} + \frac{(1-\hat{z})\hat{s}}{\mu_\rho}\right)$$

Using the expression for V_1 and $\hat{V_1}$ this simplifies to

$$V_2\left(\frac{z}{\mu_0} + \frac{(1-z)(1-s)}{\mu_v} + \frac{(1-z)s}{\mu_\rho}\right) = \hat{V_2}\left(\frac{\hat{z}}{\mu_0} + \frac{(1-\hat{z})(1-\hat{s})}{\mu_v} + \frac{(1-\hat{z})\hat{s}}{\mu_\rho}\right)$$

The quantities multiplying V_2 and $\hat{V_2}$ are both positive so that $V_2 > \hat{V_2}$ iff

$$\frac{\hat{z}}{\mu_0} + \frac{(1-\hat{z})(1-\hat{s})}{\mu_v} + \frac{(1-\hat{z})\hat{s}}{\mu_\rho} > \frac{z}{\mu_0} + \frac{(1-z)(1-s)}{\mu_v} + \frac{(1-z)s}{\mu_\rho}$$

which is equivalent to

32)
$$\left[\frac{z}{\mu_0} + \frac{(1-z)(1-s)}{\mu_v} + \frac{(1-z)s}{\mu_\rho}\right] > 0$$

But,

$$\left[\frac{z}{\mu_0} + \frac{(1-z)(1-s)}{\mu_v} + \frac{(1-z)s}{\mu_\ell}\right] = \left[\frac{P_x}{P_x}\left(\frac{z}{\mu_0} + \frac{(1-z)(1-s)}{\mu_v} + \frac{(1-z)s}{\mu_\ell}\right)\right]$$

$$= \left[\frac{1}{P_x}\right]P_x\left(\frac{z}{\mu_0} + \frac{(1-z)(1-s)}{\mu_v} + \frac{(1-z)s}{\mu_\ell}\right) + \frac{1}{\hat{P}_x}\left[P_x\left(\frac{z}{\mu_0} + \frac{(1-z)(1-s)}{\mu_v} + \frac{(1-z)s}{\mu_\ell}\right)\right]$$

the second term in this last expression is equal to zero. this can be seen by using

$$\left[\frac{z(\epsilon u + kP_x)}{\mu_0}\right] = \left[(1-z)(1-s)\left(\epsilon u + \frac{kP_x}{\mu_v}\right)\right] = \left[(1-z)s\left(\epsilon u + \frac{kP_x}{\mu_0}\right)\right] = 0$$

and the fact that [Z+(1-Z)S+(1-Z)(1-S)]=0, so 32) is satisfied provided $[1/P_x]<0$ $[P_x]>0$. This proves that for the second characteristic V_2, the one on the left is overtaking the one on the right provided $[P_x]>0$.

APPENDIX C

Here it will be shown that if the conditions on F_ℓ, F_v, and F_o hold at a shock, then there is a unique solution to the jump conditions 17) that has $0<Z<1$, $0<S<1$ on the R.H.S.

At the first shock assume $F_v<0$, $F_\ell<0$, and $F_o>0$. Equation 18) may be solved for $\hat{S}$ (the value of S on the R.H.S) in terms of $\hat{Z}$ and the values on the L.H.S of the shock.

33) $$\hat{S} = \left(\frac{\hat{Z} F_\ell F_v}{\mu_o} + (1-\hat{Z}) \frac{F_o F_\ell}{\mu_v} \right) \Bigg/ \left((1-\hat{Z}) \frac{F_o F_\ell}{\mu_v} - \frac{F_o F_v}{\mu_\ell}(1-\hat{Z}) \right)$$

If one requires that $0<\hat{S}<1$ two inequalities on $\hat{Z}$ are obtained.

$$G = \frac{F_o}{\frac{\theta}{2}\epsilon\left(1-\frac{\mu_v}{\mu_o}\right)} < \hat{Z} < \frac{F_o}{\frac{\theta}{2}\epsilon\left(1-\frac{\mu_\ell}{\mu_o}\right)} = H$$

If one evaluates the polynomial in equation 19) at G and H one obtains

$$AH^2 + BH + C = -F_o^2(1-s)(1-\hat{Z})\left(\frac{1}{\mu_v}-\frac{1}{\mu_o}\right) \Bigg/ \left(1-\frac{\mu_\ell}{\mu_o}\right) < 0$$

$$AG^2 + BG + C = -F_o^2 s(1-\hat{Z})\left(\frac{1}{\mu_\ell}-\frac{1}{\mu_v}\right) \Bigg/ \left(1-\frac{\mu_v}{\mu_o}\right) > 0$$

Let $f(\hat{Z})=AZ^2+BZ+C$, since $A<0$ we have $f(\infty)<0$, $f(H)<0$, $f(G)>0$, and $f(-\infty)<0$. Thus, one root to 19) satisfies $G<\hat{Z}<H$, the other root satisfies $\hat{Z}<G$, and will not yield $0<\hat{S}<1$.

Now to have $0<\hat{Z}<1$ it is only necessary that $G>0$, and $H<1$. This is easily shown to be so iff $F_o>0$, and $F_\ell<0$. This completes the proof that one and only one solution of 17) satisfies $0<\hat{S}<1$, $0<\hat{Z}<1$ provided F_ℓ, F_v, and F_o have the proper

signs at the first shock. Using identical arguments the corresponding result can be proven at the second shock.

APPENDIX D

Here it will be shown that

A) equation 20 has a unique solution with $0 < Z_2 < 1$ when the slug first forms,

and

B) At the point where the Buckley-Leverett shock overtakes the slug (as one varies a parameter such as P_∞), two roots of 20) satisfy $0 < Z_2 < 1$. As mentioned in section 7) this is required to have a smooth transition from the flows in section 6) to those in section 7).

Equation 20 may be written

$$F(\hat{z}) = \rho_\ell \frac{\theta}{2} \epsilon \left(\hat{\mu}_o - \mu_\ell\right) \hat{z}(\hat{z}-1) + \rho_\ell(1-\hat{z}) \hat{z} F_o \hat{\mu}_o - \hat{z}\mu_\ell \left(\rho_\ell s F_\ell + \rho_v(1-s) F_v\right)$$

$$= 0$$

Here the hatted quantities represent quantities on the R.H.S. of the shock. Note that

34) $\quad F(\pm\infty) = \infty \quad F(1) = -\left(\rho_\ell s F_\ell + \rho_v(1-s) F_v\right) \quad F(0) = F_o$

It should be recalled that just before the slug forms the value of S at the second shock is approaching 1. At this shock $F_\ell > 0$, $F_o > 0$. At a point where the slug first develops (as one varies a parameter), $S=1$, $F_\ell > 0$, and $F_o > 0$ on the L.H.S. of the shock into the slug. From 34) it is seen that there is one root with $0 < Z < 1$, and one root with $Z > 1$. This proves A.

On the L.H.S. of the Buckley-Leverett shock $F_v < 0$, $F_\ell < 0$, and $F_o > 0$. So it is easy to see from 34) that there are either

$\emptyset$ or 2 roots that satisfy $\emptyset < Z < 1$ at the point where the Buckley-Leverett shock catches up to the slug. The flows that exist immediately before the two shocks cross demonstrate that at least one root exists, so the conclusion is that B) does in fact hold.

467

Shock-like structure of phase-change flow in porous media

By L. A. ROMERO

Applied Mathematics Division

AND R. H. NILSON

Fluid Mechanics and Heat Transfer Division II
Sandia Laboratories,
Albuquerque, New Mexico 87185

Shock-like features of phase-change flows in porous media are explained, based on the generalized Darcy model. The flow field consists of two-phase zones of parabolic/hyperbolic type as well as adjacent or imbedded single-phase zones of either parabolic (superheated, compressible vapour) or elliptic (subcooled, incompressible liquid) type. Within the two-phase zones or at the two-phase/single-phase interfaces, there may be steep gradients in saturation and temperature approaching shock-like behaviour when the dissipative effects of capillarity and heat-conduction are negligible. Illustrative of these shocked, multizone flow-structures are the transient condensing flows in porous media, for which a self-similar, shock-preserving (Rankine–Hugoniot) analysis is presented.

1. Introduction

Geological applications motivate the study of transient phase-change flow in porous media. Examples include: geothermal systems (Brownell, Garg & Pritchett 1977), steam stimulation of oil fields (Weinstein, Wheeler & Woods 1977), and containment of underground nuclear tests (Morrison 1973) as well as the *in situ* combustion processes such as oil-shale retorting and coal gasification.

A mathematical statement of the conservation principles leads to partial differential equations having hyperbolic, parabolic and elliptic character within different regions of the flow. In phase-change regions, where the fluid-matrix energy transfer predominates, the transport equations are of a mixed parabolic/hyperbolic type. In adjacent or imbedded single-phase regions, the velocity field becomes nearly uncoupled from the temperature field and the pressure field is either parabolic or elliptic for the respective cases of compressible vapour and incompressible liquid. Transitions between zones are accompanied by steep gradients in saturation and temperature, approaching shock-like behaviour as capillary pressure and thermal conduction become negligible.

Saturation shock is a characteristic feature of multiphase flows in which the pressure gradient is the primary driving force rather than the gradient in capillary pressure, as expected in the applications noted above (although not in unsaturated hydrology, the infiltration problem, or some drying processes). The best known example of saturation shock is the Buckley–Leverett case of immiscible fluid/fluid displacement (Bear 1970). Comparable behaviour occurs in isothermal phase-change

systems, as reviewed by Nikolaevskii & Somov (1978), but here the isothermal restriction precludes the fluid/matrix energy transfer which is paramount in the applications noted above. When the energy transfer is included as in oil displacement by hot water (Fayers 1962), thermal shocks are found to accompany the saturation shocks, provided that convective heat transfer dominates over conduction. These fundamental examples suggest that a composite of shock-like behaviour will likely be encountered in the coupled problem of non-isothermal, phase-change flow. Although it is true that capillarity and heat conduction will always smear the shock fronts in direct analogy with viscous smearing of gasdynamic shocks (Scheidegger 1974), these dissipative effects should be moderate in the noted applications, as is already apparent in some previous numerical simulations.

Shock-like phenomena are observed in numerical simulations of non-isothermal, phase-change flows in porous media (e.g. Weinstein *et al.* 1977; Morrison 1973), but there have been no analyses which explain the mathematical and physical character of these phase-change shocks which occur as a consequence of fluid/matrix energy transfer. Such an analysis is particularly needed because the direct numerical integration of the primitive equations is a very difficult task (subject to the numerical instabilities and dispersion which result from nonlinearity, type-change, and sharp fronts (Settari & Aziz 1975)). There has been no opportunity to assess the accuracy by comparison with a reliable but non-trivial solution, and the physical structure of the flow has been obscured by numerical smearing.

In the present study of phase-change shocks, consideration is given to self-similar flows. The ordinary differential equations are solved by a shock-preserving method, using Rankine–Hugoniot (jump balance) conditions in crossing the shock fronts. A representative example problem is that of transient condensing flow of a pure substance within a porous matrix. Depending on the initial and boundary conditions, several flow structures are found to occur as described in the individual sections of the paper:

(*a*) two-phase flow divided by a saturation shock (§ 4);

(*b*) two-phase flow divided by an imbedded slug of subcooled liquid, with shocks on both sides of the slug (§ 5);

(*c*) superheated inflow shocking into a two-phase zone like either (*a*) or (*b*) above (§ 6),

(*d*) two-phase inflow shocking into a superheated vapour zone, followed by a two-phase zone like either (*a*) or (*b*) above (§ 7);

(*e*) entry flow like either (*c*) or (*d*), shocking into a central two-phase zone, followed by a fully-wet subcooled far-field flow (§ 5).

Thus, the central structure is generally two-phase, divided by either a shock or an imbedded slug of liquid. The inner and outer zones respectively depend upon the boundary (inflow) data and the initial (far-field) data.

The primary purpose is to communicate the structure of the flow, based on a widely-used mathematical description of the physics. To accent the shock-like structure, the dispersive effects of capillarity and heat conduction are suppressed. The shock-preserving, self-similar method of solution is well suited because it affords the opportunity for rigorous analysis as well as reliable numerical computation based on well-established algorithms for ordinary differential equations. Qualitative

observations and structural aspects are representative of a broad class of flows, not just the considered self-similar examples.

2. Transport equations

The transient, two-phase flow of a pure substance in a porous medium is governed by conservation of mass, energy and momentum (Cheng 1978; Whitaker 1977):

$$\frac{\partial}{\partial t}\left[\epsilon S\rho_l + \epsilon(1-S)\rho_v\right] + \frac{\partial}{\partial x}\left[\rho_l u_l + \rho_v u_v\right] = 0; \tag{1a}$$

$$\frac{\partial}{\partial t}\left[\epsilon S\rho_l h_l + \epsilon(1-S)\rho_v h_v + (1-\epsilon)\rho_m h_m\right]$$
$$+ \frac{\partial}{\partial x}\left[\rho_l h_l u_l + \rho_v h_v u_v\right] - \frac{\partial}{\partial x}\left[\langle k \rangle \frac{\partial T}{\partial x}\right] - \frac{DP}{Dt} = 0; \tag{1b}$$

$$\left. \begin{array}{ll} u_v = -\alpha_v \dfrac{K}{\mu_v}\dfrac{\partial P}{\partial x}, & \alpha_v = 1-S; \\[4mm] u_l = -\alpha_l \dfrac{K}{\mu_l}\dfrac{\partial P}{\partial x}, & \alpha_l = S^3, \end{array} \right\} \tag{1c}$$

where the subscripts l, v, and m refer to liquid, vapour and solid matrix; K and ϵ are permeability and porosity; and S is the volume fraction of the pore space containing liquid. All other variables have the usual meaning. In the generalized Darcy equations, which relate velocity to pressure gradient at low Reynolds number, the relative permeability functions α_l and α_v are taken in a simple form which facilitates the analysis while still representing the proper qualitative behaviour (Scheidegger 1974; Wooding & Morel-Seytoux 1976). Although experimentally-determined α_l and α_v are considerably more complex, particularly near the single-phase extremes at $S = 0$ and $S = 1$, the basic qualitative behaviour of the flow should be essentially the same for any smooth monotonic functions (as verified by obtaining some comparative solutions in which both a_l and α_v were presumed linear in S).

Body forces and capillary pressure are neglected, thermal equilibrium between fluid and solid is presumed, and under the supposition of a high Peclet number, the conduction terms need only be included for the discussion of shock structure. Viscosities are assumed constant, the liquid is incompressible, the gas is ideal ($\rho = P/\breve{R}T$), and the enthalpies $h_i = e_i + P/\rho_i$ depend linearly on T with slope C_i for $i = l, v, m$. Consistent with the low-Reynolds-number Darcy approximation, the kinetic energy and $\mathbf{u}.\nabla P$ work terms are neglected.

In a region of two-phase flow, the pressure and temperature are related by the Clausius–Clapeyron equation

$$\frac{dP}{dT} = \frac{h_{lv}}{Tv_{lv}}, \quad T = T_{sat}(P) \tag{2a}$$

in which $h_{lv} = h_v - h_l > 0$ and $v_{lv} = \rho_v^{-1} - \rho_l^{-1} > 0$. In a single-phase region, it is instead required that

$$\begin{array}{ll} S = 1, & T < T_{sat}(P), \\ S = 0, & T > T_{sat}(P), \end{array} \tag{2b}$$

for the cases of subcooled liquid and superheated vapour, respectively.

The initial and boundary conditions to be imposed are

$$S(x, 0) = S_\infty, \quad P(x, 0) = P_\infty, \quad T(x, 0) = T_\infty;$$
$$S(0, t) = S_0, \quad P(0, t) = P_0, \quad T(0, t) = T_0. \tag{3}$$

To induce a forward flow $(\partial P/\partial x < 0)$ and vapour condensation, the boundary pressure and temperature are abruptly increased to $P_0 > P_\infty, T_0 > T_\infty$. If the driving state is saturated, $T_0 = T_{\text{sat}}(P_0)$, and S_0 must be specified. If superheated, T_0 and P_0 are independent, but S_0 must vanish. In either case, there are two independent boundary conditions at $x = 0$; and similarly, there are two independent initial conditions.

The system reduces to a set of ordinary differential equations under the similarity transformation (Morrison 1973; Nikolaevskii & Somov 1978)

$$\theta = \frac{x}{t^{\frac{1}{2}}} \left(\frac{\epsilon \mu_v}{P_0 K} \right)^{\frac{1}{2}}.$$

Normalizing P, T, ρ, h_{lv}, C_i and k by $P_0, T_0, \rho_{v0}, h_{lv0}, h_{lv0}/T_0$ and k_0, respectively, the transformed equations are

$$\tfrac{1}{2}\theta(\rho_l S + (1-S)\rho_v)' + ((\rho_v \alpha_v + R\rho_l \alpha_i)P')' = 0, \tag{4a}$$

$$T'(F_h) - h_{lv}(\tfrac{1}{2}\theta\rho_l S' + R\rho_l(\alpha_i P')') - \tfrac{1}{2}\theta\Gamma P' + Pe^{-1}(kT')' = 0, \quad \rho_v = P/T, \tag{4b,c}$$

in which the derivatives, denoted $(\ )'$, are taken with respect to the similarity variable θ, and the parameters

$$R = \mu_v/\mu_l, \quad \Gamma = \tilde{R}T_0/h_{lv0}, \quad Pe^{-1} = k_0 T_0 \mu_v \epsilon/\rho_0 h_{lv0} K P_0$$

are all small numbers.† The convective energy flux involves the group

$$F_h = C_l F_l + C_v F_v + \rho_m C_m(\tfrac{1}{2}\theta)(1-\epsilon)/\epsilon$$

in which we introduce the notation

$$F_l = \rho_l(\tfrac{1}{2}\theta S + R\alpha_i P'), \quad F_v = \rho_v \alpha_v(\tfrac{1}{2}\theta + P')$$

for the mass flux of liquid and vapour relative to the moving self-similar co-ordinate system. The transformed boundary conditions are

$$S(0) = S_0, \quad P(0) = 1, \quad T(0) = 1;$$
$$S(\infty) = S_\infty, \quad P(\infty) = P_\infty, \quad T(\infty) = T_\infty, \tag{5}$$

with $P_\infty < 1$ and $T_\infty < 1$.

Within a two-phase zone, the equations are conveniently written

$$\mathbf{A} \begin{pmatrix} P'' \\ S' \end{pmatrix} = \mathbf{b}, \tag{6a}$$

$$\mathbf{A} = h_{lv} \begin{pmatrix} \rho_v \alpha_v & -\rho_v(\tfrac{1}{2}\theta + P') \\ \rho_l \alpha_i R & \rho_l(\tfrac{1}{2}\theta + 3RS^2 P') \end{pmatrix}, \tag{6b}$$

$$\mathbf{b} = \begin{pmatrix} -h_{lv}\rho_v'\alpha_v(\tfrac{1}{2}\theta + P') - T'F_h \\ T'F_h \end{pmatrix}, \tag{6c}$$

$$\det \mathbf{A} = h_{lv}^2 \rho_l \rho_v(\alpha_v(\tfrac{1}{2}\theta + 3RS^2 P') + R\alpha_i(P' + \tfrac{1}{2}\theta)). \tag{7}$$

† From now on, both Γ and Pe^{-1} will be neglected, except for the discussion of shock structure in §6.

In single-phase regions, the energy equation (4b) reduces to

$$T'(F_h) = 0 \tag{8}$$

(in which F_h is somewhat degenerate since either F_v or F_l vanishes in one-phase regions), and the continuity equation (4a) reduces to either

$$P'' = 0, \tag{9a}$$

or

$$(\rho_v(P' + \tfrac{1}{2}\theta))' = \tfrac{1}{2}\theta\rho_v, \tag{9b}$$

for the liquid and vapour cases, respectively.

Although the system is third order, there are four independent boundary conditions suggesting that added flexibility is needed. It is noted that for $S_0 > 0$, det $\mathbf{A} < 0$ at the origin, but that det $\mathbf{A} \to +\infty$ as $\theta \to \infty$. Either the flow contains a singularity at which det $\mathbf{A} = 0$ or a shock at which det $\mathbf{A}$ changes sign. The first alternative affords the needed flexibility only if $\mathbf{b}$ becomes orthogonal to all solutions of $\mathbf{A}^T y = 0$ whenever det $\mathbf{A} = 0$ – this being a sufficient condition for the existence of a singular subinterval of variable breadth. Since this compatibility condition is not automatically satisfied, a shock must be present.

3. Shock conditions

Mass, energy and momentum must be conserved in crossing a shock. From this fact (or by integrating (4) across a shock), we obtain the following shock conditions (Slattery 1972):

$$[F_l] + [F_v] = 0, \tag{10a}$$

$$[T]F_h + \hat{h}_{lv}[F_v] = 0, \tag{10b}$$

$$[P] = 0, \tag{10c}$$

in which the circumflex on h_{lv} indicates that it is to be evaluated on a different side of the shock than the quantities in F_h. Since h_{lv} may be evaluated on either side, and since h_{lv} has the same (positive) sign on both sides, so must F_h have the same sign on both sides. The pressure cannot jump (in 10c) because the Reynolds number is presumed low in Darcy flow and the inertial terms are, therefore, absent.

The entropy cannot decrease in crossing a shock. Letting ϕ denote the specific entropy, this condition can be written

$$[\phi_l F_l + \phi_v F_v + \phi_m \rho_m (\tfrac{1}{2}\theta)(1-\epsilon)/\epsilon] \leqslant 0. \tag{11}$$

Since the pressure does not change in crossing shocks

$$d\phi_i = \frac{dh}{T} = \frac{C_i dT}{T} \Rightarrow [\phi_i] = C_i[\ln T]; \quad i = v, l, m.$$

Using this result and the identity $\hat{\phi}_{lv} = \hat{h}_{lv}/T$, the second law (11) is combined with the energy equation (10b) to arrive at the inequality

$$\hat{T}\left([\ln T] - \frac{1}{\hat{T}}[T]\right)F_h \leqslant 0. \tag{12}$$

in which quantities with circumflexes lie on the two-phase side. To examine the consequences of this statement, first note that

$$[\ln T] - \frac{1}{\hat{T}}[T] \geqslant 0$$

whenever the two-phase region is on the right, and that this inequality changes direction whenever the two-phase region is on the left. It is, therefore, concluded that only three possibilities are consistent with the second law:

$$[T] = 0, \tag{13a}$$

$$[T] \neq 0, \text{ the two-phase region is on the left, and } F_h \geqslant 0, \tag{13b}$$

$$[T] \neq 0, \text{ the two-phase region is on the right, and } F_h \leqslant 0. \tag{13c}$$

4. Two-phase/two-phase

Consider the simplest case of a strictly two-phase flow (containing no single-phase regions) as occurs whenever $N = P_1/P_0$ and $S(\infty)$ are not too large and $S(0)$ is not too small. As already mentioned, there must be a shock at which det **A** jumps from negative to positive. But, in passing from a two-phase region into another two-phase region, $[P] = 0 \Rightarrow [T] = 0$, so that the jump conditions $(10a, b)$ reduce to

$$[F_l] = [F_v] = 0$$

or, equivalently,

$$[S](\tfrac{1}{2}\theta + RP'(S^2 + \hat{S}^2 + S\hat{S})) + R\hat{S}^3[P'] = 0 \tag{14a}$$

$$(1 - \hat{S})[P'] = [S](\tfrac{1}{2}\theta + P') \tag{14b}$$

where quantities with circumflexes will now represent quantities on the right side of the shock.

The two-phase shock conditions $(14a, b)$ combine to give a cubic equation for $\hat{S}$

$$F(\hat{S}) = (\tfrac{1}{2}\theta + RP'(S^2 + S\hat{S} + \hat{S}^2))(1 - \hat{S}) + R\hat{S}^3(\tfrac{1}{2}\theta + P') = 0. \tag{15}$$

The existence of a unique physical solution is demonstrated by examining the behaviour of $F(\hat{S})$.

$$F(-\infty) = -\infty, \quad F(0) = \tfrac{1}{2}\theta + RP'S^2 \geqslant 0, \tag{16a,b}$$

$$F(S) = \frac{\det \mathbf{A}}{\rho_l \rho_v h_{lv}^2} < 0, \quad F(1) = R(\tfrac{1}{2}\theta + P') \leqslant 0, \quad F(\infty) = +\infty. \tag{16c,d,e}$$

The above inequalities on $F(1)$ and $F(0)$ are based on the observation that the velocities of vapour and liquid, each measured with respect to the shock,

$$V_v = -(\tfrac{1}{2}\theta + P') \quad \text{and} \quad V_l = -(\tfrac{1}{2}\theta + RP'S^2) \tag{17}$$

must have positive and negative signs, respectively, in order that it be possible for det **A** to have the necessary sign-change in crossing. (The supportive argument is based on the following observations: det **A** is roughly a linear combination of V_v and V_l, V_v and V_l have the same sign at the origin, V_v and V_l cannot both change sign to the left of the shock without a singularity, neither V_v nor V_l can change sign at the

shock, and $V_v > V_l$.) The sign changes in (16) show that there are three real roots to the cubic equation $F(\hat{S}) = 0$.

$$\hat{S}_1 < 0, \quad \hat{S}_2 > 1, \quad 0 < \hat{S}_3 < S.$$

Since only $\hat{S}_3$ is physically meaningful, it is concluded that:

(a) a unique solution exists;

(b) $[S] < 0$, so the shock faces forward;

(c) $[P'] > 0$, from (14b);

(d) $\det \hat{\mathbf{A}} = R\hat{P}'\alpha_v(S + 2\hat{S})[S] + [P'](\hat{S}^2 + S^2 + S\hat{S})\alpha_v + R\alpha_l > 0$, from (15).

The last inequality guarantees that $\det \mathbf{A}$ has the necessary sign-change in crossing the shock.

The stability of the shock can be assessed from the local features noted above. The inequalities (17) on V_v and V_l are sufficient to establish the one-dimensional stability in the sense that the characteristics on the left are overtaking the characteristics on the right. In addition, the inequality on $[P']$ is, according to the steady planar analyses of Miller (1975) and of Laude & Morrison (1979), sufficient to suggest the stability of the present flows under two-dimensional perturbations. In some of the more complex flow structures to be discussed in later sections it is not so easy to determine the stability from an *a priori* analysis, but an examination of the computed results (particularly the sign of $[P']$) suggests that the criterion is satisfied.

Numerical solutions are obtained by a forward-marching shooting method, as described in the appendix. The shooting parameters are $P'(0)$ and θ_s. The ordinary differential equations (6) are integrated outward to θ_s; the jump conditions (14a, b) are used to cross the shock; integration of (6) is resumed. The values of the shooting parameters are adjusted until the far-field boundary conditions are satisfied.

Typical profiles of S, P, and T are shown in figure 1. Upon increasing $S(0)$, as in figure 2, the saturation profile becomes spike-shaped at the leading edge. For large enough $S(0)$, say $S^*(0)$, the peak of the spike rises to $S = 1$, indicating liquid-full conditions behind the shock. The algorithm still converges for $S(0) > S^*(0)$, but the answers are unphysical since $S > 1$ in the region immediately behind the shock. Thus, for $S(0) \geqslant S^*(0)$ we seek to accommodate the excess liquid by making allowance for a liquid-full zone of finite width, as described in the next section.

5. Two-phase/subcooled liquid/two-phase

A condensing flow may contain a subcooled-liquid zone which lies imbedded within an otherwise two-phase region (figure 3). Such a situation arises as the continuous extension of a strictly two-phase flow under a change of data which favours liquid-flooding of the pore space: increase of $S(0)$ as in figure 2, increase of $S(\infty)$, increase of $\Delta T = T_0 - T_\infty$. In the transition from a strictly two-phase flow to an imbedded-liquid flow, the shock-line of the two-phase flow broadens into a liquid-filled zone of finite width.

Within the subcooled zone the structure is simple: $S = 1$, $T' \approx 0$ from (8) with $\Gamma \ll 1$, and $P' =$ constant for an incompressible liquid. The last implies uniformity of the liquid velocity as in a so-called slug-flow. Aside from these consequences of the

474   *L. A. Romero and R. H. Nilson*
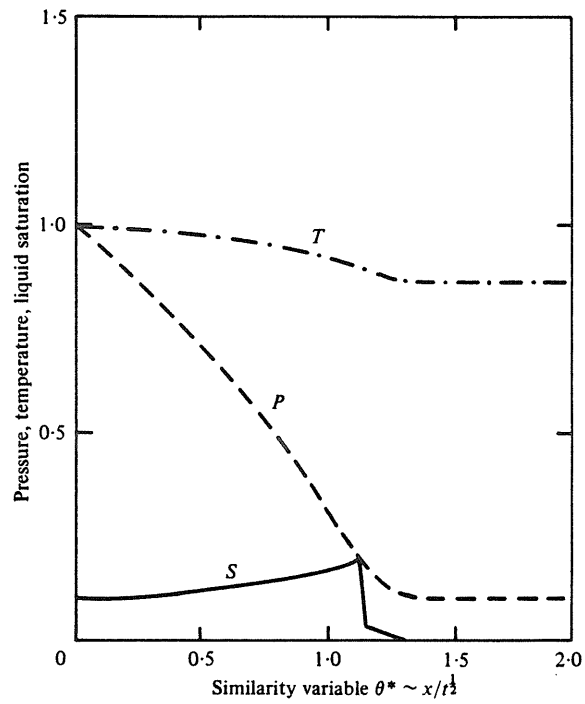
FIGURE 1. Strictly two-phase flow divided by a saturation jump.
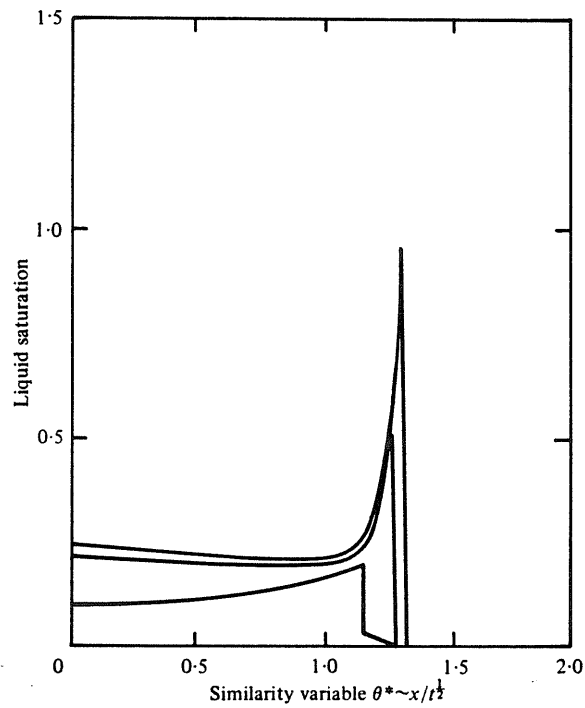
FIGURE 2. Family of saturation profiles for different prescriptions of the inflow saturation $S(0)$.
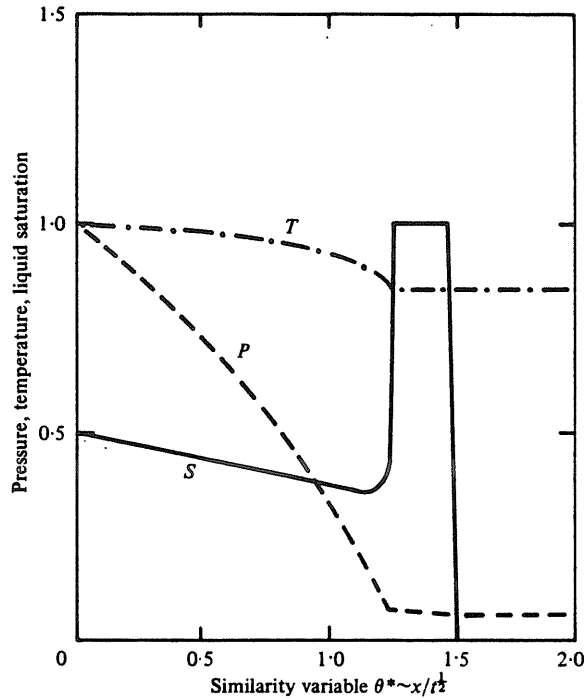
FIGURE 3. Two-phase flow divided by imbedded slug of subcooled liquid.

conservation equations, there is the thermodynamic requirement that $T \leqslant T_{\text{sat}}(P)$ everywhere within the subcooled slug.

A temperature jump $[T] < 0$ must occur at the left end of the slug $\theta = \theta_s$. Recall that the fluid temperature T and the saturation temperature $T_{\text{sat}}(P)$ are identical at θ_{s-}. Now, in crossing the slug, the saturation temperature must decrease (since $P' < 0$), while the fluid temperature remains nearly uniform (from (8))

$$\frac{dT_{\text{sat}}}{d\theta} < 0 \quad \text{and} \quad \frac{dT}{d\theta} = 0.$$

Were it not for an abrupt temperature drop upon entering the slug $(T(\theta_{s-}) > T(\theta_{s+}))$, the saturation temperature would fall below the fluid temperature, indicating super-heated rather than subcooled conditions. The thermal shock which prevents this situation is physically indicative of a narrow thermal boundary-layer (of thickness Pe^{-1}) which lies within the slug at its left extremity.

The second law (13b) admits the temperature jump at θ_s, provided that $F_h \geqslant 0$ at θ_{s+}. Using the definition of F_h and the condition that $P' = $ constant within the slug, it is seen that

$$\frac{dF_h}{d\theta} > 0.$$

It follows that $F_h > 0$ at the right end of the slug which, from second-law considerations (13c), rules out a temperature jump at the right. The absence of a right-hand temperature jump serves to determine the extent of the liquid slug, as explained in the numerical procedure of the appendix.

A typical imbedded-slug flow is presented in figure 3. Although a thermal shock occurs only at the left end of the slug, a saturation shock is found to occur at both ends, as in the back-to-back shocks of Fayers' hot-water flood problem. The width of the slug depends upon the given data.

(a) Upon decreasing $S(0)$, the slug solution properly transforms into the strictly two-phase solution of § 4. As $S(0) \to S^*(0)$ from above, the width of the slug and the jump in T both approach zero.

(b) An increase in $S(0)$ causes increased slug-width but only to a finite extent as $S(0) \to 1$.

(c) An increase in ΔT (i.e. T_0/T_∞) causes increased slug-width, because more condensate is then produced in raising the temperature of the solid matrix.

(d) An increase in $S(\infty)$ causes increased slug-width. As $S(\infty) \to 1$, the slug extends toward infinity, and the liquid compressibility ψ must be taken into account. For a fully-wet far field (i.e., $S(\infty) = 1$), the pressure disturbance penetrates to a relatively large depth $\theta \sim (P_0 \psi \mu_v/\mu_l)^{\frac{1}{2}}$, (roughly, $P \sim \text{erfc}\,(x(\mu_l \epsilon \psi/Kt)^{\frac{1}{2}})$ in the far field) compared to the two-phase condensation region which remains confined to a boundary-layer of thickness $\theta \sim (\rho_v/\rho_l)^{\frac{1}{2}}$.

6. Superheated/two-phase...

Under superheated inflow conditions

$$S_0 = 0, \quad T_0 \geqslant T_{\text{sat}}(P_0),$$

there is a narrow superheated-vapour zone adjacent to the entrance, followed by a two-phase downstream region (perhaps containing an imbedded slug of liquid) like that described previously.

A shock with $[T] < 0$ must occur in passing from the superheated region into the two-phase region. To show this, first note that $F_h < 0$ at $\theta = 0$ and that F_h must then remain negative throughout the superheated region. Otherwise, there is a singularity in the energy equation (8). Now, with $F_h < 0$ and $P' < 0$,

$$T' = 0 \quad \text{and} \quad \frac{dT_{\text{sat}}}{d\theta} < 0,$$

indicating that the flow becomes more superheated as θ increases. A temperature drop must, therefore, occur in the superheated/two-phase transition.

The shock into the two-phase region occurs when $F_h = 0$. This is demonstrated by examining the shockless behaviour of the system for small (but now non-zero) values of the thermal conductivity $\langle k \rangle$ and the capillary pressure P_c which respectively appear as multipliers of T_{xx} and S_{xx}.

(a) In the shock-like transition region there are sharp gradients in T but not in P. Such a situation cannot occur in a two-phase region where the Clausius–Clapeyron equation relates T' and P'. Thus, the sharp gradients in T must occur in the single-phase region.

(b) When $\langle k \rangle$ and P_c are both non-zero, T and T' are both continuous in going from the superheated region to the two-phase. Thus, the sharp temperature gradients of the single-phase region must flatten out *before* entering the two-phase region.

(c) F_h must change sign (i.e., become positive) in the single-phase region. Otherwise, T' could not flatten out. This assertion is based on the extended form of the energy equation (8) which includes thermal conduction

$$Pe^{-1}T'' = -(F_h)T', \quad 0 < Pe^{-1} \ll 1.$$

Once the temperature gradient becomes negative ($T' < 0$), it grows progressively steeper ($T'' < 0$), unless F_h becomes positive ($F_h = +\delta$).

(d) F_h must not change sign (i.e. remains negative) throughout the single-phase region and in crossing the shock into the two-phase region. This condition is a consequence of the shock relations, as previously noted in § 3.

To resolve the apparent contradiction between (c) and (d), it is concluded that $F_h = +\delta \simeq 0$ at the superheated/two-phase transition. This conclusion rigorously satisfies the continuous boundary-layer argument (c) and approximately satisfied the lower-order shock-layer argument (d) as $\delta \to 0$. The condition that $F_h = 0$ serves to determine the position of the superheated/two-phase shock, as described in the numerical procedure of the appendix.

The typical superheated/two-phase flow of figure 4 is somewhat comparable to Morrison's numerical calculation for a condensing steam/water flow in the presence of confluent air. The superheated region is always quite small, even for large values of $T_0/T_{sat}(P_0)$. Furthermore, an increase in T_0 has very little effect on the downstream solution, as apparent in a comparison of figures 1 and 4. The effects of superheat are small because C_v is small (compared to h_{lv}), and hence the flow is desuperheated in a region which is narrow (compared to the condensation region). In taking the limit as $C_v \to 0$, the superheated region shrinks to zero, the temperature shock moves to the inlet, and the two-phase equations start off singular.

When the amount of superheat approaches zero, (i.e. $(T(0) - T_{sat}(P(0))) \to 0$), the breadth of the superheated region remains finite. This behaviour is a consequence of the energy equation (4b) which demands that $T'(0) = 0$ whenever $S(0) = 0$ (provided that $C_v \neq 0$). Since

$$T' = 0 \quad \text{and} \quad P' < 0 \Rightarrow \frac{dT_{sat}}{d\theta} < 0 \quad \text{at} \quad \theta = 0,$$

it is concluded that for $S(0) = 0$ the saturation temperature dives below the fluid temperature, resulting in a superheated region at the inlet. It turns out that this tendency toward superheat persists for small (but non-zero) values of $S(0)$ as described in the next section.

7. Two-phase/superheated/two-phase/...

For small values of S_0 there is a two-phase region adjacent to the boundary, followed by a superheated zone, followed by a two-phase downstream region (perhaps containing an imbedded slug of liquid). The occurrence of an imbedded superheated region can be explained on the basis of mathematical or physical arguments. The differential equations demand that, for $S(0) \neq 0$, $S'(0) \sim h_{lv}P'(0)$, as also apparent in figure 2, indicating that the flow must become dryer as it moves forward into the medium. Physically, the inflowing fluid experiences a decreasing pressure ($DP/Dt < 0$) which, according to the Clausius-Clapeyron equation, must be accompanied
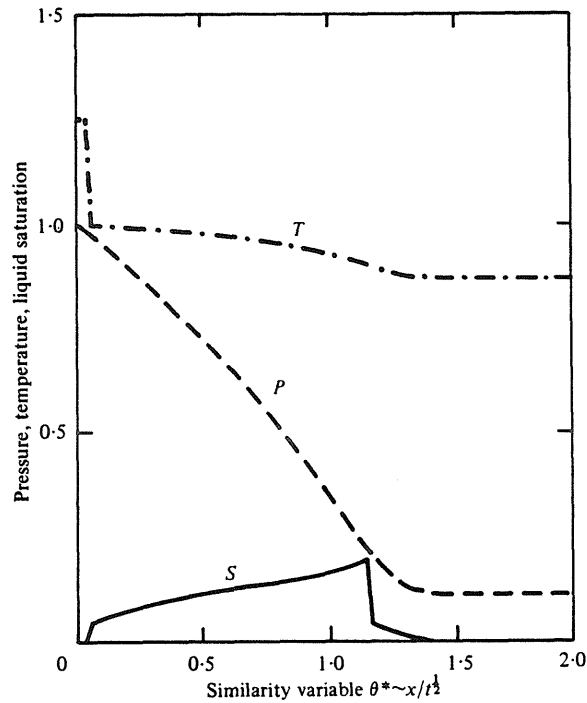
FIGURE 4. Two-phase flow with superheated inflow region (otherwise same as figure 1).

by a decreasing temperature $(DT/Dt < 0)$, and this cooling is apparently accomplished by evaporation of the liquid $(DS/Dt \sim \partial S/\partial x < 0$, at the boundary where conditions are fixed in time).

Downstream of the two-phase entry, the structure is identical to the previous superheated flow. So, the only new feature is the two-phase/superheated transition. There cannot be a temperature jump in passing forward from the two-phase region into the superheated region. Supposing to the contrary that $[T] \neq 0$, the second law (13b) requires that $F_h \geqslant 0$. Then, from the continuity equation (9b) and the definition of F_h, it is seen that

$$\frac{dF_h}{d\theta} > 0$$

in the superheated region, so $F_h > 0$ at the right end of the region. This is in contradiction with the logic of the previous section which showed that $F_h \leqslant 0$ at the right end. Hence, $[T] = 0$ at the two-phase/superheated transition.

A stopping condition is needed to determine the location of the two-phase/superheated transition. Since $[T] = 0$, the shock conditions require that $[F_v] = [F_l] = 0$. Further, since $S = 0$ and $F_l = 0$ on the superheated side, it follows that

$$F_l = (\tfrac{1}{2}\theta + P'RS^2)\,S = 0 \Rightarrow \tfrac{1}{2}\theta + P'RS^2 = 0, \tag{19}$$

on the two-phase side. Here we have ruled out the possibility that $S = 0$, since this would require a singularity (det $\mathbf{A} = 0$) in the two-phase region.

Flows which enter under two-phase conditions may have different character, depending on the value of $S(0)$. The two-phase/superheated/two-phase solution of
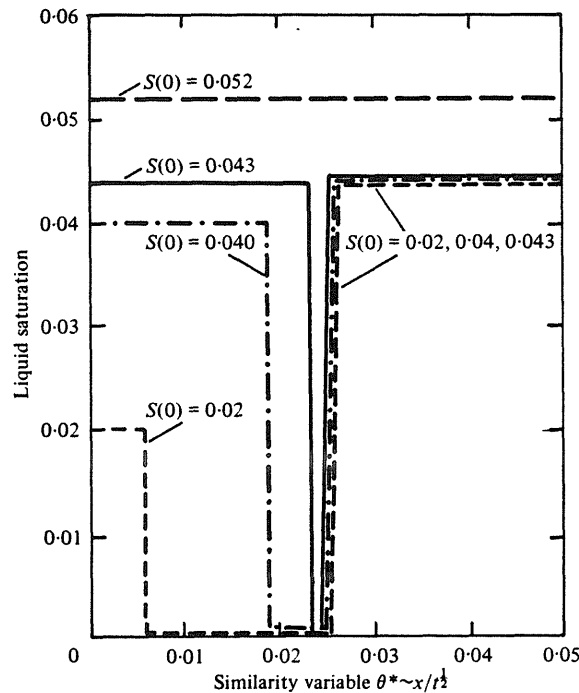
FIGURE 5. Family of saturation profiles showing imbedded superheated zone
for small enough $S(0)$.

this § 7 is valid for small $S(0)$ but fails when $S(0)$ is too large. Conversely, the strictly two-phase solution of § 4 is valid for large $S(0)$ but fails when $S(0)$ is too small. To demonstrate continuous dependence on data (i.e. on $S(0)$) and the nature of the type 7/type 4 transition, computer runs were made for a succession of $S(0)$ values, starting from $S(0) = 0$, as illustrated in figure 5. Letting θ^* be the point at which the two-phase region ends and the superheated region begins, a necessary condition for the superheated region to exist is that $F_h(\theta^*) \leqslant 0$. As $S(0)$ increases, $F_h(\theta^*)$ increases until it approaches 0. At this point, the superheated region has shrunk to zero length, since it ends when $F_h = 0$. Above this value of $S(0)$, the method of § 4 is applicable.

8. Summary

Shock-like phenomena are seen to occur in transient condensing flow through porous media. A pressure-driven, phase-changing flow will develop steep gradients in saturation and temperature, approaching shock-like behaviour when the dispersive effects of capillarity and heat conduction are small. Several different flow structures may occur, depending upon the initial (i.e. far field) and boundary (i.e. inflow) data:

(a) *Two-phase/two-phase*. Strictly two-phase flows occur when: $S(0)$ is not too small; $S(\infty)$ is not too large; and ΔT is not too large. A two-phase/two-phase saturation shock divides the flow, but thermal shock is absent.

(b) *Two-phase/subcooled liquid/two-phase*. For large $S(0)$, large $S(\infty)$, or large ΔT,

the two-phase/two-phase shock line broadens into a subcooled liquid region of finite width. Saturation shock occurs at both ends of the liquid slug, accompanied by thermal shock on the trailing end.

(c) *Two-phase/subcooled liquid.* As $S(\infty) \to 1$, the subcooled region extends to infinity and the compressibility of the liquid must be taken into account.

(d) *Two-phase/superheated/two-phase/....* For small $S(0)$, an imbedded superheated region appears near the boundary. Saturation shock occurs at both ends of the superheated zone accompanied by thermal shock on the leading end. As $S(0) \to 0$, the superheated zone extends backward to the entrance and the left-hand shock shrinks to zero leaving only a superheated/two-phase/...structure.

(e) *Superheated/two-phase/....* With $S(0) = 0$, the inflow may be superheated, causing accentuation of the superheated region. However, the width of the superheated zone depends strongly on the specific heat ratio (vapour to solid), not on the amount of superheat. As $C_V \to 0$, the superheated zone collapses into the origin, leaving a thermal-shock and a singularity (det $\mathbf{A} = 0$) at the origin.

In all cases, the transitions from one flow-structure into another depend continuously on the data. There are many possible combinations of inflow and far-field structure, for example, two-phase/superheated/two-phase/subcooled/two-phase.

Further study of the condensing flow problem is reported in another paper (Nilson & Romero 1980) where we restrict to a representative case in which the inflow and far-field are both prescribed as dry saturated-vapour states. Particular emphasis is given to the various length scales which arise in the phase-change flows. The overall penetration depth of the flow is a consequence of the gross energy-balance and momentum-balance, as embodied in the scaling of the similarity variable (used in the present figures),

$$\theta* = \frac{x}{t^{\frac{1}{2}}} \left(\frac{\epsilon\mu_v}{K\Delta P}\right)^{\frac{1}{2}} \left(\frac{\Delta S \rho_{lv}}{\rho_{v0}}\right)^{\frac{1}{2}}$$

in which

$$\Delta S = \langle \rho C \rangle_0 \Delta T / \epsilon \rho_l (h_{lv})_0 \quad \text{and} \quad \langle \rho C \rangle_0 = (1-\epsilon)\rho_m C_m + \epsilon \Delta S \rho_l C_l.$$

But, there are several boundary-layer zones within the flow field:

1. The imbedded superheated zone (as in figure 5) collapses into a singularity at $\theta = 0$, as $C_v \Delta T / h_{lv} \to 0$.

2. The precursor two-phase zone, which lies ahead of the subcooled-liquid zone, vanishes as $(\Delta S \rho_{lv}/\rho_{v0}) \to \infty$.

3. The thermal boundary-layer, which lies at the trailing edge of the subcooled-liquid zone, approaches a thermal shock as $Pe \to \infty$.

4. The increasing saturation region ($S' > 0$), which lies to the left of all shocks, collapses into the origin as $R = (\mu_v/\mu_l) \to 0$. The central shock front moves backward into the origin in this singular immobile-liquid limit.

In the companion paper (Nilson & Romero 1980) discussion of these matters is illustrated by a family of calculations concerning steam-flow in sandstone.

A complex flow structure has been encountered, even in a rather elementary single-component, one-dimensional problem. It is not, however, suggested that a detailed knowledge of the flow structure is always a critical issue in the analysis of engineering systems, particularly in the geologic applications where there is only limited knowl-

edge concerning the structure of the porous medium. Nevertheless, it is important to understand the fine structure which is predicted by the customary and well-established mathematical model. It is only through this knowledge that the appropriate engineering approximations and computational tools can be formulated and tested.

Appendix

The numerical integration procedure is based upon the well-known shooting method. Standard library routines perform the major operations: integration by a fifth-order Runga–Kutta method and iterative adjustment of the shooting parameters by a simplex minimization procedure. A general outline which includes all of the special cases is as follows:

(1) Guess the values of $P'(0)$ and θ_s.

(2) Integrate the two-phase equations (6) until $F_l = 0$.

(3) Shock according to (10) with $S = 0$ on the right.

(4) Integrate the superheated equations (8) and (9b) until $F_h = 0$.

(5) Shock according to (14a, b) with $T = T_{sat}(P)$ on the right. Here (14a, b) replaces (10) because $F_h = 0$ in (10b).

(6) Integrate the two-phase equations (6) until $\theta = \theta_s$.

(7) Shock according to (10) with $S = 1$ on the right.

(8) Integrate the subcooled liquid equations (8) and (9a) until $T = T_{sat}(P)$.

(9) Shock according to (14a, b) with $T = T_{sat}(P)$ on the right.

(10) Integrate the two-phase equations (6) out to large θ.

A minimization procedure adjusts the values of the shooting parameters, $P'(0)$ and θ_s, until both of the far-field boundary conditions are satisfied.

Although it is possible that all of the integration steps might apply to a particular flow, there are also a number of subset procedures which generate the simpler flows that are described in the individual sections of the paper.

§4. Two-phase/two-phase	(1), (6), (9)–(10)
§5. Two-phase/subcooled/two-phase	(1), (6)–(10)
Two-phase/subcooled	·(1), (6)–(8)
§6. Superheated/two-phase...	(1), (4)–(7), (8), (9), (10)
§7. Two-phase/superheated...	(1)–(7), (8), (9), (10)

The presence of the subcooled slug, (7) and (8), is optional in §§6 and 7.

REFERENCES

BEAR, J. 1970 Two-liquid flows in porous media. *Advances in Hydroscience* **6**, 141–251.

BROWNELL, D. H., GARG, S. K. & PRITCHETT, J. W. 1977 Governing equations for geothermal reservoirs. *Water Resources Res.* **13**, 929–934.

CHENG, P. 1978 Heat transfer in geothermal systems. *Adv. Heat Transfer* **14**, 1–106.

482   *L. A. Romero and R. H. Nilson*

FAYERS, F. J. 1962 Some theoretical results concerning the displacement of a viscous oil by a hot fluid in a porous medium. *J. Fluid Mech.* **13**, 65–76.

LAUDE, J. M. & MORRISON, F. A. 1979 Stability of flow from a nuclear cavity. *J. Fluid Engng* **101**, 335–340.

MILLER, C. A. 1975 Stability of moving surfaces in fluid systems with heat and mass transfer, III, Stability of displacement fronts in porous media. *A.I.Ch.E. J.* **21**, 474–479.

MORRISON, F. A. 1973 Transient multiphase multicomponent flow in porous media. *Int. J. Heat Mass Transfer* **16**, 2331–2342.

NIKOLAEVSKII, V. N. & SOMOV, B. E. 1978 Heterogeneous flows of multi-component mixtures in porous media. *Int. J. Multiphase Flow* **4**, 203–217.

NILSON, R. H. & ROMERO, L. A. 1980 Self-similar condensing flow in porous media. *Int. J. Heat Mass Transfer* **23**, 1461–1470.

SCHEIDEGGER, A. H. 1974 *The Physics of Flow Through Porous Media*. University of Toronto Press.

SETTARI, A. & AZIZ, K. 1975 Treatment of nonlinear terms in the numerical solution of partial differential equations for multiphase flow in porous media. *Int. J. Multiphase Flow* **1**, 817–844.

SLATTERY, J. C. 1972 *Momentum, Energy, and Mass Transfer in Continua*. McGraw-Hill.

WEINSTEIN, H. G., WHEELER, J. A. & WOODS, E. G. 1977 Numerical model for thermal processes. *Soc. Petroleum Eng. J.* February, 65–77.

WHITAKER, S. 1977 Simultaneous heat, mass, and momentum transfer in porous media: A theory of drying. *Adv. Heat Transfer* **13**, 119–203.

WOODING, R. A. & MOREL-SEYTOUX, H. J. 1976 Multiphase fluid flow through porous media. *Ann. Rev. Fluid Mech.* **8**, 233–274.

SELF-SIMILAR CONDENSING FLOWS IN POROUS MEDIA*

R. H. NILSON

Fluid and Thermal Sciences Division

and

L. A. ROMERO

Applied Mathematics Division, Sandia National Laboratories†, Albuquerque, NM 87185, U.S.A.

Abstract – Similarity solutions are obtained for the propagation of a condensation wave into an initially dry porous matrix which receives an inflow of saturated vapor due to a step increase in temperature and pressure at the boundary. The generalized Darcy (low Reynolds number) formulation of two-phase flow leads to hyperbolic/parabolic equations in which capillarity and heat conduction are suppressed in order to emphasize the shock-like behavior. Application of the $x/\sqrt{t}$ similarity transformation gives ordinary differential equations which are solved by shooting methods, using jump-balance (Rankine–Hugoniot) conditions to preserve discontinuities in saturation (quality), pressure gradient and sometimes temperature. The distribution of condensate (saturation) is wave-shaped, with a forward-facing shock on the leading side. For a small temperature difference, there is little condensate and it is nearly immobile; the saturation shock lies close to the boundary, and the outer region is described by a reduced system of equations. With increasing temperature difference, the shock moves forward into the flow and gains in strength until the medium is liquid-full behind the shock. Beyond this, the shock splits into a pair of back-to-back shocks separated by a subcooled liquid slug. The considered prototypic problem is representative of a broad class of two-phase flows which occur in energy-related and geologic applications.

NOMENCLATURE

Independent variables

$x, X = x/L$;	position;
$\tau, \mathcal{T} = \tau/\tau_0$,	time $[\tau_0 = \Gamma \epsilon L/u_0]$;
$\theta, \Theta = \theta/R$,	similarity variable θ $= X/\sqrt{\mathcal{T}}$.

Dependent variables

$c, C = c\Delta T/(h_{lv})_0$,	specific heat;
$h, H = h/(h_{lv})_0$,	enthalpy $[(h_{lv})_0 = h_{lv}(P_0)]$;
$k, K = k/k_0$,	thermal conductivity;
$p, P = (p - p_0)/\Delta p$,	pressure $(\Delta p = p_1 - p_0)$;
$s, S = s/\Delta s$,	saturation: liquid fraction by volume
$t, T = (t - t_0)/\Delta t$,	temperature $(\Delta t = t_1 - t_0)$;
$u, U = u/u_0$,	Darcy velocity $(u_0$ $= \kappa \Delta p/L\mu_v.)$;
$v, V = v/u_0$,	interstitial velocity;
$\kappa_l, K_l = \kappa_l/\Delta s^3$,	relative permeability of liquid;
$\kappa_v, K_v = \kappa_v$,	relative permeability of vapor;
$\rho, P = \rho/N\rho_0$,	density $[\rho_0 = \rho_v(p_0, t_0)]$;
$\phi, \Phi = \phi t_0/(h_{lv})_0$,	entropy;
$\langle \rho c \rangle, \langle \rho C \rangle,$	
$= \langle \rho c \rangle / \langle \rho c \rangle_0$,	bulk specific heat, $\langle \rho c \rangle$ = $(1 - \epsilon)\rho_m c_m + \epsilon s \rho_l c_l,$ $\langle \rho c \rangle_0$ $= (1 - \epsilon)\rho_m c_m + \epsilon \Delta s \rho_l c_l.$

Physical constants

$\tilde{R}$,	gas constant;
δ,	characteristic pore dimension;
ϵ,	porosity;
κ,	permeability;
μ,	viscosity.

Dimensionless parameters

$N = p_1/p_0$,	pressure ratio;
$Pe = \dfrac{N\rho_0 u_0 h_{lv}}{\langle k \rangle \Delta t/L}$,	Peclet number;
$R = \dfrac{\mu_v}{\mu_l} \dfrac{\rho_l}{\rho_0} \dfrac{\Delta s^3}{N}$,	relative liquid mobility;
$Re = \dfrac{u_0 \delta \rho_0}{\mu_v}$,	Reynolds number;
$\Gamma = \dfrac{\Delta s \rho_{lv}}{N\rho_0}$,	relative density change;
$\beta = \dfrac{\epsilon \rho_l c_l}{(1 - \epsilon)\rho_m c_m}$,	specific heat ratio;
$\Delta s = \dfrac{\langle \rho c \rangle_0 \Delta t}{\epsilon \rho_l (h_{lv})_0}$,	nominal liquid saturation;
$\lambda = \Delta t/t_0$,	relative temperature change.

1. INTRODUCTION

CONDENSING flows in porous media occur in a number of energy-related applications. Steam injection into oil fields produces a condensation wave which heats the oil sands and reduces crude oil viscosity. *In situ*

R. H. NILSON and L. A. ROMERO

combustion processes such as oil shale retorting and coal gasification are accompanied by propagating zones of evaporation and condensation. Hypothetical reactor accidents may involve boiling and condensation in fragmented debris and in porous concrete which is subjected to intense heating. Other examples arise in geothermal systems and in the containment of underground nuclear tests.

A distinctive feature of pressure-driven condensing flows in porous media is the occurrence of a sharp, wave-like saturation front. The steep gradients of a condensation front are apparent in numerical simulations such as those of Morrison [1] and Weinstein, Wheeler and Woods [2]. However, the customary integration techniques permit smearing of the saturation shocks [3] in a manner analogous to the artificial viscosity effects of numerical gas dynamics. Also, the previous studies include application specific aspects such as multiple chemical species in either the liquid or the vapor phase, which de-emphasize the generic features of condensing flows in porous media. In contrast, the present study is concerned with a more fundamental condensation wave, and our primary purpose is to describe the mathematical and physical features of the shock phenomena.

The prototype condensation problem to be considered is the one-dimensional, transient flow of a compressible pure substance. Hot, dry vapor flows into a cold, initially dry, solid matrix, therein forming condensate which flows concurrently with the vapor. Energy transfer occurs by convection and condensation, and for each fluid phase the balance between viscous and pressure forces is accounted for by the generalized Darcy law which incorporates relative permeability functions. To emphasize the shock-like behavior, capillary pressure and heat conduction are suppressed.

The parabolic/hyperbolic transport equations reduce to ordinary differential equations under the similarity transformation, $\theta = x/\sqrt{\tau}$. Since the system is only third order but has four independent boundary conditions, a saturation shock must occur. The ordinary differential equations are solved by a shooting method which uses jump-balance relations in crossing the shocks. A family of steam flows in geologic media serves to illustrate solution behavior over a broad range of the parameters. A summary of the main results is given at the end of the paper.

2. FORMULATION

The transport equations for transient, one-dimensional, two-phase, compressible flow of a pure substance in a porous medium are as follows [4]:

$$\frac{\partial}{\partial \tau}\{\epsilon s \rho_l + \epsilon(1-s)\rho_v\} + \frac{\partial}{\partial x}\{\rho_l u_l + \rho_v u_v\} = 0$$

$$\frac{\partial}{\partial \tau}\{\epsilon s \rho_l h_l + \epsilon(1-s)\rho_v h_v + (1-\epsilon)\rho_m h_m\}$$

$$+ \frac{\partial}{\partial x}\{\rho_l h_l u_l + \rho_v h_v u_v\}$$

$$- \frac{\partial}{\partial x}\left\{\langle k \rangle \frac{\partial t}{\partial x}\right\} - \frac{Dp}{D\tau} = 0. \quad (1)$$

The subscripts l, v and m, respectively, refer to the liquid, the vapor, and the solid matrix; s is the local volume fraction of the pore space which is occupied by a liquid, ϵ is porosity, $\langle k \rangle$ is bulk thermal conductivity of the fluid saturated medium, and the other symbols have their usual meaning. The apparent velocities, u_l and u_v, represent average volumetric flow rates per unit sectional area of the medium. Darcy's law serves as a constitutive equation which relates velocity to pressure gradient in low Reynolds number flow ($Re \equiv u\delta/\nu$) where viscous forces are in balance with pressure forces,

$$u_v = -\kappa_r \frac{\kappa}{\mu_v} \frac{\partial p}{\partial x}$$

$$u_l = -\kappa_l \frac{\kappa}{\mu_l} \frac{\partial p}{\partial x}. \quad (2)$$

The relative permeability functions κ_r and κ_l are introduced as a means of extending Darcy's law to a two-phase flow. The utility of this approach derives from the experimental observation that κ_l and κ_r are, for a given medium, primarily functions of saturation alone [5]. The present study will make use of analytical expressions similar to those given by Scheidegger [6],

$$\kappa_l = s^3 \quad \kappa_r = 1 - s, \quad (3)$$

with the understanding that these functions are only representative of the expected behavior. In addition, it is assumed that the fluid and the solid are in local thermal equilibrium; that buoyancy forces are negligible, and that interfacial tension is accounted for implicitly through the relative permeability functions.

Thermodynamic relationships are described by the conventional analytical approximations. The liquid is incompressible; the gas is ideal, $\rho_r = p/\bar{R}t$, and in two-phase regions, the pressure and temperature are related by the Clausius–Clapeyron equation

$$\frac{dp}{dt} = \frac{h_{lv}\rho_v}{t}\frac{\rho_l}{\rho_{lv}} \simeq \frac{ph_{lv}}{\bar{R}t^2}\frac{\rho_l}{\rho_{lv}} \quad (4)$$

in which $h_{lv} = h_v - h_l > 0$ and $\rho_{lv} = \rho_l - \rho_v > 0$. The enthalpies h_l, h_v and h_m of the liquid, the saturated vapor and the matrix each depend linearly on temperature with respective slopes (specific heats) c_l, c_r and c_m. To eliminate secondary parameters, let $c_r = 0$, and suppose that the viscosities, μ_l and μ_r, and the matrix properties, κ and ϵ, are constants.

Regarding initial and boundary conditions, consider the case of a semi-infinite porous medium which initially contains dry saturated vapor at a temperature t_0 and corresponding saturation pressure p_0. The transient is begun by suddenly subjecting the boun-

dary to an external environment which contains dry saturated vapor at t_1 and p_1, such that $\Delta t = t_1 - t_0 > 0$, and $\Delta p = p_1 - p_0 > 0$. Condensation occurs as the hot, high pressure fluid penetrates into the cold, porous matrix.

Upon normalization (as defined in the Nomenclature) and introduction of Darcy's law, the conservation equations are rewritten in a form which isolates the effects of phase change and emphasizes the primary dependent variables (P, T, S)

$$\frac{\partial S}{\partial \tau} - \frac{\partial}{\partial X}\left\{(P_v\mathcal{K}_v + R\mathcal{K}_l)\frac{\partial P}{\partial X}\right\} = -\frac{1}{\Gamma}(1 - S\Delta s)\frac{\partial P_v}{\partial \tau}$$

$$\langle PC\rangle\frac{\partial T}{\partial \tau} - H_{lv}\left\{\frac{\partial S}{\partial \tau} - R\frac{\partial}{\partial X}\left(\mathcal{K}_l\frac{\partial P}{\partial X}\right)\right\}$$
$$-\left(\frac{\Delta s\beta}{1 + \Delta s\beta}\right)R\mathcal{K}_l\frac{\partial P}{\partial X}\frac{\partial T}{\partial X}$$
$$= Pe^{-1}\frac{\partial}{\partial X}\left(\langle K\rangle\frac{\partial T}{\partial X}\right) + \Gamma^{-1}\frac{\tilde{R}t_0}{\epsilon h_{lv}}\frac{(N-1)}{N}\frac{DP}{D\tau} \quad (5)$$

$$\langle PC\rangle = \frac{(1 + \Delta s\beta S)}{(1 + \Delta s\beta)}; \quad \mathcal{K}_v = 1 - \Delta sS; \quad \mathcal{K}_l = S^3$$

$$\rho_v = \frac{1 + (N-1)P}{N}\left\{\frac{1}{1 + \lambda T}\right\}$$

$$H_{lv} = 1 - \left(\frac{\Delta s\beta}{1 + \Delta s\beta}\right)T.$$

Here and hereafter we make the approximation that $\rho_l/\rho_{lv} \simeq 1$. The principal parameters are N, λ and β as defined in the Nomenclature; as well as the characteristic saturation $\Delta s = \langle \rho c\rangle_0\Delta t/\epsilon\rho_l(h_{lv})_0$, which represents the amount of condensation nominally required to produce the temperature change Δt; and the relative liquid mobility $R = \mu_v\rho_l\Delta s^3/\mu_l N\rho_0$, which characterizes the relative significance of mass flow in the liquid and vapor phases. An important scaling consideration is the choice of a characteristic time τ_0

$$\tau_0 = \Gamma\frac{\epsilon L}{u_0}, \quad \Gamma = \frac{\Delta s\rho_{lv}}{N\rho_0} \quad (6)$$

which recognizes that the two-phase wave speed is very slow ($\Gamma \gg 1$) compared to a single-phase pressure wave (for which $\tau_0 = \epsilon L/u_0$, [17]), because the representative density change is $\Delta s\rho_{lv}$ rather than $N\rho_0$. Since Γ and the Peclét number, Pe, are usually very large, we can safely neglect: the time derivative of vapor density, the material derivative of pressure and the heat conduction which all appear on the RHS of the above transport equations.

The partial differential equations cannot be classified as any one of the three basic types. Superheated vapor regions are generally parabolic. Subcooled liquid regions generally appear to be elliptic because the compressibility is negligible. Two-phase regions are of a mixed parabolic/hyperbolic type [8], but become strictly parabolic as R (the liquid mobility) $\to 0$. The hyperbolic character is therefore attributed to

liquid mobility and the dependence of relative permeability on saturation.

Under the similarity transformation [1, 7, 9]

$$\theta \equiv \frac{X}{\sqrt{\tau}} = \frac{x}{\sqrt{\tau}}\left(\Gamma\frac{\epsilon\mu_v}{\kappa\Delta p}\right)^{1/2} \quad (7)$$

the partial differential equations become ordinary differential equations

$$\frac{\theta}{2}S' + \{(P_v\mathcal{K}_v + R\mathcal{K}_l)P'\}' = 0 \quad (8)$$

$$\frac{\theta}{2}\langle PC\rangle T' + H_{lv}(P_v\mathcal{K}_vP')'$$
$$+ \left(\frac{\Delta s\beta}{1 + \Delta s\beta}\right)R\mathcal{K}_lP'T' = 0 \quad (9)$$

subject to the boundary conditions $P(0) = T(0) = 1$, $S(0) = 0$; $P(\infty) = T(\infty) = S(\infty) = 0$.

If shock-like discontinuities occur at a singular point $\theta = \theta_s$, local conservation must be enforced through the jump-balance [10] or Rankine–Hugoniot conditions. The jump-balance of momentum, roughly $[p] = \text{ord}\{\rho u^2\}$, usually admits a first-order pressure jump at a shock, but the estimates $u \sim \text{ord}\{\Delta p\kappa/\mu L\}$ and $\kappa \sim \text{ord}\{\delta^2\}$ suggest that $[P] \sim \text{ord}\{Re\ \delta/L\}$, so that $[P]$ becomes negligible once the flow has penetrated deep enough ($L/\delta \gg Re$) to be considered asymptotically self-similar (i.e., independent of Re, which is the Darcy assumption). The jump-balances of mass and energy are then

$$[\epsilon(1 - s)P_v(V_v - V_s) + \epsilon s P_l(V_l - V_s)] = 0 \quad (10)$$

$$[\epsilon(1 - s)P_vH_v(V_v - V_s) + \epsilon s P_lH_l(V_l - V_s)$$
$$+ (1 - \epsilon)P_mH_m(-V_s)] \quad (11)$$
$$= Pe^{-1}\left[K\frac{dT}{d\theta}\right]$$

in which $V_s = (dx/dt)/u_0$ is the interface velocity of the discontinuity, and $V_v = U_v/(1 - s)\epsilon$ and $V_l = U_l/s\epsilon$ are the so-called pore velocities or interstitial velocities of the liquid and vapor. The second law of thermodynamics must also be satisfied in crossing a shock

$$[\epsilon(1 - s)\Phi_vP_v(V_v - V_s) + \epsilon s\Phi_lP_l(V_l - V_s)$$
$$+ (1 - \epsilon)\Phi_mP_m(-V_s)] \quad (12)$$
$$\geq Pe^{-1}\left[\frac{K}{1 + \lambda T}\frac{dT}{d\theta}\right].$$

Since P does not change in crossing, changes in the specific entropy ϕ are calculated as $d\phi = dh/t$ or $d\phi = c_l dt/t$ and, hence,

$$[\Phi_i] = C_i[\ln(1 + \lambda T)]/\lambda; \quad i = l, v, m.$$

As in the differential equations, heat conduction will be ignored in the jump equation under the supposition that $Pe \gg 1$.

3. WEAKLY-SHOCKED, STRICTLY TWO-PHASE FLOW: MODERATE N

Since saturation conditions, $T = T_{sat}(P)$, are prescribed at both ends of the interval, it is reasonable to suspect that the intermediate states might also be saturated. Such strictly two-phase flows are found to occur, provided that the temperature difference (or pressure ratio) is sufficiently small, that a liquid-full condition does not occur at any cross section.

Within two-phase regions, the temperature and pressure are related by the Clausius–Clapeyron equation [now in a dimensionless form which reflects the boundary conditions: $T(P = 0) = 0$, $T(P = 1) = 1$]

$$\frac{dP}{dT} = \frac{\{1 + (N - 1)P\}H_{lv}}{(1 + \lambda T)^2}\left\{\int_0^1 \frac{dP}{\{1 + (N - 1)P\}}\middle/ \int_0^1 \frac{H_{lv}\,dT}{(1 + \lambda T)^2}\right\} \quad (13)$$

and the conservation equations reduce to a third-order system of the form

$$A\begin{bmatrix} P'' \\ S' \end{bmatrix} = \mathbf{b} \quad (14)$$

subject to four independent boundary conditions,

$$P(0) = 1,\ S(0) = 0;\quad P(\infty) = 0,\ S(\infty) = 0. \quad (15)$$

The system is therefore overconstrained.

A sign change of the determinant, det A, suggests the presence of a shock. By application of the boundary conditions, it can be seen that det $A > 0$, as $\theta \to \infty$. Conversely, at $\theta = 0$ (where the equations are singular), an expansion in powers of $\theta^{1/2}$ shows that

$$S = \frac{\theta^{1/2}}{\sqrt{(-6P_0'R)}} + \dots \quad (16)$$

$$P' = P_0'\left\{1 + \Delta s\frac{\theta^{1/2}}{\sqrt{(-6P_0'R)}}\right\} + \dots \quad (17)$$

$$\det A = 0, \quad \text{and}\ \frac{d}{d\theta}(\det A) < 0 \quad \text{at}\ \theta = 0.$$

Thus, det A must change sign in crossing the interval.

Allowance is made for a shock on the interior of the two-phase interval. Since both phases are present on

both sides of the shock, $[P] = 0$ implies $[T] = 0$, and hence, $[\rho_i] = [H_i] = 0$, $i = l, v, m$. Thus, with $Re \ll 1$ and $Pe \gg 1$, the jump-balances of mass and energy jointly require continuity of both the vapor flux and the liquid flux

$$[(1 - S\Delta s)(V_v - V_s)] = 0$$

$$\Rightarrow \left[\kappa_v\left(P' + \frac{\theta}{2}\Gamma^{-1}\right)\right] = 0 \Rightarrow [\kappa_v P'] \simeq 0$$

$$[S\Delta s(V_l - V_s)] = 0 \Rightarrow \left[R\kappa_l P' + \frac{\theta}{2}S\right] = 0. \quad (18)$$

This means that there is no local phase change at the shock and that the second law is automatically satisfied through equality.

Letting 'hatted' quantities represent function values downstream of the shock, the two conditions can be combined as follows to eliminate $\hat{P}'$

$$\hat{\kappa}_v\left\{\frac{\theta}{2} + RP'(\hat{S}^2 + S^2 + S\hat{S})\right\} + R\hat{\kappa}_l P'\Delta s = 0. \quad (19)$$

Which, on simplification, provides a quadratic in S having only one positive, real root. Thus, for given θ, S, P, and P' there is a unique shock strength. Once $\hat{S}$ is available, $\hat{P}'$ is readily determined from the first shock condition. It is interesting to note that if $S = \hat{S}$, the above requirement reduces to the condition for det $A = 0$. It can also be shown that det A has the necessary sign change in crossing the shock, provided that $[S] = \hat{S} - S < 0$. So, the two-phase saturation shock must face forward, although not as a consequence of entropy change.

The system of equations is solved numerically by a shooting method. For chosen values of $P'(0) = \alpha$, a three-term expansion from the singular origin is followed by rightward numerical integration, stopping at a presumed shock location θ_s. Integration is then restarted with values of $\hat{S}$ and $\hat{P}'$ determined from the shock conditions. The two shooting parameters α and θ_s are adjusted until the asymptotic boundary conditions, $P(\infty) = S(\infty) = 0$, are both satisfied.

As an illustrative family of solutions, consider the case of dry saturated steam flowing into sandstone (β

Table 1. A family of steam flows

	Configuration parameters			Shock locations		Pressure gradient	
N	Δs	R	λ	(θ_l)	θ_s	P_0' $(R \to 0)$	
$N \to 1$	0	0	0			$(-1/\sqrt{\pi})$	
2	0.034	0.009	0.040		0.035	-0.533	(-0.554)
5	0.084	0.083	0.098		0.435	-0.512	(-0.557)
10	0.127	0.185	0.148		0.961	-0.505	(-0.574)
15	0.161	0.292	0.180		1.17	-0.505	(-0.589)
19.5	0.184	0.371	0.202	(1.18)	1.18	-0.507	(-0.601)
100	0.359	0.924	0.360	(1.00)	1.13	-0.515	(-0.726)
1000	0.855	2.56	0.688	(0.91)	1.21	-0.525	(-2.161)
2500	1.26	4.38	0.874	(0.89)	1.28	-0.521	(∞)
5000	1.75	7.31	1.04	(0.89)	1.34	-0.510	
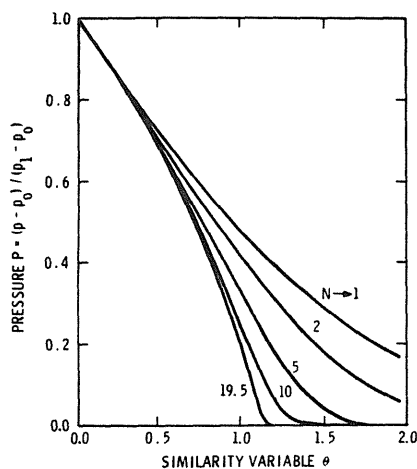
FIG. 1. Pressure profiles for various pressure ratios $N = p_1/p_0$.

$\simeq$ 0.6) and suppose that the initial temperature in the medium is $530°R$, corresponding to an initial pressure of $P_0 = 0.025$ atm. For such a choice of fluid, medium and initial state, Δs, R, and λ become increasing functions of N. The parameter values corresponding to particular choices of N are listed in Table 1 along with the shock location θ_s and the surface pressure gradient $P'(0)$ which were determined. Figures 1 and 2 illustrate the results.

The pressure profiles of Fig. 1 lie within a rather narrow range of θ which (based on the scaling considerations) suggests that the process is largely controlled by mass transfer in the vapor phase. As $N \to 1$ the pressure is given by $P(\theta) = \text{erfc}(\theta/2)$, and for large N the pressure profiles become proximate. The local condensation rate, $(\rho_v K_v P')'$, is non-negative everywhere in the flow and reaches a maximum in the vicinity of the pressure inflection. With increasing N the saturation shock becomes more pronounced and moves forward into the flow. There is a limiting
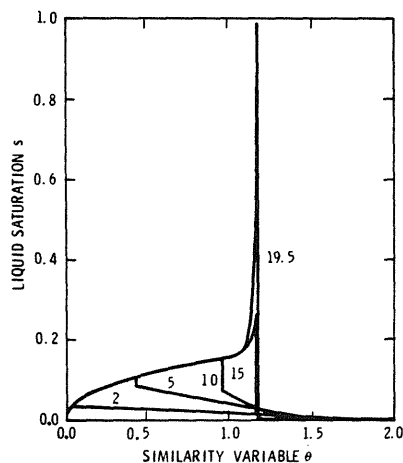
FIG. 2. Saturation profiles for various pressure ratios N.

pressure ratio $\tilde{N}$ (here $\tilde{N} \simeq 19.5$) for which the pore space becomes liquid-full behind the shock.

It is generally true that the low-velocity liquid is overtaken by the shock and that the high-velocity vapor passes forward through the shock. As $N \to \tilde{N}$ the shock conditions (for $\Gamma \to \infty$) require that $P'_+ \to 0$ (suppressing a slight precursor ahead of the shock) and that $V_{l^-} \to V_s$, indicating that the wall of liquid advances with the shock velocity.

4. UNSHOCKED IMMOBILE-LIQUID LIMIT: SMALL N

When N is small, there is little condensate, it is relatively immobile, and the shock lies close to the surface. A secondary, inner scale in θ results from the disparity in phase velocities, as evident both in the saturation profiles of Fig. 2 and in the $(\theta/R)^{1\,2}$ terms which appear in the inner series expansion. Such behavior suggests the existence of an outer, down-stream solution complemented by a singular-perturbation boundary-layer.

In the limit of vanishing liquid mobility ($R \to 0$) the transport equations reduce to the following form

$$\frac{\theta}{2}\langle\rho C\rangle P' + \frac{dP}{dT} H_{lv}(\rho_v K_v P')' = 0 \qquad (20)$$

$$\frac{dT}{H_{lv}} = \frac{dS}{\langle\rho C\rangle} \quad \text{or} \quad S = \frac{T}{1 + \Delta s\beta(1 - T)}. \qquad (21)$$

The first equation describes the transient, Darcy flow of a vapor with a large apparent compressibility because of the phase change. The second ensures energy conservation by attributing local temperature change to local condensation, whereupon T becomes an explicit function of S. With $S[T(P)]$ now available in analytical form, it is only necessary to solve a second-order, parabolic equation for the pressure. The dependence of S on P is such that the two outer boundary conditions are simultaneously satisfied if $P(\infty) = 0$, but the inner boundary conditions become incompatible. In choosing to satisfy the pressure condition $P(0) = 1$, it must also be accepted that $S(0) = 1$ and the surface can no longer be dry. This change in boundary conditions is physically reasonable because the condensate which forms near the origin must now remain in place.

The immobile liquid approximation is illustrated in Fig. 3 by a family of saturation profiles corresponding to parameter values (N, Δs, and λ) of Table 1, except that $R = 0$ is now imposed. A comparison with the liquid-mobile solutions from Fig. 2 emphasizes the typical singular perturbation behavior [11]. For small R, there is a narrow inner region where saturation gradients are steep, while the outer region remains nearly unaffected by the boundary layer and, to a good approximation, still satisfies the condition $S \to 1$ as $\theta \to 0$. As apparent in comparing the last two columns of Table 1, the immobile liquid approximation ($R \to 0$) gives a good approximation to the inflow pressure gradient.
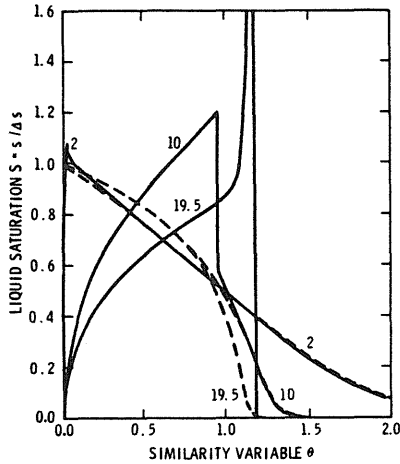
FIG. 3. Immobile liquid approximation (dotted lines) compared with shocked solutions (solid lines) for various pressure ratios $N = p_1/p_0$.

The most natural description of the boundary layer, if it exists, should involve a rescaling of the variables and matching with the outer region, a matter not pursued here. It is, however, interesting to replot the saturation profiles using $\Theta = \theta/R$ as the independent variable. For small Θ, all of the curves are nearly coincident, and as R becomes small ($N \to 1$), the shock position approaches a nonzero limit.

5. STRONGLY-SHOCKED, IMBEDDED-SLUG FLOW: LARGE N

Recall from Section 3 that for large enough N (e.g. $N \to \tilde{N} = 19.5$ in Fig. 2) the medium becomes liquid-full behind the forward-facing shock. When N exceeds $\tilde{N}$, the peak of the saturation wave· broadens into a subcooled liquid zone. Within the subcooled zone $\theta_l < \theta < \theta_s$ the saturation is uniform at $S = 1/\Delta s$, but P and T are independently variable, so that the transport equations become

$$P'' = 0 \tag{22}$$

$$\frac{\Delta s\beta}{1 + \Delta s\beta}\left(RK_lP' + \frac{\theta}{2}S\frac{1+\beta}{\beta}\right)T' + \frac{1}{Pe}T'' = 0.$$

The pressure therefore decreases linearly in crossing the slug (i.e. velocity is uniform), and with conduction neglected (i.e. $Pe \to \infty$) the temperature must be uniform within the slug.

Allowance is now made for shocks both on the leading side and on the trailing side of the liquid slug. Letting hatted quantities refer to the slug side (wet side) of either shock and letting $[P] \equiv P(\theta_+) - P(\theta_-) = 0$, $Pe \to \infty$, and $\Gamma \to \infty$; conservation of mass and energy, respectively, require that

$$\left[RK_lP' + \frac{\theta}{2}S\right] + [\rho_vK_vP'] = 0 \tag{23}$$

$$\frac{\Delta s\beta}{1 + \Delta s\beta}[T]\left(R\hat{K}_l\hat{P}' + \frac{\theta}{2}\hat{S}\frac{1+\beta}{\beta}\right)$$
$$+ H_{lv}[\rho_v K_v P'] = 0. \tag{24}$$

Phase change is, therefore, allowable, provided that the change in liquid flux relative to the shock is offset by the change in vapor flux and that the enthalpy of phase change accounts for the temperature jump of the mass flowing through the shock, including the mass of the solid phase. In addition, it is necessary to satisfy the second-law of thermodynamics (entropy-jump inequality)

$$\frac{\Delta s\beta}{1 + \Delta s\beta}\frac{[\ln(1 + \lambda T)]}{\lambda}\left(R\hat{K}_l\hat{P}' + \frac{\theta}{2}\hat{S}\frac{1+\beta}{\beta}\right)$$
$$+ \frac{H_{lv}}{1 + \lambda T}[\rho_v K_v P'] \le 0, \tag{25}$$

which reflects the identity, $\Phi_{lv} = H_{lv}/(1 + \lambda T)$. Finally, there is a temperature-jump inequality, $\hat{T} \le T$, which ensures that the slug side is not superheated.

In checking the necessity and the admissibility of temperature jumps, it is found that $T = T_{sat}[P(\theta_s)]$ everywhere within the slug. The argument consists of two main points:

(1) There must be a downward temperature jump at θ_l. Suppose to the contrary that $T = T_{sat}(P)$ at θ_{l+}. Then, upon moving rightward into the slug, T stays constant (from energy equation) while $T_{sat}(P)$ decreases as the pressure falls. So, $T_{sat}(P)$ falls below T, suggesting superheated conditions in a liquid region — a contradiction.

(2) There cannot be a temperature jump at θ_s. At any shock location, θ, the jump conditions on energy and entropy jointly require that

$$\left\{[\ln(1 + \lambda T)] - \frac{[1 + \lambda T]}{(1 + \lambda T)}\right\}$$
$$\times\left(R\hat{K}_l\hat{P}' + \frac{\theta}{2}\hat{S}\frac{1+\beta}{\beta}\right) \le 0. \tag{26}$$

Now, at θ_l the slug side is ahead of the shock, so that the script brackets above cannot be positive. Conversely, at θ_s the slug side is behind, so that the script brackets cannot be negative. Thus, a temperature jump is second-law admissible at θ_l and/or at θ_s, only if

$$R\hat{K}_l\hat{P}' + \frac{\theta}{2}\hat{S}\frac{1+\beta}{\beta} \ge 0$$

and/or $\tag{27}$

$$R\hat{K}_l\hat{P}' + \frac{\theta}{2}\hat{S}\frac{1+\beta}{\beta} \le 0$$

at θ_l and θ_s, respectively. Since the first condition must be satisfied [because (1) above demands a T-jump at θ_l], and since $\theta_s > \theta_l$, $\beta > 0$, and $R K_l \hat{P}'$ is the same at θ_l and θ_s (from continuity); it is impossible to satisfy the later inequality. There can be no temperature jump at θ_s.

In view of the above observations and the previously noted absence of an internal temperature gradient, it is concluded that $T = T_{sat}[P(\theta_s)]$ on $[\theta_{l+}, \theta_s]$.

Since temperature jump cannot occur at the leading edge, θ_s, phase change cannot occur and the energy balance requires that $\rho_v \kappa_v P' = 0$ at θ_{s+}. The density cannot vanish; and if $\kappa_{v+} = 0$, then $S = 1/\Delta s$ on both sides, and det A does not change sign in crossing. Thus, it must be that $P'_+ = 0$, whereupon S'_+ vanishes along with all of the higher-order derivatives, ruling out downstream variation in the dependent variables. So, in view of the boundary conditions, it must also be true that

$$P = 0, \ S = 0, \ T = 0 \quad \text{at } \theta_{s+} \qquad (28)$$

and it only remains to satisfy the jump-mass balance which now reads as

$$R\hat{\kappa}_l\hat{P}' + \frac{\theta_s}{2}\hat{S} = 0 \quad \text{at } \theta_{s-}. \qquad (29)$$

This is recognized as the liquid-wall condition, $\hat{V}_l = V_s$, which previously accompanied the vanishing (suppressed) precursor in the limiting case as $N \to \tilde{N}$. So, the slug solution appears to be a continuous extension of the earlier two-phase flows.

Now, consider the trailing shock which lies behind the slug at θ_l. A temperature drop, $[T] = -T(\theta_l)$, must occur here to ensure subcooled conditions throughout the slug. Using this, the jump-balances of mass and energy are alternatively combined to give both of the following expressions:

$$\rho_v \kappa_v P' + T\frac{\Delta s\beta}{1 + \Delta s\beta}\left\{R\kappa_l P' + \left(S + \frac{1}{\Delta s\beta}\right)\frac{\theta}{2}\right\} = 0$$

$$\qquad (30)$$

$$\hat{P}' = \frac{\Delta s^3}{R}\left\{H_{lv}\left(R\kappa_l P' + \frac{\theta}{2}S\right)\right.$$

$$\left. - \theta T\frac{(1 + \beta)}{2(1 + \Delta s\beta)} - \frac{H_{lv}\theta}{2\Delta s}\right\}.$$

The first is a compatibility condition which must be satisfied on the upstream side of the shock. It is used to determine the shock location. The second gives $\hat{P}'$ in terms of upstream data. This is all that is needed to resume downstream integration since $\hat{P} = P$, $\hat{T} = 0$, and $\hat{S} = 1/\Delta s$.

The computational procedure for a doubly shocked flow is simple because there is only one shooting parameter. For chosen $\alpha = P'(0)$, the two-phase equations are integrated forward until the compatibility condition is satisfied, thereby determining θ_l. Then, $\hat{P}'(\theta_l)$ is calculated from the upstream data. Recalling that $P'' = 0$ in the slug and that $P(\theta_s) = 0$, the leading shock must lie at $\theta_s = \theta_l - P(\theta_l)/\hat{P}'(\theta_l)$. Then, since $\hat{P}'(\theta_s) = \hat{P}'(\theta_l)$, there is sufficient information to indicate whether or not the remaining shock condition $(\hat{V}_l = V_s)$ is satisfied at θ_s; this being the sole criterion for iterative adjustment of α.

Doubly-shocked solutions are illustrated by the
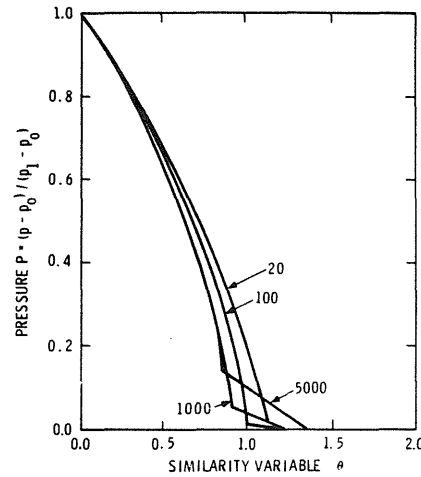
FIG. 4. Pressure profiles for various pressure ratios $N = p_1/p_0$.

pressure and saturation profiles of Figs. 4 and 5. With increasing N, the slug broadens (see Table 1), and the pressure rises at θ_l to overcome the viscous drag on the slug. Both the liquid and the vapor overtake the condensation shock. At the leading edge θ_s the liquid velocity matches the shock speed. However, on both sides of θ_l the liquid velocity exceeds the local shock speed, providing a mechanism for the timewise growth (self-similar stretching) of the slug.

6. DISPERSIVE MECHANISMS

Smearing of saturation shocks by the capillarity of a porous medium is analogous to viscous smearing of gas-dynamic shocks, as discussed previously [5, 6] for the classical Buckley–Leverett problem. If a finite capillary pressure were explicitly included in the present model, s_{xx} would appear along with s_x and s_t in the continuity equation, the system would become fourth order with a proper number of boundary
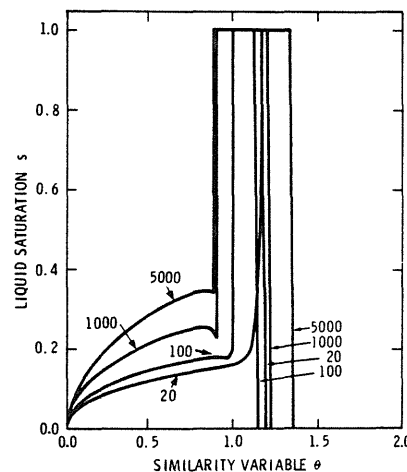
FIG. 5. Saturation profiles for various pressure ratios N.

conditions, and there would be no mathematical necessity for a shock (although computational difficulties may still persist). Although the mechanisms of capillarity and hydrodynamic dispersion preclude a true discontinuity in saturation, these smearing effects should be local, as in gas dynamic shock. Likewise, the effects of macroscopic fingering instability (which might occur in two-phase drive of a liquid slug) should be negligible because of the stabilizing influence of volumetric contraction at the moving condensation front [12].

Smearing of thermal shock by heat conduction is assessed by reformulation of the current problem under the suppositionof asymptotically large, but now finite, Peclét number. Within two-phase regions, the perturbation (due to $\epsilon = 1/Pe \ll 1$) is regular [11] because the T'' conduction term in the energy equation can be grouped (using Clausius–Clapeyron) with the stronger P'' terms and, hence, the order of the equation is not changed. However, in the subcooled liquid slug, the addition of T''' raises the order of the energy equation. The temperature distribution then remains uniform across the slug, except within a thermal boundary layer which replaces the temperature jump at θ_l. The singular perturbation [11] of the slug solution shows that the boundary layer thickness is of order $1/Pe$ and that the temperature gradient at θ_l is, to the first order

$$T' = [T]Pe\frac{\Delta s\beta}{1 + \Delta s\beta}\left(R\hat{\kappa}_l\hat{P}' + \frac{\theta}{2}\hat{S}\frac{1 + \beta}{\beta}\right), \quad (31)$$

in which $[T]$ is now interpreted as the temperature change in crossing the boundary layer. In writing the jump energy balance for the saturation shock which still persists at θ_l, temperature jump is now omitted, but a conduction term $[T'/Pe]$ is included, thereby arriving at identically the same shock conditions. As $Pe \to \infty$, the solution is, therefore, the same as before.

Regarding second-law considerations, it is noteworthy that a necessary condition for existence of the (exponential) thermal boundary layer at high Pe is that

$$\left(R\hat{\kappa}_l\hat{P}' + \frac{\theta}{2}\hat{S}\frac{1 + \beta}{\beta}\right) > 0. \quad (32)$$

Since this criterion is identical to the entropy-jump inequality (27a) for a thermal shock, it follows that the second-law becomes extraneous when heat conduction is included. An analogous situation occurs in shocked gas flows where the inviscid equations must be supplemented by entropy considerations, but the complete Navier–Stokes equations (including viscous smearing through u'') are self-sufficient.

7. SUMMARY

The considered prototype problem retains only the essential features of a condensing flow in a porous medium: concurrent gas/liquid mass transfer, convective energy transfer, and condensation due to fluid/solid energy exchange. Since capillarity and heat conduction are suppressed, the transport equations

are of a mixed parabolic/hyperbolic type which demands shock-like jumps in saturation and temperature. In the considered case of a dry saturated-vapor inflow there is a singularity at the injection surface which suppresses the inner structure in order to focus on a representative, but relatively simple, outer structure. In a subsequent paper [13], we consider the behavior under other boundary conditions, particularly those which result in imbedded regions of superheated vapor, as well as the case of a partially wet or fully wet far field.

Physical characteristics of the flow are strongly dependent on the magnitude of the temperature difference ΔT (parameterized by the pressure ratio, N), since it determines the nominal amount of condensation, Δs.

1. When ΔT is small, there is little condensation and the liquid is nearly immobile. The flow contains a weak saturation shock which lies close to the inflow boundary. The outer downstream region is second-order parabolic and resembles a single-phase vapor flow with a large (phase-change) compressibility.

2. So long as ΔT is moderate, the amount of condensate is insufficient to cause liquid-blockage of the pore space. At the saturation shock both phases are present on both sides, and the jump conditions require that: the shock faces forward, that there be no local phase change, that there be no local temperature jump. The low-mobility liquid is overtaken by the shock while the high-mobility vapor passes forward through the shock. Each mass flow is continuous in the shock frame, as in the classical Buckely–Leverett flow [5, 6].

3. At large ΔT, the liquid-full condition prevails over an interval in which the (incompressible) flow velocity and the temperature are uniform. The leading edge of this liquid slug is simply a wall of liquid, and the medium is undisturbed ahead (for $\Gamma \to \infty$). This full strength forward-facing shock is the continuous extension of the previous two-phase shock and, accordingly, there is no local phase change. On the trailing side of the slug there is a backward-facing saturation shock. Both liquid and vapor overtake the shock, and there is a temperature jump and some local condensation.

A family of steam flows in geologic media serves to illustrate solution behavior over a broad range of the parameters. It is noteworthy that the penetration depth $\theta_s \simeq 1$ and the pressure gradient $P'(0) \simeq -0.5$, are very weak functions of the parameters, because the scaling considerations absorb the first-order dependency (as also checked for other fluid/solid systems). Thus, the scaling considerations and the computational results have considerable generality in estimating penetration depth, flow rates, and flow structure for condensing flows in initially dry porous media.

REFERENCES

1. F. A. Morrison, Jr., Transient multiphase multicomponent flow in porous media, *Int. J. Heat Mass Transfer* **16**, 2331–2342 (1973).
2. H. G. Weinstein, J. A. Wheeler and E. G. Woods, Numerical model for thermal processes. *Soc. Pet. Engrs J.* **17**, 65–77 (1977).
3. A. Settari and K. Aziz, Treatment of nonlinear terms in the numerical solution of partial differential equations for multiphase flow in porous media, *Int. J. Multiphase Flow* **1**, 817–844 (1975).
4. P. Cheng, Heat transfer in geothermal systems, *Adv. Heat Transf.* **14**, 1–106 (1978).
5. R. A. Wooding and H. J. Morel-Seytoux, Multiphase fluid flow through porous media, *A. Rev. Fluid Mech.* **8**, 233–274 (1976).
6. A. H. Scheidegger, *The Physics of Flow Through Porous Media*, University of Toronto Press, Toronto (1974).
7. F. A. Morrison, Jr., Transient gas flow in a porous column, *I/EC Fundamentals* **11**, 191–197 (1972).
8. R. Courant, *Methods of Mathematical Physics II*, Interscience, New York (1966).
9. V. N. Nikolaevskii and B. E. Somov, Heterogeneous flows of multicomponent mixtures in porous media — Review, *Int. J. Multiphase Flow* **4**, 203–217 (1978).
10. J. C. Slattery, *Momentum, Energy, and Mass Transfer in Continua*, McGraw-Hill, New York (1972).
11. M. Van Dyke, *Perturbation Methods in Fluid Mechanics*, Academic, New York (1964).
12. C. A. Miller, Stability of moving surfaces in fluid systems with heat and mass transfer — III. Stability of displacement fronts in porous media, *A. I. Ch. E. Jl* **21**, 474–479 (1975).
13. L. A. Romero and R. H. Nilson, Shock-like structure of phase-change flow in porous media, *J. Fluid Mech*, in press.

ECOULEMENTS SELF-SIMILAIRES AVEC CONDENSATION DANS LES MILIEUX POREUX

Résumé—On obtient des solutions similaires pour la propagation de l'onde de condensation dans une matrice poreuse initialement sèche et qui reçoit un flux de vapeur saturée dû à un accroissement en échelon de température et de pression à la frontière. La formulation généralisée de Darcy (faible nombre de Reynolds) d'un écoulement diphasique conduit à des équations hyperboliques/paraboliques dans lesquelles la capillarité et la conduction thermique sont supprimées de façon à dégager le comportement semblable à un choc. L'application de la transformation en $X/\sqrt{t}$ donne des équations aux dérivées partielles qui sont résolues en utilisant un bilan de saut (Rankine–Hugoniot) pour traiter des discontinuités de saturation (qualité) de gradient de pression et de température éventuellement. La distribution du condensat (saturation) présente un front. Pour une faible différence de température, il y a un faible condensat proche de l'immobilité; le choc de saturation est proche de la frontière et la région externe est décrite par un système d'équations réduit. Lorsque la différence de température augmente, le choc se déplace en avant et gagne en intensité jusqu'à ce que le milieu soit plein de liquide derrière le choc. Le choc se déplace en avant et gagne en intensité jusqu'à ce que le milieu soit plein de liquide derrière le choc. Le choc se sépare en deux chocs dos-à-dos, séparés par un noyau de liquide sous-refroidi. Le problème considéré est représentatif d'une grande classe d'écoulements diphasiques qui sont rencontrés dans les applications liées à l'énergie et à la géologie.

ÄHNLICHE KONDENSIERENDE STRÖMUNGEN IN PORÖSEN MEDIEN

Zusammenfassung—Für die Ausbreitung einer Kondensations-Welle in eine anfänglich trockene poröse Matrix, in die durch ein sprunghaftes Ansteigen von Temperatur und Druck an ihrem Rande gesättigter Dampf einströmt, werden Ähnlichkeitslösungen gewonnen. Die verallgemeinerte Darcy-Formulierung (kleine Reynolds-Zahl) für Zwei-Phasen-Strömung führt auf hyperbolisch/parabolische Gleichungen, in denen zur Betonung des stoßartigen Verhaltens Kapillarwirkung und Wärmeleitung vernachlässigt werden. Die Anwendung der $X/\sqrt{t}$—Ähnlichkeits-Transformation führt zu gewöhnlichen Differential-Gleichungen, die durch Monte-Carlo-Verfahren gelöst werden; hierbei werden Sprungbedingungen (Rankine–Hugoniot) verwendet, um Unstetigkeiten der Sättigung (Dampfgehalt) des Druckgradienten und manchmal der Temperatur zu erhalten. Die Kondensat-Verteilung (Sättigung) ist wellenförmig, mit einer Stoßfront an der Vorderseite. Bei einer kleinen Temperatur-Differenz entsteht wenig Kondensat, und es ist fast unbewegt; der Sättigungs-Stoß liegt nahe am Rand, das Gebiet außerhalb wird durch ein reduziertes Gleichungssystem beschrieben. Mit zunehmender Temperatur-Differenz bewegt sich der Stoß vorwärts in die Strömung und nimmt dabei an Stärke zu, bis hinter dem Stoß gesättigte Flüssigkeit vorliegt. Danach teilt sich der Stoß auf in ein Paar durch einen unterkühlten flüssigen Pfropfen getrennter Stöße. Das betrachtete beispielhafte Problem steht für eine große Gruppe von Zwei-Phasen-Strömungen, die im Bereich der Energietechnik und der Geologie Anwendung finden.

REFERENCES

1) A.E. Scheidegger, The Physics of Flow Through Porous Media, University of Toronto Press, (1974).

2) S.E. Buckley and M.C. Leverett, Trans. AIME, (1942), 146, 107.

3) G.B. Whitham, Linear and Nonlinear Waves, John Wiley and Sons, (1974).

4) R.H. Nilson and L.A. Romero, Self-Similar Condensing Flows in Porous Media, Int. J. Heat and Mass Transfer, (1980), V.23, pp 1461-1470.

5) L.A. Romero and R.H. Nilson, Shock-like Structure of Phase Change Flow in Porous Media, J. Fluid Mech., (1981), V.104, pp 467-482.

6) K.H. Coats, Simulation of Steamflooding with Distillation and Solution Gas, Soc. of Petr. Eng. Journal, (Oct., 1976), p. 235.

7) P.G. Saffman and G.I. Taylor, The Penetration of a Fluid into a Porous Medium or Hele-Shaw Cell, Proc. Roy, Soc. A, (1958), V.245, pp 312-329.

8) C.A. Miller, Stability of Moving Surfaces with Heat and Mass Transfer, AIChE Journal, (1975), V.21, #3, pp 475-479.

Part II

THE FINGERING PROBLEM IN A HELE SHAW CELL

1) INTRODUCTION

There is an analogy between two dimensional flow in a porous medium and flow between two flat plates that are very close together. The latter apparatus is known as a Hele-Shaw cell. In such an apparatus, since the two plates are very close together, Stokes' equations for low Reynolds number flow are applicable.

$$\nabla P = \mu \nabla^2 \underline{u} \qquad \underline{u} = (u, v, w)$$

If one assumes that w is negligible compared to u and v, and that $\frac{\partial^2}{\partial x^2}$ and $\frac{\partial^2}{\partial y^2}$ are negligible compared to $\frac{\partial^2}{\partial z^2}$, one obtains the equations

$$P_x = \mu \, u_{zz}$$

$$P_y = \mu \, v_{zz}$$

$$P_z = 0$$

If the plates are separated by a distance h, after averaging the above equations with respect to z, one finds the equations for the net rate of fluid transport in the xy plane

$$\langle \underline{u} \rangle = -\frac{k}{\mu} \nabla P \qquad k = \frac{h^2}{12}$$

These are identical to the equations in a two dimensional porous medium. From now on the brackets on U will be dropped, and it will always be assumed that all the velocities refer to velocities averaged with respect to z. If the fluid is assumed to be incompressible, one finds

1) $\nabla^2 \phi = 0$ $\phi = -\dfrac{kP}{\mu}$

Saffman and Taylor (ref 1) analyzed the stability of a
moving plane interface in a porous medium or a Hele-Shaw cell.
They found that if no body force or surface tension effects
are included, the interface is stable if and only if the more
viscous fluid is pushing the less viscous fluid. They did
experiments in a Hele-Shaw cell to confirm this result. The
experiments also showed that an unstable plane interface will
at first develop several finger-like protrusions. As time
develops the larger fingers grow at the expense of the smaller
ones until a steady state is reached where there is just one
long finger present.

Saffman and Taylor were able to analyze the shapes of
these steady fingers. They assumed that the less viscous
fluid that pushes the more viscous fluid is of such negligible
viscosity that the pressure is essentially constant throughout
it. Assuming that the walls of the Hele-Shaw cell are a
distance L apart (not to be confused with the small distance h
that separates the plates of the cell), the problem can be
stated as follows.

On the surface of the finger,

a) $\phi = 0$

2)

b) $\phi_n = u \cdot \hat{n}$

here $\hat{n}$ is the unit normal to the finger, and U is the velocity of the finger. At $y=\pm L$

c) $\quad \phi_n = 0$

and as $x \rightarrow \infty$

d) $\phi_x \rightarrow \lambda v$ 2λ=width of finger

this last condition follows from conservation of mass.
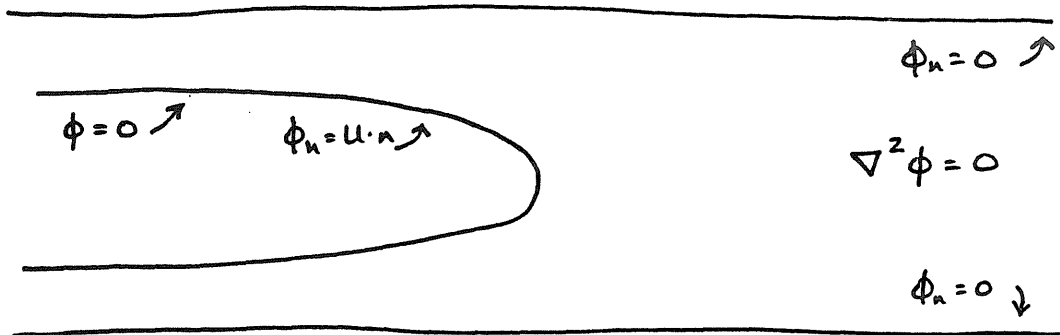
The condition $\phi=0$ on the surface of the finger is valid only if surface tension is neglected. Introducing $w=\phi+i\psi$, writing the equations in a coordinate system with the finger at rest, and rewriting the conditions 1) and 2a-d) in the hodograph plane, one gets

a) $\quad y = \dfrac{\psi}{u} \quad$ on $\quad \phi = 0$

3) b) $\quad y = \pm L \quad$ on $\quad \psi = \pm \lambda L U$

c) $\quad \nabla^2 y = 0$

The solution to this boundary value problem can be shown to be

4) $$z = x + iy = \frac{w}{\lambda L} + \frac{2(1-\lambda)}{\pi} \ln \frac{1}{2} \left[1 + e^{-\pi w/Lv} \right]$$

The shape of the finger can be found by plugging $\phi = 0$, and $y = \psi/U$ into the above formula.

5) $$x = \frac{1-\lambda}{\pi} \ln \frac{1}{2} \left(1 + \cos \frac{\pi y}{\lambda L} \right)$$

There are two dimensionless parameters that indicate the relative importance of viscous stresses to surface stresses. Depending on whether one scales the surface stresses by the radius of curvature of the mean two dimensional surface, or the radius of curvature of the meniscus in the narrow gap, one obtains the dimensionless parameters $\frac{\mu U L^2}{T h^2}$, or $\frac{\mu U L}{T h}$. Experiments show that as long as these are very small, the finger width is 1/2. The finger shapes computed by Saffman and Taylor agree very well with the experimental shape provided $\lambda = 1/2$ is plugged into their formula for the shape. Unfortunately they could not explain why $\lambda = 1/2$ was the appropriate value. Additional confirmation of these experimental results may be found in reference 4.

Saffman and Taylor analyzed the stability of these steady fingers and found that under the assumptions they were making the fingers are unstable. This is not at all in agreement with the experiments.

Recently McLean (references 2 and 3) analyzed the

problem of steady fingers in a Hele-Shaw cell taking into account the affects of surface tension. When surface tension is taken into account, the boundary condition at the surface of the finger is $\Delta P = T(1/R_1 + 1/R_2)$. Here R_1 is the radius of curvature of the two dimensional interface seen by an observer looking at the Hele-Shaw cell from above. R_2 is the radius of curvature of the very thin meniscus that one would see if one were to look at the narrow gap between the two plates. Obviously the second term is much larger than the first. However if the second term is assumed to be constant, then it merely plays the part of an additive constant in the problem. McLean proceeded on this assumption and got some interesting results.

By using analytic function techniques he was able to reduce the free surface problem to a nonlinear singular integral equation. He then solved this problem numerically using Newton's method. He found that if one includes surface tension in the problem (ignoring R_2), then there is a unique value of λ for each value of the surface tension. Furthermore, as the surface tension goes to zero the value of λ goes to 1/2.

It seemed as though one would be able to determine the value of λ as T went to 0 using a perturbation expansion. But neither McLean nor Saffman was able to do this. When the expansion was done, there was no condition to determine λ .

McLean also analyzed the stability of the fingers with

surface tension included and found that surface tension did not seem to stabilize the fingers.

McLean's results were a significant contribution to the problem, but there are still loose ends.

1) The perturbation analysis does not agree with the numerics.

2) The experiments show that the fingers are stable, but the analysis does not.

3) The curve of λ as a function of $\frac{\mu u \ell^2}{T h^2}$ does not agree with the experiments as well as one might hope.

The above loose ends are enough to keep one from calling the Saffman-Taylor problem a closed issue. The present work considers the effect of changes in the radius of curvature that McLean assumed was constant. McLean's problem may be considered to be a subclass of the problems to be considered here. Part of the motivation for the present study is to check McLean's results by an independent numerical scheme, and thus to bolster confidence in his results.

It is not an easy matter to take into account the effect of the radius of curvature in the small dimension. Unless one solves the full three dimensional Stokes equations, one must make an assumption on how R_2 is related to the two dimensional flow field. It is felt that it is reasonable to assume that R_2 is some function f(v) of the normal velocity of the two dimensional interface. For lack of any data on such a problem it is assumed that f(v) is a linear function of the normal velocity. It should be mentioned that it would be interesting

to try to obtain the function f(v) by modeling the full flow in   the narrow gap, and in fact this problem is currently being studied.

Besides the possibility of clearing up the stability issue and the agreement with experimental data, it was felt that it would be interesting to see if unique solutions are still obtained when only the effect of R_2 is taken into account. One reason this issue is interesting is that if the boundary condition using R_1 is so significant in determining the value of λ , then it seems clear that one must be careful in using a Hele-Shaw cell as an apparatus to model fingering in a porous medium. This is because in a porous medium the real interface is a very jagged one that only statistically can be thought of as being smooth. The radius of curvature of this mean interface is not necessarily significant in determining the pressure drop across the interface. The problem of determining whether the pressure drop depends on the mean radius of curvature is an interesting problem, and to the author's knowledge has not been solved. The condition $\Delta P=f(v)$ is possibly more realistic of the condition at the surface of an interface in a porous medium.

2) FORMULATION OF PROBLEM

The problem to be considered is identical to the Saffman-Taylor problem and the problem that McLean solved except for the boundary condition on the surface of the finger.

The fluid satisfies

6a)
$$\nabla^2 \phi = 0$$

On the finger

b)
$$\frac{\mu}{k} \phi = \frac{T}{R_1} + \frac{T}{R_2} \quad , \quad k = \frac{h^2}{12} \quad \frac{T}{R_2} = \beta \phi_n$$

c)
$$\phi_n = u \cdot \hat{n}$$

On the walls $y = \pm L$

d)
$$\phi_n = 0$$

Also,

e)
$$\phi_x \rightarrow V \quad \text{as} \quad x \rightarrow \infty \quad V = \lambda u$$

From now on it will be assumed that L=1.

If the shape of the finger was known, the conditions 6acde) would alone determine ϕ. The problem is to find the particular shapes of the boundary such that the equations labcde) can all be satisfied.

It is possible to proceed as McLean did and derive an integral equation to determine the shape of the boundary.

However, since part of the motivation for the present study is to check McLean's results by an independent numerical scheme, this is not done. Instead, the more direct approach of iterating on the shape of the boundary until all the boundary conditions are satisfied is used.

To do this one must have a way of solving Laplace's equation quickly for an irregular region. One does not have to know the solution in the whole region, but only on the boundary. An effective method for doing this is to use Theodorsen's method of numerical conformal mapping. Using this technique one can solve Laplace's equation and find the necessary information on the boundary in only $O(N\log N)$ operations where N is the number of points on the boundary. In order for Theodorsen's method to converge one must first map the region of interest onto a region that is fairly close to a circle. The Saffman Taylor solution can be used to do this.

Consider the function $Z=f(W(\Gamma))$, where $Z=f(W)$ is the function given in equation 4), and

$$W(\Gamma) = \frac{-V}{\pi} \ln \Gamma$$

This function can easily be shown to map the Saffman-Taylor finger of width λ onto the unit circle. When surface tension is included, it will map fingers of width λ onto a region that is approximately circular. Also, whether surface tension is included or not, it will map the walls $y=\pm 1$ onto the strip

$$\text{Im}(\Gamma) = 0, \quad -1 < Re(\Gamma) < 0$$

This cut in the Γ plane may be removed if one assumes the fingers are symmetrical. Finally one may use Theodorsen's method to map this near circle onto a circle. One can then solve Laplace's equation using fast Fourier transforms. Diagrams of these mappings are sketched in figure 1.

Let $\Delta = \Delta(\Gamma)$ be the mapping that maps the near circular finger shape in the Γ plane onto the unit circle. One must write down the boundary conditions 6bcde) in terms of the mapped variable Δ.

Let $\Omega(s)$ describe the finger in any plane Ω. The normal derivative of ϕ in this plane may be written

7) $$\phi_{n_\Omega} = \text{Im}\left(\frac{dw}{|d\Omega|}\right)$$

where dW and dΩ are the changes of W and Ω along the curve $\Omega(s)$. In the Z plane equation 6c) and 7) can be seen to yield

$$\text{Im}\left(\frac{dw}{|d\bar{z}|} - U\frac{d\bar{z}}{|d\bar{z}|}\right) = 0 \implies \text{Im}\left(dw - U d\bar{z}\right) = 0$$

so in the Δ plane

$$\phi_{n_\Delta} = \text{Im}\left(\frac{dw}{|d\Delta|}\right) = -\text{Im}\left(U\frac{d\bar{z}}{d\bar{\Delta}}\frac{d\bar{\Delta}}{|d\Delta|}\right)$$

this last equation can be seen to be equivalent to

8) $$\phi_{n_\Delta} = \tilde{u} \cdot \hat{n}_\Delta \quad \text{where} \quad \tilde{u} = U\frac{d\bar{z}}{d\bar{\Delta}} \quad \text{and} \quad \hat{n}_\Delta = \text{normal in } \Delta \text{ plane}$$

At this point it might be well to explain what

Theodorsen's method is, and how it is used to determine dZ/d$\triangle$

in equation 8). Let $\Gamma = \rho(\alpha) e^{i\alpha}$ describe a curve in the Γ

plane. Let $\Gamma(\triangle)$ be the function that maps the unit circle

onto this curve, and that satisfies $\Gamma(\emptyset)=\emptyset$. This mapping maps

any point on the unit circle with angle Θ onto a point on the

curve with angle $\alpha(\Theta)$. This function $\alpha(\Theta)$ can be shown to

satisfy

9)
$$\alpha(\Theta) = \Theta + \mathcal{A}(\ln \rho(\alpha))$$

Here $\mathcal{A}(h(\hat{z}))$ denotes the conjugate harmonic function of h that

satisfies $h(\emptyset)=\emptyset$.

Theodorsen's method solves this equation using picard

iteration (ref 5).

$$\alpha^{j+1}(\Theta_k) = \Theta_k + \mathcal{A}\left(\ln \rho(\alpha^j(\Theta_k))\right) \qquad \Theta_k = \frac{2\pi k}{N} \qquad k = 0, 1, \ldots, N-1$$

The function $\mathcal{A}(\ln(\rho(\alpha)))$ may be evaluated using fast

Fourier transforms. (It will be seen that for the problem

under consideration this last step must be slightly modified)

The end result is that one knows $\alpha_k = \alpha(\Theta_k)$ k=1,N-1, and hence

$\Gamma(\Theta_k) = \rho(\alpha_k) e^{i\alpha_k}$. One can now evaluate dΓ/d$\triangle$ by using

$$\frac{d\Gamma}{d\Theta} = \frac{d\Gamma}{d\triangle}\frac{d\triangle}{d\Theta} = i\triangle\frac{d\Gamma}{d\triangle} \implies \frac{d\Gamma}{d\triangle} = -i\,\bar{\triangle}\,\frac{d\Gamma}{d\Theta}$$

Then dZ/d$\triangle$=(dZ/dΓ)(dΓ/d$\triangle$), where dZ/dΓ can be evaluated

analytically.

To evaluate 6b) in the mapped plane one has to know how

to express 1/R$_1$, and ϕ_n in terms of the function Z($\triangle$). To

evaluate the curvature one only has to know how to evaluate the first two derivatives of $Z(\Theta)$, where $Z(\Theta)$ describes the finger in the physical plane in terms of the angle Θ in the mapped plane. These derivatives are

10a)
$$\frac{d\bar{z}}{d\Theta} = i\Delta\frac{d\bar{z}}{d\Delta}$$

b)
$$\frac{d^2\bar{z}}{d\Theta^2} = -\frac{d^2\bar{z}}{d\Delta^2}\Delta^2 - \frac{d\bar{z}}{d\Delta}\Delta$$

The expression for $\phi_n = U \cdot n$ in terms of $Z(\Delta)$ is

11)
$$U \cdot n = Im\left(U\frac{d\bar{z}}{|d\bar{z}|}\right) = Im\left(U\frac{d\bar{z}}{d\bar{\Delta}}\left|\frac{d\Delta}{d\bar{z}}\right|\frac{d\bar{\Delta}}{|d\Delta|}\right) \qquad \frac{d\bar{\Delta}}{|d\Delta|} = \frac{-i}{\Delta}$$

To evaluate 6e) in the mapped plane, note that as $x \to \infty$, $\Gamma \to 0$. Also,

$$\frac{d\bar{z}}{d\Gamma} = -\frac{1}{\pi}\left(\frac{1}{\Gamma} + 2\frac{\lambda-1}{1+\Gamma}\right)$$

From 6e) it is known that $dW/dZ \to V$ as $x \to \infty$. So as $\Gamma \to 0$,

$$\frac{dw}{d\Gamma}\frac{d\Gamma}{d\bar{z}} \longrightarrow -\pi\Gamma\frac{dw}{d\Gamma} \longrightarrow V$$

So there is a point source of strength $-V/\pi$ at $\Gamma=0$.

12)
$$W \sim \frac{-V}{\pi}\ln\Gamma \quad near \quad \Gamma = 0$$

This point source is mapped into a point source of the same strength in the Δ plane.

Z plane

w plane

Γ plane

Δ plane
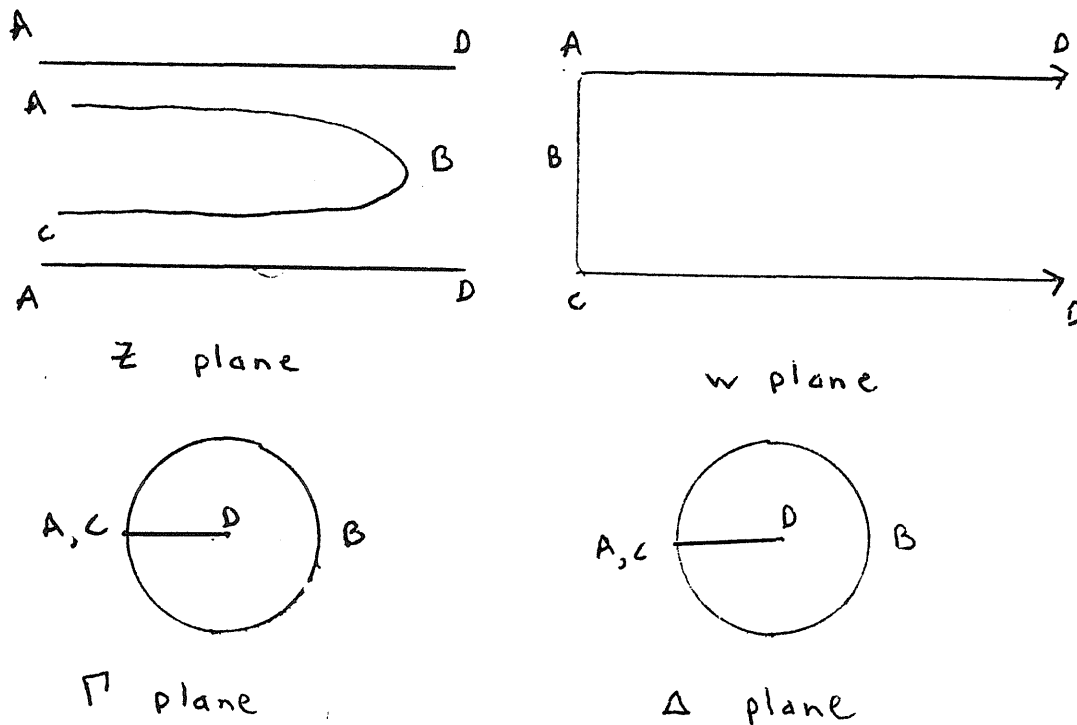
Figure 1

The function $w = w(z)$ defined by $z = \frac{w}{v} + \frac{z(1-\lambda)}{\pi} \ln^{1/2}\left(1 + e^{-\pi w/v}\right)$

maps the region bounded by the Saffman-Taylor finger of width λ and

the walls $y = \pm 1$, onto the semi-infinite strip $|\psi| < v$ $\phi > 0$. The

mapping $\Gamma = e^{-\pi w/v}$ maps this region onto the unit circle. The walls

$\psi = \pm v$ map onto the cut $-1 < \text{Re } \Gamma < 0$. Finally, if the finger shape

in the z plane was only close to the Saffman-Taylor shape, the region

in the Γ plane is only approximately circular. One can use Theodorsen's

method to find a mapping $\Delta = \Delta(\Gamma)$ that maps the Γ plane onto a circle.

3) ANALYSIS OF SINGULARITY OF THE MAPPING

The basic plan of attack is to find the shape of the finger in the T plane. Let $\Gamma = r(\alpha)e^{i\alpha}$ describe the shape of the finger in this plane. For the case of no surface tension, $r \equiv 1$. Before proceeding with the numerics it is necessary to find the form of $r(\alpha)$ near $\alpha = \pi$. If care is not taken in solving the equations around this point, the numerics are found not to converge as one raises the number of points used to describe the finger.

It will soon be shown that the solution near $\alpha = \pi$ depends on the asymptotic behavior of the solution as $x \to -\infty$. First however, this asymptotic form will be found.

As $x \to -\infty$ assume that y has the form $y = \lambda + Ae^{\gamma x}$. To first order $1/R = -A\gamma^2 e^{\gamma x}$

and

$$u \cdot n = -\gamma A u e^{\gamma x}$$

Now assume that ϕ also decays like $e^{\gamma x}$. In order to satisfy Laplace's equation, and the condition $\phi_n = 0$ at $y=1$, ϕ must have the form

$$\phi = B e^{\gamma x} \cos(\gamma(y-1)) \quad as \quad x \to -\infty$$

Now if these asymptotic forms are plugged into 6b) and c), one finds that to have A and B be nonzero γ must satisfy

13)
$$\cot \gamma(1-\lambda) = \frac{k}{\mu}\left(\frac{T}{u}\gamma^2 + \beta\gamma\right)$$

If T and β are zero, $\gamma = \dfrac{\pi}{2(1-\lambda)}$. If T and β are positive $\gamma < \dfrac{\pi}{2(1-\lambda)}$.

The dependence of r near $\alpha = \pi$ will now be found. Assume that near $\alpha = \pi$,

$$r(\alpha) = 1 + A(\pi - \alpha)^{\sigma}$$

Using $dZ/d\alpha = \dfrac{d\mathcal{Z}}{d\Gamma}\dfrac{d\Gamma}{d\alpha}$ one gets

$$\dfrac{dy}{dx} = \dfrac{[1 + r^2 + 2r\cos\alpha + 2(\lambda-1)r(r+\cos\alpha)]\dfrac{r'}{r} - 2(\lambda-1)r\sin\alpha}{1 + r^2 + 2r\cos\alpha + 2(\lambda-1)r(r+\cos\alpha) + \dfrac{r'}{r}2(\lambda-1)\sin\alpha} \qquad r' = \dfrac{dr}{d\alpha}$$

Near $\alpha = \pi$ the leading order terms give

14) $$\dfrac{dy}{dx} = \dfrac{-(\pi-\alpha)^{1-\sigma}}{A(1+\sigma)}$$

One can use equation 4) to find that as $x \to -\infty$ and $\alpha \to \pi$

$$x \sim \dfrac{-2(1-\lambda)}{\pi}\ln\dfrac{1}{2}\left(1 + r^2 + 2r\cos\alpha\right)^{1/2} \sim \dfrac{2(1-\lambda)}{\pi}\ln(\pi-\alpha)$$

so

15) $$\pi - \alpha \sim c\, e^{\frac{\pi x}{2(1-\lambda)}} \qquad near \;\; \alpha = \pi$$

Combining 14) and 15) one gets

$$\dfrac{dy}{dx} = c\, e^{\frac{\pi x}{2(1-\lambda)}(\sigma-1)} \qquad as \;\; x \to -\infty$$

so that

$$y \sim c'\, e^{\frac{\pi x}{2(1-\lambda)}(\sigma-1)} \qquad as \;\; x \to -\infty$$

Comparing this to equation 13) yields

16) $$\frac{\pi(\sigma-1)}{2(1-\lambda)} = \gamma$$

Since $\gamma < \frac{\pi}{2(1-\lambda)}$, we see that $\sigma < 2$. This means that the second derivative of $r(\alpha)$ blows up as $\alpha \to \pi$. If one were to try to expand r in a Fourier series, the coefficients would decay like $1/n^{\sigma+1}$. To find the curvature one must take the second derivative of r. The second derivative would decay like $1/n^{\sigma-1}$. Since $\sigma-1<1$, this is totally unsatisfactory.

For the numerical calculations the function r is assumed to have the form

$$r(\alpha) = 1 + A \sin^2\alpha \left(\cos\frac{\alpha}{2}\right)^{\sigma-2} + a_2(\cos 2\alpha - 1) + a_3(\cos 3\alpha - \cos\alpha) + \cdots$$

17)

The first term on the right hand side has the proper behavior near $\alpha = \pi$, and is zero at $\alpha = 0$. The remaining terms are just a Fourier expansion that is restricted to have $r(0)=1$. This last condition merely assures that the tip of the finger will be at $x=0$.

The singularity near $\alpha = \pi$ must also be accounted for in other ways. When finding the conformal mapping one must account for the singularity when evaluating $\ln(\rho(\alpha))$ in equation 9). If the function $\rho(\alpha)$ was analytic at $\alpha = \pi$, then one could find the conjugate harmonic by using fast Fourier transforms. Due to the singularity at $\alpha = \pi$, the Fourier expansion of $\ln(\rho(\alpha))$ only decays like $1/n^{\sigma+1}$. One obtains better accuracy if one splits the function up into two parts.

$$\ln\rho(\alpha) = \left(\ln\rho(\alpha) - A\frac{Re(\Gamma+1)^\sigma}{\cos\frac{\pi}{2}\sigma}\right) + A\frac{Re(\Gamma+1)^\sigma}{\cos\frac{\pi}{2}\sigma}$$

The Fourier components of the first part decay like $1/n^{2\sigma}$, and its conjugate may be found using fast Fourier transforms. The conjugate of the second part may be found analytically.

In order to evaluate the curvature, and $U \cdot n$, it is necessary to evaluate $dZ/d\Delta$. and hence $d\Gamma/d\Delta$. To determine $d\Gamma/d\Delta$, one uses equation 10), so $d\Gamma/d\theta$ must be evaluated accurately. The function $d\Gamma/d\theta$ can be evaluated by either doing finite differences, or by using fast Fourier transforms. Whichever technique is used (in the present work the first was chosen), one must subtract off the singularity before taking the derivative, differentiate the singular part analytically, and add this onto the less singular part of the derivative.

After one has determined the mapping $\Delta = \Delta(Z)$, and found the boundary conditions in the Δ plane, one must account for the singularity when solving Laplace's equation in a circle. Using equation 8) (except evaluating all quantities in the Γ plane instead of the Δ plane) one can find a formula for near $\alpha = \pi$. Near $\alpha = \pi$, if $r(\alpha) = 1 + A(\pi - \alpha)^{\sigma}$, then

18)
$$\phi_n \sim A \frac{u}{\pi} 2(\lambda - 1)(\sigma - 1)(\pi - \alpha)^{\sigma - 2}$$

In the Γ plane ϕ has a singularity at $\Gamma = -1$.

$$\phi = Re\left(2(1-\lambda)\frac{u}{\pi} \frac{(\Gamma+1)^{\sigma-1}}{\cos \frac{\pi}{2}(\sigma-2)}\right)$$

so in the Δ plane, ϕ has a singularity at $\Delta = -1$.

$$\phi = Re\ 2(1-\lambda)\frac{u}{\pi} \frac{(\Delta+1)^{\sigma-1}}{\cos \frac{\pi}{2}(\sigma-2)} \left(\frac{d\Gamma}{d\Delta}\Big|_{\Delta=-1}\right)^{\sigma-1}$$

To solve the Neumann problem in equation 8) one should analytically find the solution to the most singular part of the potential. Then one can use fast Fourier transforms to solve for the remaining part.

4) IMPLEMENTATION OF NUMERICS

The shape of the interface in the Γ plane is represented using 17). For McLean's problem the values of λ, A, and 2^n-2 Fourier coefficients a_n are used to represent the boundary. After mapping this region to a circle, the Neumann problem given by 6c) is solved, and the residuals from equation 6b) are computed. Newton's method is then used to adjust λ, A, and the a_ns, until the residuals go to zero. A few details of the implementation should be pointed out.

To begin with, it is interesting to note that the representation 17) is unique only if one imposes the extra condition that the Fourier coefficients die down as rapidly as possible. To see this note that the mapping from the Z plane to the Γ plane is a function of λ.

19)
$$ z(\Gamma) = -\frac{1}{\pi} \ln \Gamma + \frac{2(1-\lambda)}{\pi} \ln \frac{1}{2}(1+\Gamma) $$

Suppose that $r(\alpha)$ has a nonzero derivative at $\alpha = \pm\pi$. Then,

$$ Arg(\Gamma+1) = \pm\frac{\pi}{2}a \qquad \text{as} \quad \alpha \longrightarrow \pm\pi \qquad a \neq 1 $$

From 19) it is seen that as $\alpha \longrightarrow \pm\pi$

$$ x \longrightarrow -\infty $$

$$ y \longrightarrow \pm(a-1) \mp \lambda a $$

If the value of λ used in the transformation 19) is the same as the width of the finger, a=1, and there is no

discontinuity in $r'(\alpha)$ at $\alpha = \pm\pi$, otherwise there is a discontinuity. It is seen that the Fourier coefficients die down fastest when λ is chosen to correspond to the width of the finger, but if λ is chosen differently, then there is still a represenatation of the form 17).

The same point also applies to the coefficient A in equation 17). For any value of A, there is a representation of the form 17), but only for the correct value will the Fourier coefficients die down faster than $1/n^{\sigma+1}$. When actually implementing the numerics, it turns out that one does not have to explicitly impose the constraint that the Fourier coefficients die down rapidly. Newton's method just naturally chooses A and λ so that the coefficients die down as fast as possible.

It was felt that it was too difficult to find the exact Jacobian of this numerical scheme. However, it was too expensive merely to evaluate the Jacobian by brute force numerical differentiation. This would require finding a new conformal mapping for each row of the Jacobian. Instead, the following method is used.

Let $\epsilon \mathcal{V}(\alpha)$ be the perturbation in the normal direction to the finger in the Γ plane. An equation for $\dfrac{\partial \phi}{\partial \epsilon} = \hat{\phi}$ can be derived (appendix A). This equation involves the solution to the unperturbed problem, and may be solved numerically to find the Jacobian. There is no need to evaluate the conformal mapping each time. This method is used for finding the

derivatives with respect to the a_ns. The derivatives with respect to λ, and A are found by brute force numerical differentiation.

Let $M=2^m$ be the number of points used in finding the conformal mapping, and in solving the Neumann problem. Let $N=2^n$ be the number of points at which boundary condition 6c) is required to be satisfied, and also the number of points used to describe the boundary. Since the solutions are symmetric, it is only necessary to satisfy 6b) at half the points. If n=m-1 it is found that Newton's method does not converge. This is because the Jacobian is not evaluated exactly, and there is considerable error in the derivatives of the high frequency components of the Fourier series. If 6b) is only required to be satisfied at every 2nd , 4th, or 8th point, this problem does not occur. In the calculations to follow using every 4th point was found to work quite well.

After Newton's method has converged, the points that were not required to satisfy 6b) can be looked at, and the errors can be evaluated. It was found that for McLean's problem, the maximum of these errors $E_M(N)$, decayed about like $1/N^2$. In the following section this error is included in the table of results.

5) COMPARISON WITH MCLEAN'S RESULTS

To begin with, β was set to zero, and the results were compared with McLean's. Just as McLean found, for positive values of T, λ could not be determined arbitarily. However, a solution branch other than the one McLean found was also found. McLean's program was obtained to see if it would also give this branch. By modifying his initial guess, this branch was obtained. The two methods appear to be in excellent agreement.

Table 1) shows how the numbers vary as one raises the number of points used to describe the boundary. Note that as one raises N, the maximum error decreases about like $1/N^2$, and that $\lambda_{2N} - \lambda_N$ decays like $1/N^3$.

In table 2) are shown the Fourier coeficients for N=32. The decay is faster than $1/N^4$.

For both branches, λ approaches 1 as the surface tension becomes very large. For McLean's branch, it appears that $\lambda \to 1/2$ as $T \to 0$. This does not appear to be the case for the other branch. Figure 2) shows the branches plotted as functions of the dimensionless parameter $\frac{\mu u L^2}{T h^2}$. Plotted along with these two branches is a third branch that was found using McLean's code. An initial guess could not be found that yielded this branch using the conformal mapping approach.

It should be noted that both codes have trouble computing solutions for very small values of the surface tension. If one makes the surface tension small enough, both codes give

solutions with $\lambda < 1/2$, but these solutions are most likely not valid. As one raises N, λ increases, but before it settles down, the solutions become too costly to compute.

McLean's method of solving an integral equation turns out to be less cumbersome than the method described in this work. The main advantage is that the amount of programming is considerably less. As the number of points N used to describe the boundary becomes large, the major expense of both codes is solving Newton's method. Since the Fourier coefficients in 17) decay about like $1/N^4$, the present method is less expensive if very high accuracy is desired. However, unless very high accuracy is desired, McLean's method is considerably less expensive.

Table 1

N	λ^1	E_M^1	λ^2	E_M^2
4	.5222342	.18E-3	.5841376	.41E-3
8	.5217650	.40E-4	.5863854	.13E-3
16	.5217398	.13E-4	.5863619	.32E-4
32	.5217349	.35E-5	.5863599	.81E-5
64	.5217345	.93E-6	.5863600	.20E-5

Dependence of λ, and E_M on the number of points N used to describe the boundary. Superscripts indicate which branch is being considered.

Table 2

.28E0	.31E-3	-.12E-3	.49E-4	-.23E-4	.12E-4
-.70E-5	.43E-5	-.28E-5	.18E-5	-.13E-5	.91E-6
-.68E-6	.49E-6	-.37E-6	.28E-6	-.22E-6	.17E-6
-.13E-6	.10E-6	-.78E-7	.60E-7	-.45E-7	.33E-7
-.23E-7	.14E-7	-.96E-8	.52E-8	-.22E-8	.51E-9

Example of typical decay of the Fourier coefficients for N=32, $P=0$, $T\neq0$, $\lambda=.5217$. The coefficients are listed in increasing order from left to right, and from top to bottom.
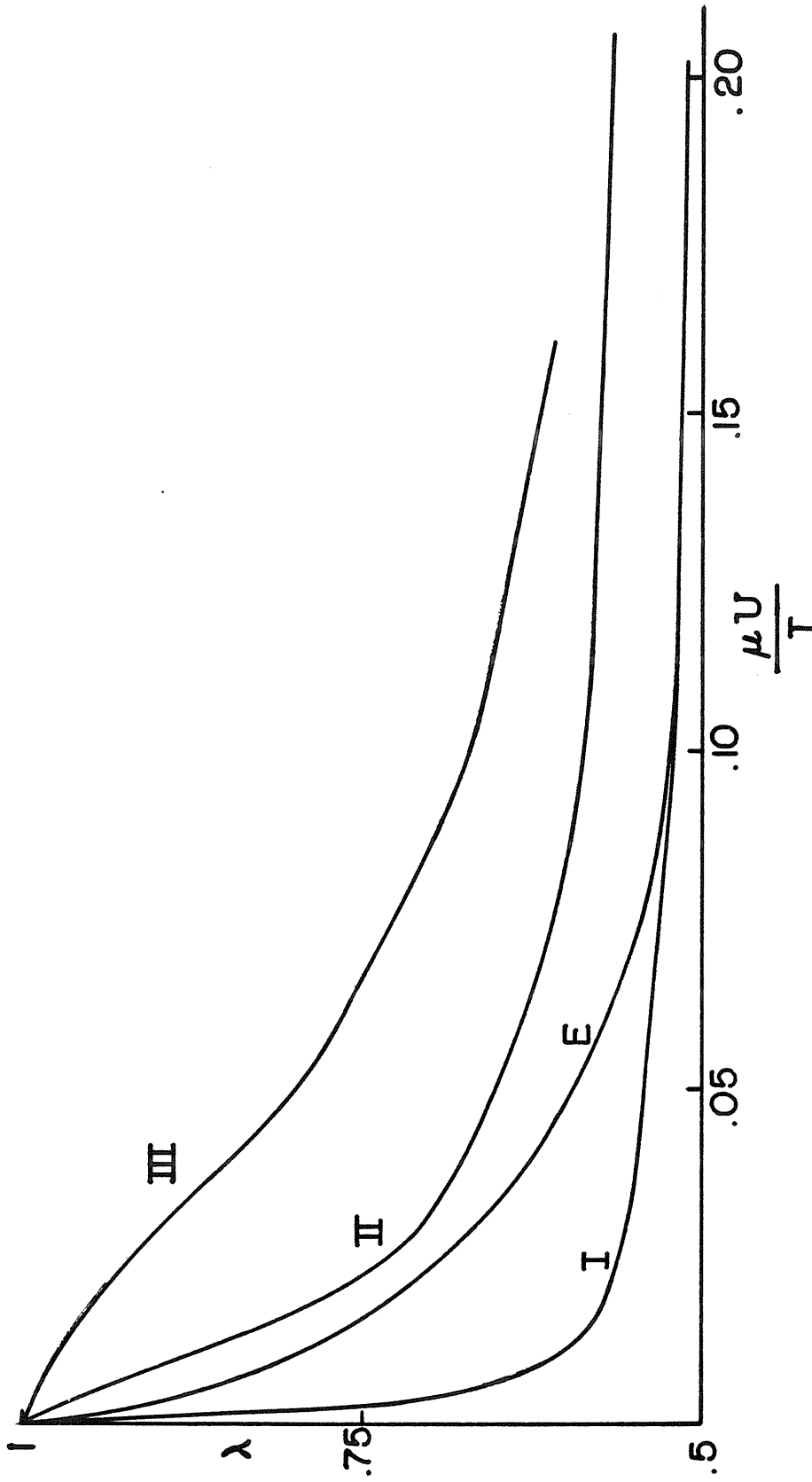
Figure 2

Finger width λ versus $\frac{\mu U}{T}$. I-McLean's branch; II-Branch found by both methods; III-Branch found only with McLean's code; E-Experimental data.

6) MODIFIED BOUNDARY CONDITION

After checking to see that when $\beta = 0$ the results agreed with McLean's, shapes were computed with $T \neq 0$, and $\beta \neq 0$. Then T was gradually reduced to see if the determinant of the system went to zero as in the case when $\beta = 0$. It was found that this in fact did happen. Table 3 shows how the determinant of the system decreases as one lets the dimensionless parameter $\dfrac{Th^2}{\mu u L^2}$ go to zero keeping β fixed.

T was set to zero, and the code was then adjusted so that λ was specified instead of being an adjustable parameter in Newton's method. It was found that the solutions converged nicely. All indications are that the boundary condition with $\Delta P = \beta \phi_n$ does not eliminate the arbitrariness of λ in the problem. Table 4 shows an example of how the maximum error E_M and the coefficient A in the representation 17) vary as one varies N (the number of points used to describe the boundary).

It is reasonable to assume that β is proportional to T/h. Also, it is reasonable to assume that as the normal velocity of the interface increases, the curvature $1/R_2$ also increases. This corresponds to requiring that β be positive. One finds that for any particular value of $T \neq 0$ or 1, the finger widths grow larger as one increases β. The values of λ as $T \to 0$ or 1, remain the same as in the case where $\beta = 0$. The effect of modeling $1/R_2$ is to modify McLean's curve $\lambda(\mu u L^2 / Th^2)$ so that it stays fixed at 0 and ∞, but it is raised for intermediate values. As seen in figure 2, this is qualitatively what is

needed to bring the curves into agreement with experimental data.

The code was also run assuming that $1/R_2 = \beta \phi_n^2$. The conclusion was the same. A unique value of λ was not determined unless one took into account $1/R_1$. In table 5 it is shown how the determinant goes to zero as one lowers $\frac{Th^2}{\mu u L^2}$.

Also the curve $\lambda(\mu L^2 U/Th^2)$ was raised for intermediate values of $\mu L^2 U/Th^2$ as when the dependence on ϕ_n was assumed to be linear.

By slightly modifying McLean's derivation, it is easy to derive an integral equation for the shape of the finger when both radii of curvature are taken into account.

$$q = Tqs \frac{d}{ds}\left(sq \frac{d\theta}{ds}\right) + \cos\theta + \beta qs \frac{d}{ds}\left(\frac{\sin\theta}{qs}\right)$$

$$\ln q = -\frac{s}{\pi} P\!\!\int \frac{\theta(s')}{s'(s'-s)} ds' \qquad \begin{array}{ll} \theta(0)=0 & \theta(1)=\frac{-\pi}{2} \\[4pt] q(0)=1 & q(1)=0 \end{array}$$

The definitions of q, θ, and s may be found in McLean's thesis. It is interesting to note that when the parameter T is nonzero, the second derivative of θ is brought into the problem, but when β is nonzero, only the first derivative of θ is brought in. The parameter T appears to perturb the equations in a more singular way than the parameter β. It is not surprising that β by itself does not fix the value of λ the way that T does.

Table 3

$\dfrac{\mu u L^2}{T h^2}$	det
.124	.27E-3
.156	.70E-4
.195	.18E-4
.24	.50E-5
.30	.15E-5
.48	.29E-6
.61	.13E-6
.81	.23E-8

Table 4

N	A	E_M
8	.7675	.2E-4
16	.6816	.7E-5
32	.6525	.2E-5
64	.6405	.5E-6

Table 5

$\dfrac{\mu u L^2}{T h^2}$	det
.17	.14E2
.28	.80E-1
.39	.72E-3
.59	.11E-4
.88	.30E-6
1.3	.19E-7

7) CONCLUSIONS

McLean's results were checked by a different numerical scheme, and the agreement between the two methods was found to be quite good. Another solution branch was found on which it appears that λ does not approach 1/2 as T approaches 0. The physical significance of this branch is not known.

The effect of the radius of curvature R_2 was modeled by assuming that $1/R_2 = \rho \phi_n$. It was found that if one ignores the large radius of curvature R_1, λ is arbitrary as in the case where one completely ignores the surface tension. One finds that when both radii of curvature are taken into account, the effect of $1/R_2$ is to modify the curve $\lambda = \lambda(\mu u^2 / T h^2)$ in a way that is qualitatively in agreement with experiments.

APPENDIX A

Let the finger shape in the Γ plane be given by 17). In this appendix it will be shown how to evaluate the derivatives of the function given by the residuals in equation 6b), with respect to the parameters a_n in 17). If one perturbs the shape in the Γ plane by changing one of the a_n's by $\epsilon \hat{a}_n$, it changes the shape of the finger in the Δ plane to $(1+\epsilon \hat{\nu}(\theta))e^{i\Theta}$, where $\hat{\nu}(\theta)$ can be calculated knowing $d\Gamma/d\Delta$ and the perturbation to the shape in the Γ plane. The problem then reduces to finding how a small perturbation to the shape in the Δ plane affects the residuals in 6b).

Let $\phi = \phi_0 + \epsilon \hat{\phi}$ be the potential for the problem with the perturbed finger shape. One can derive a Neumann problem for $\hat{\phi}$ on the unit circle that is accurate to $o(\epsilon)$. In equation 8) both $\tilde{U}$ and n_Δ are changed. To first order

$$\tilde{u}\left((1+\epsilon\hat{\nu})\Delta\right) = \tilde{u}(\Delta) + \epsilon \hat{\nu} \Delta \frac{d\tilde{u}}{d\Delta}$$

$$n_\Delta = (n_\Delta)_0 + \epsilon \hat{\nu}' T_\Delta \qquad \text{where} \quad T_\Delta = \text{unit tangent vector}$$

so

$$\tilde{u} \cdot n_\Delta = \left(\tilde{u} \cdot n_\Delta\right)_0 + \epsilon\left(\tilde{u} \cdot T_\Delta \hat{\nu}' + \Delta \frac{d\tilde{u}}{d\Delta} \cdot n_\Delta \hat{\nu}\right)$$

Also,

$$\frac{\partial \phi}{\partial n} = \nabla\left(\phi + \epsilon\hat{\phi}\right) \cdot \left(n_\Delta + \epsilon\hat{\nu}' T_\Delta\right) = \left(\frac{\partial \phi}{\partial n}\right)_0 + \epsilon\left(\nu' \frac{\partial \Theta}{\partial T} + \frac{\partial \hat{\phi}}{\partial n}\right) + O(\epsilon^2)$$

The above, along with equation 8) determine $\dfrac{\partial \hat{\phi}}{\partial n}$ up to $o(\epsilon)$ on the perturbed boundary. To the same order, the value on the unperturbed boundary is found by subtracting $\epsilon \hat{\vartheta}\, \dfrac{\partial^2 \phi}{\partial n^2}$. The final result is

$$\frac{\partial \hat{\phi}}{\partial n} = \epsilon \left(-\hat{\vartheta}' \frac{\partial \phi}{\partial t} + \tilde{u} \cdot T_\Delta \hat{\vartheta}' + \hat{\vartheta} \frac{d\tilde{u}}{d\Delta} \Delta \cdot n_\Delta \right)$$

One can use fast Fourier transforms to compute $\hat{\phi}(\Theta)$.

Let $\Delta' = \Delta'(\Delta)$ be the mapping obtained from Theodorsen's method that maps the perturbed shape in the Δ plane onto the unit circle. To order ϵ Theodorsen's method gives

$$\Theta(\Theta') = \Theta' + \mathcal{A}\, \ell n \left(1 + \epsilon \hat{\vartheta}\, \Theta'(\Theta) \right) = \Theta' + \epsilon \mathcal{A} \hat{\vartheta}(\Theta) + O(\epsilon^2)$$

We thus get

$$\Theta(\Theta') - \Theta' = \epsilon \mathcal{A} \hat{\vartheta}(\Theta)$$

The term on the right can be evaluated using fast Fourier transforms. Dividing by ϵ and taking the limit as $\epsilon \to 0$, we obtain an expression for $d\Theta/d\epsilon$. This derivative tells at what angle points in the Δ' plane must have originated from in the Δ plane. To evaluate the contribution to 6b), the change in the potential, one must first take into account the contribution of $\hat{\phi}$, and one must then take into account the fact that the function ϕ is being evaluated at both a different radius and a different angle. The total contribution is

$$\hat{\phi} + \epsilon \frac{\partial \phi}{\partial T} \frac{d\Theta}{d\epsilon} + \epsilon \hat{\vartheta} \frac{\partial \phi}{\partial n}$$

One now must calculate the change in $\phi_n = U \cdot n$ in 6b) caused

by perturbing the boundary in the $\triangle$ plane. One can do this by noting that the normal in the z plane can be written

$$\underline{n} = \frac{d\hat{z}}{|d\hat{z}|} = \frac{d\hat{z}}{d\triangle} \left| \frac{d\triangle}{d\hat{z}} \right| \frac{d\triangle}{|d\triangle|} = f(\triangle) \frac{d\triangle}{|d\triangle|}$$

Where $d\hat{z}$ and $d\triangle$ are taken along the boundary of the finger in the z and $\triangle$ plane respectively. Taking into account the perturbation in the $\triangle$ plane one gets

$$\underline{n} = \underline{n}_0 + \epsilon \left(\hat{\nu} f'(\triangle) \triangle \frac{d\triangle}{|d\triangle|} + \hat{\nu}' f(\triangle) \triangle \right)$$

To evaluate U·n one merely takes the x component of the vector $\underline{n}$.

Again one must correct for the fact that one wants to evaluate the function in the $\triangle'$ plane and not the $\triangle$ plane. To do this one must correct ϕ_n by adding a term

$$\epsilon \frac{d\theta}{d\epsilon} \frac{d}{d\theta} \phi_n$$

To calculate the change in the curvature one uses

$$\frac{1}{R_1} = \frac{x' y'' - y' x''}{(x'^2 + y'^2)^{3/2}} \qquad \text{primes refer to derivatives w.r.t. } \theta$$

The perturbations to the derivatives of x and y may be calculated using

$$\frac{d\hat{z}}{d\theta} = \frac{d\hat{z}}{d\triangle} \frac{d\triangle}{d\theta} \qquad \triangle = (1 + \epsilon \hat{\nu}) e^{i\theta}$$

The perturbation to the curvature can easily be obtained by gathering the contributions of order ϵ. One again must add a term due to the fact that all quantities should be evaluated in the $\triangle'$ plane.

$$\epsilon \frac{d\theta}{d\epsilon} \frac{d}{d\theta} \left(\frac{1}{R_1} \right)$$

REFERENCES

1) P.G. Saffman and G.I. Taylor, The Penetration of a Fluid Into a Porous Medium or Hele-Shaw Cell, Proc. Roy., Soc. A, V. 245, (1958), pp 312-329.

2) J.W. McLean, The Fingering Problem in Flow Through Porous Media, Ph.D. Thesis, Cal Tech, (1980).

3) J.W. McLean and P.G. Saffman, The Effect of Surface Tension on the Shape of Fingers in a Hele-Shaw Cell, J.F.M, V. 102, (1981), pp 455-469.

4) E. Pitts, Penetration of a Fluid into a Hele-Shaw Cell, J.F.M, 97, (1980), pp 53-64.

5) P. Henrici, Fast Fourier Methods in Complex Analysis, S.I.A.M. Review, V. 21, #4, (1979), pp 481-527.